



**NTNU – Trondheim**  
Norwegian University of  
Science and Technology

# Automatic Reliability-based Control of Iceberg Towing in Open Waters

**Andreas Orsten**

Marine Technology

Submission date: June 2014

Supervisor: Roger Skjetne, IMT

Norwegian University of Science and Technology  
Department of Marine Technology



## PROJECT DESCRIPTION SHEET

<b>Name of the candidate:</b>	Andreas Orsten
<b>Field of study:</b>	Marine control engineering
<b>Thesis title (Norwegian):</b>	Automatisk pålitelighetsbasert tauing av isfjell i åpne farvann.
<b>Thesis title (English):</b>	Automatic reliability-based control of iceberg towing in open waters.

### Background

Icebergs pose serious threats to existing and planned offshore structures, vessels, and operations in Arctic waters such as the East Coast of Canada, East and West Greenland, the Barents Sea, and the Kara Sea. The intrusion of icebergs into an operational area must be detected within safety time limits, continuously tracked, and their future motion must be forecasted in order to assess the threat of structures and operations. This is typically done by an *iceberg management system*. If an iceberg is evaluated as a threat, then *physical iceberg management* must be mobilized to mitigate the threat. This is typically done by single vessel towing of the iceberg using a synthetic floating towline.

In this project the candidate will consider a Line-Of-Sight- (LOS-) based control method to tow an iceberg safely along a predetermined path in presence of ocean current. Moreover, reliability-based control was introduced for thruster-assisted position mooring systems to avoid breaking the mooring lines during rough weather conditions. It is believed that this method will also be applicable to the iceberg towing control problem. Hence, reliability-based methods shall be considered to keep the tension in the towline within its limits and avoid towline rupture, towline slippage, and iceberg overturning.

### Work description

- 1) Perform a literature review to provide background and relevant references on:
  - Iceberg statistics and iceberg towing operations for various geographic locations.
  - Iceberg towing operation, towing vessel, towing configuration, towlines, winches, and sensors.
  - Reliability index methods and reliability-based control.
  - LOS-based guidance and control of ships.Write a list with abbreviations and definitions of terms and concepts, explaining relevant concepts related to icebergs and iceberg towing.
- 2) Develop a simulation model for an iceberg, a synthetic towline, and a towing vessel, and integrate these models through the tension of the towline. The simulation model shall as minimum include an ocean current that affects the vessel, the iceberg, and the towline.
- 3) Implement the failure modes of towline rupture, towline slippage, and iceberg overturning in your simulation model.
- 4) Derive a LOS-based control algorithm for towing the iceberg along a straight-line path, verify its stability, simulate, and present the resulting responses.
- 5) Derive a reliability-index for the towline. Based on this, derive a control law that controls the forward towing motion of the towing vessel (considering speed control or direct force control) to minimize the risk of towline rupture, towline slippage, and iceberg overturning.
- 6) Propose an overall control strategy combining safe forward towing motion with LOS-based steering of the iceberg along the straight-line path. Implement this in your simulation model and present the resulting responses.
- 7) Implement your simulation and control algorithms on the HIL setup for C/S Enterprise I, run simulations, and present the HIL setup and resulting responses.
- 8) Experimentally test the iceberg towing system in MC Lab with C/S Enterprise I, towing an “iceberg-like” object and interfacing the tension measurements for the towline.

### **Guidelines**

The scope of work may prove to be larger than initially anticipated. By the approval from the supervisor, described topics may be deleted or reduced in extent without consequences with regard to grading.

The candidate shall present his personal contribution to the resolution of problems within the scope of work. Theories and conclusions should be based on mathematical derivations and logic reasoning identifying the various steps in the deduction.

The report shall be organized in a rational manner to give a clear exposition of results, assessments, and conclusions. The text should be brief and to the point, with a clear language. The report shall be written in English (preferably US) and contain the following elements: Abstract, acknowledgements, table of contents, main body, conclusions with recommendations for further work, list of symbols and acronyms, references, and (optionally) appendices. All figures, tables, and equations shall be numerated. The original contribution of the candidate and material taken from other sources shall be clearly identified. Work from other sources shall be properly acknowledged using quotations and a Harvard citation style (e.g. *natbib* Latex package). The work is expected to be conducted in an honest and ethical manner, without any sort of plagiarism and misconduct. Such practice is taken very seriously by the university and will have consequences. NTNU can use the results freely in research and teaching by proper referencing, unless otherwise agreed upon.

The thesis shall be submitted with two printed and electronic copies, to 1) the main supervisor and 2) the external examiner, each copy signed by the candidate. The final revised version of this thesis description must be included. The report must appear in a bound volume or a binder according to the NTNU standard template. Computer code and a PDF version of the report shall be included electronically.

**Start date:** 1 February, 2014                      **Due date:** As specified by the administration.

**Supervisor:** Prof. Roger Skjetne  
**Co-advisor(s):** Prof. Bernt J. Leira and PhD cand. Petter Norgren

---

**Roger Skjetne**  
Supervisor



# Abstract

Icebergs pose serious threats to existing and planned offshore structures, vessels, and operations in Arctic waters. In order to eliminate the threat, iceberg handling must be performed. This is typically done by single vessel towing of the iceberg, using a floating towline laid encircling the iceberg in the waterline. Common challenges during towing of icebergs are *towline rupture*, that the *towline slips* off the iceberg, or that the *iceberg overturns*. These are denoted *failure modes* of iceberg towing operations. Motivated by finding a way to safely alter the iceberg trajectory such that it no longer poses a threat, this thesis discusses automatic reliability-based control of iceberg towing in open waters.

A mathematical model for single vessel iceberg towing in the presence of a constant and irrotational ocean current is developed. A reliability index is defined for each failure mode of the towline. The index is based on towline tension measurements and maximum tension limits for the failure mode, for instance the towline rupture tension limit.

A line-of-sight guidance and control method is developed in order to tow an iceberg to and along a pre-defined straight-line path in the presence of an ocean current, using a towing vessel and a towline. The method assumes that the iceberg position is measured, and calculates a desired iceberg course angle. Using a reference model and backstepping controller, the towing vessel is positioned in order to apply a tow force in the desired iceberg course direction.

Two reliability index-based penalty control schemes are proposed. The first penalizes the commanded thrust when the reliability index is too close to the lower limit. The second penalizes the velocity reference for the tow operation. A limitation to the rate of change of the penalty is proposed for reducing how fast the penalty decreases, in order to achieve a steady velocity reference.

The mathematical model and control methods are tested, both in simulations, and experimentally in the Marine Cybernetics Laboratory (MC Lab) at the Norwegian University of Science and Technology (NTNU). Simulations and experiments show that it is advisable to avoid transients in the towline tension, and that the penalty on commanded thrust is not sufficiently effective.

Using the line-of-sight method, simulations and experiments show that the vessel tows the iceberg to and along the desired path. A combination of the line-of-sight method and the velocity reference penalty scheme is simulated, and shown to safely tow the iceberg along the path, while avoiding failure modes.

A hardware-in-the-loop (HIL) setup, containing position measurement errors, is developed for iceberg towing in the Marine Cybernetics Laboratory (MC Lab), using CS Enterprise I, a 1 : 50 scaled model vessel.



# Sammendrag

Isfjell utgjør en trussel for både eksisterende og planlagte strukturer, skip og operasjoner offshore. Hvis et isfjell er en trussel, fjernes det vanligvis ved å taue isfjellet ved hjelp av et slepefartøy og en flytende tauline som legges rundt isfjellet i vannlinjen. Vanlige utfordringer ved isfjelltauing er *brudd i taulinen*, at *taulinen sklir* av isfjellet, eller at *isfjellet kantrer*. Disse utfordringene kalles *feilmoder* for isfjelltauing. Motivert av et ønske om å finne en trygg metode for å endre kursen til isfjellet slik at det ikke lenger er en trussel, vil denne oppgaven undersøke automatisk pålitelighetsbasert tauing av isfjell i åpne farvann.

En matematisk modell for tauing av isfjell blir utviklet, med en konstant, virvelfri havstrøm inkludert i modellen. En pålitelighetsindeks defineres for hver feilmode. Indeksen baserer seg på målinger av taukraften og maksimalkraft før en feilmode oppstår, for eksempel hvilken taukraft som gir brudd.

En siktelinje-reguleringsmetode blir utviklet for å taue et isfjell, påvirket av havstrøm, langs en forhåndsdefinert rett linje, ved bruk av slepefartøy og tauline. Metoden antar at isfjellets posisjon måles, og beregner deretter den ønskede kursen for isfjellet. Slepefartøyet posisjoneres, ved hjelp av en referansmodell og en backsteppingregulator, slik at det påfører taukraften i den ønskede retningen for kursen til isfjellet.

To vektingbaserte reguleringsmetoder basert på pålitelighetsindeksen blir foreslått. Den første metoden nedjusterer pådraget til skipet når pålitelighetsindeksen er for nære en nedre grense. Den andre nedjusterer hastighetsreferansen til taueoperasjonen. En begrensning av nedjusteringens endringsrate blir foreslått for å redusere hvor hurtig nedjusteringen avtar, slik at hastighetsreferansen blir stabil.

Den matematiske modellen og reguleringsmetodene testes, både ved simulering og ved å teste dem eksperimentelt i laboratoriet for Marin Kybernetikk (MC Lab) ved Norges Tekniske og Naturvitenskapelige Universitet (NTNU). Simuleringer og eksperimenter viser at det er ønskelig å unngå transienter i taukraften, og at metoden som nedjusterer pådraget til skipet ikke fungerer godt nok.

Simuleringer og eksperimenter med siktelinjemetoden viser at slepefartøyet tauer isfjellet langs den ønskede banen. En kombinasjon av siktelinjemetoden og vektingmetoden på hastighetsreferansen blir simulert, og viser at isfjellet taues langs den ønskede banen samtidig som feilmodene unngås.

Til slutt utvikles et programvaretest-oppsett (HIL) for isfjelltauing, ved bruk av modellfartøyet CS Enterprise I, i laboratoriet for Marin Kybernetikk (MC Lab). Oppsettet inneholder simulerte feil i posisjonsmålingene.



# Acknowledgements

This report is the final result of my master thesis within marine technology at NTNU. During my five years in Trondheim, at the Department of Marine Technology, I have developed much - both personally and academically. My knowledge within both marine engineering and cybernetics, but also my world knowledge, has thoroughly expanded during these years, and I can safely say that I now know of a lot more that I still do not have a clue about.

The master thesis has been encouraging to work with. The topic of towing icebergs has been exciting, and I would like to thank my supervisor, Professor Roger Skjetne, for introducing me to the topic, and for his guidance and help throughout the thesis work. I would also like to thank my co-advisor PhD candidate Petter Norgren for his great help and inputs throughout the semester, and my co-advisor Professor Bernt J. Leira for his inputs on reliability-based control.

Especially encouraging about the thesis work, was the hands-on experience in the Marine Cybernetics Lab (MC Lab) at NTNU. Being able to work with the model vessel CS Enterprise I in a model tank, has helped much in understanding the different concepts of guidance and control of marine vessels. My lab work would not have been possible without senior engineer Torgeir Wahl, who has continuously aided me with my experiments. My work was also heavily accelerated by the help I received from fellow MSc student Nam Dinh Tran, who is somewhat of an expert on laboratory experiments with CS Enterprise I. Some of the lab experiments would have been impossible without the help of good friends to aid me, so I would like to thank MSc students Jostein Follestad and Christian H. Sunde for their help. I would also like to express my appreciation for the work Mika Sundland performed on his Master thesis in 2013. His thesis has been the foundation for my work on iceberg towing.

Lastly, I would like to thank my fellow students, and especially our student organization Mannhullet, for making the last five years unforgettable.

**Andreas Orsten**  
Trondheim, June 9, 2014



# Contents

<b>Abstract</b>	<b>iii</b>
<b>Sammendrag</b>	<b>v</b>
<b>Acknowledgements</b>	<b>vii</b>
<b>List of acronyms and symbols</b>	<b>xiii</b>
<b>1 Introduction</b>	<b>1</b>
1.1 Former work on iceberg towing . . . . .	1
1.2 Scope of work . . . . .	2
1.3 Thesis outline . . . . .	2
1.4 Publications . . . . .	3
<b>I Literature review</b>	<b>5</b>
<b>2 Definitions</b>	<b>7</b>
<b>3 Iceberg statistics and operations</b>	<b>9</b>
3.1 Introduction and motivation for towing of icebergs . . . . .	9
3.1.1 Iceberg handling . . . . .	9
3.2 Areas of iceberg management . . . . .	9
3.2.1 Iceberg management in the Grand Banks area . . . . .	10
3.2.2 Iceberg management in the Barents Sea . . . . .	11
3.3 Detection of icebergs . . . . .	12
3.3.1 Iceberg classification . . . . .	12
3.3.2 Detecting icebergs . . . . .	14
3.3.3 Threats of icebergs . . . . .	15
3.4 Limitations of iceberg towing . . . . .	16
3.4.1 Iceberg shape limitations . . . . .	16
3.4.2 Iceberg size limitations . . . . .	17
3.4.3 Sea state limitations . . . . .	18
3.4.4 Towing limitations during the Fylla exploration drilling program	18
<b>4 Single vessel iceberg towing operation</b>	<b>19</b>
4.1 Current tow operations . . . . .	20
4.2 Mathematical model . . . . .	20
4.2.1 Towing method . . . . .	20
4.2.2 Model by Marchenko and Eik . . . . .	21

4.2.3	Model by Sundland . . . . .	22
<b>5</b>	<b>LOS-based guidance of ships</b>	<b>25</b>
5.1	Modelling of offshore vessels . . . . .	25
5.2	LOS guidance . . . . .	26
5.2.1	Traditional LOS guidance . . . . .	26
5.2.2	LOS method with constant ocean current . . . . .	29
<b>6</b>	<b>Reliability-based control</b>	<b>31</b>
6.1	Reliability-based control of risers . . . . .	31
6.2	Reliability-based control of mooring lines . . . . .	32
6.3	Application of reliability index in control . . . . .	33
<b>II</b>	<b>Simulation setup for iceberg towing</b>	<b>35</b>
<b>7</b>	<b>Mathematical model for iceberg towing</b>	<b>37</b>
7.1	Ocean current model . . . . .	37
7.2	Towline tension observer . . . . .	37
7.3	Towing vessel model . . . . .	40
7.4	Iceberg model . . . . .	41
<b>8</b>	<b>Towing vessel observer</b>	<b>43</b>
8.1	Nonlinear passive observer (NPO) . . . . .	43
8.1.1	Dead reckoning . . . . .	44
<b>9</b>	<b>Iceberg LOS guidance and control</b>	<b>45</b>
9.1	LOS algorithm for an iceberg . . . . .	45
9.2	Ideal towing vessel position . . . . .	47
9.3	Towing vessel reference model . . . . .	48
9.3.1	Saturation . . . . .	48
9.4	Backstepping controller . . . . .	49
<b>10</b>	<b>Reliability-index for the towline</b>	<b>53</b>
10.1	Failure mode implementation . . . . .	53
10.1.1	Combined implementation . . . . .	54
<b>11</b>	<b>Reliability-based control</b>	<b>55</b>
11.1	Thrust penalty control . . . . .	55
11.2	Velocity reference penalty control . . . . .	56



<b>III</b>	<b>Simulations and experiments in the MC Lab</b>	<b>59</b>
<b>12</b>	<b>MC Lab overview</b>	<b>61</b>
12.1	MC Lab setup . . . . .	61
12.2	CS Enterprise I . . . . .	62
12.2.1	Thrust allocation . . . . .	64
12.2.2	Thruster mapping . . . . .	65
12.3	Iceberg model . . . . .	66
12.4	Towline modelling and tension measurements . . . . .	66
12.5	HIL setup . . . . .	67
12.5.1	Position measurement error . . . . .	68
<b>13</b>	<b>Simulation study</b>	<b>69</b>
13.1	Mathematical model performance . . . . .	70
13.1.1	Scenario 1 . . . . .	70
13.1.2	Scenario 2 . . . . .	71
13.1.3	Discussions, mathematical model . . . . .	72
13.2	Reliability index implementation . . . . .	72
13.2.1	Scenario 3 . . . . .	72
13.2.2	Discussions, reliability-index . . . . .	72
13.3	Failure mode implementation . . . . .	73
13.3.1	Scenario 4 . . . . .	73
13.3.2	Discussions, failure mode implementation . . . . .	75
13.4	Thrust penalty control . . . . .	75
13.4.1	Scenario 5 . . . . .	75
13.4.2	Scenario 6 . . . . .	77
13.4.3	Discussions, thrust penalty control . . . . .	78
13.5	Iceberg LOS guidance and control . . . . .	79
13.5.1	Scenario 7 . . . . .	79
13.5.2	Discussions, iceberg LOS control . . . . .	81
13.6	Combined strategy, LOS iceberg- and reliability control . . . . .	81
13.6.1	Scenario 8 . . . . .	81
13.6.2	Discussions, combined LOS- and reliability-control . . . . .	86
13.7	HIL test, with position measurement errors . . . . .	86
13.7.1	Scenario 9 . . . . .	87
13.7.2	Discussions, position measurement errors . . . . .	87
<b>14</b>	<b>Experiments</b>	<b>89</b>
14.1	Thrust penalty control . . . . .	89
14.2	Iceberg LOS guidance and control . . . . .	92
14.2.1	Updated thruster mapping . . . . .	94
14.2.2	Iceberg LOS towing with ocean current . . . . .	96

<b>Conclusion</b>	<b>99</b>
Further work . . . . .	100
<b>Conference Paper</b>	<b>109</b>
LOS guidance for towing an iceberg along a straight-line path	109
<b>Appendix</b>	<b>III</b>
A Tuning for LOS guidance and control	III

# List of acronyms and symbols

BODY-frame	A body-fixed coordinate system
CPM	Control Plant Model
CSE1	CyberShip Enterprise I
CoB	Center of Buoyancy
CoG	Center of Gravity
DOF	Degrees of Freedom
DP	Dynamic Positioning
FEM	Finite Element Method
FPSO	Floating Production, Storage and Offloading
GPS	Global Positioning System
HIL	Hardware-in-the-Loop
IAHR	International Association of Hydro-Environment Engineering and Research
LOS	Line-of-Sight
MC Lab	the Marine Cybernetics Laboratory at NTNU
NPO	Nonlinear Passive Observer
NTNU	The Norwegian University of Science and Technology
OSV	Offshore Supply Vessel
UGES	Uniformly Globally Exponentially Stable
UGS	Uniformly Globally Stable
VSP	Voith Schneider Propeller
cRIO	compact Reconfigurable Input/Output
$[x_{fp}, y_{fp}]^T$	Local placement of the towline fastening point on the towing vessel.
$[x_{tl}, y_{tl}]^T$	Global, Cartesian towline fastening point on the towing vessel.

$[x_{vp}, y_{vp}]^\top$	Local placement of the towing vessel position on the towing vessel.
$\alpha_{LOS}^{xy}$	Desired, Cartesian, current-modified LOS iceberg course.
$\alpha_1$	Stabilizing function for the backstepping controller.
$\alpha_{LOS}$	Iceberg towline angle for line-of-sight calculation.
$\beta_c$	Ocean current direction.
$\beta_{tl}$	Towline angle.
$\chi_i$	Stability criteria functions for the backstepping controller. $i = 1, 2, 3$ .
$\Delta L$	Deformation of the towline.
$\delta_x$	Reliability index for towline rupture, towline slippage and iceberg overturning. $x = \{T = rupture, slip, overturn\}$
$\delta_{near}$	Reliability index limit, higher than, but close to the lower limit.
$\delta_{x,limit}$	Reliability index minimum limit for towline rupture, towline slippage and iceberg overturning. $x = \{T = rupture, slip, overturn\}$
$\dot{p}_k^+$	Limitation to the positive change rate of the penalty $p_k$ of sample $k$ .
$\dot{p}_{max}^+$	Maximum positive change rate for $p_k$ at zero penalty ( $p_k = 1$ ).
$\dot{p}_{min}^+$	Maximum positive change rate for $p_k$ at full penalty ( $p_k = 0$ ).
$\epsilon$	Strain of the towline.
$\eta_d$	Desired towing vessel position.
$\eta_i = [x_i, y_i]^\top$	Cartesian iceberg position.
$\eta_s = [x_s, y_s, \psi_s]^\top$	Position and heading of towing vessel in Cartesian coordinates.
$\eta_{ref}$	Ideal towing vessel position for towing according to the LOS iceberg course.
$\hat{\eta}_s$	Estimated towing vessel position in Cartesian frame.
$\hat{\nu}_s$	Estimated towing vessel velocity in BODY-frame.
$\hat{b}_s$	Estimated towing vessel bias state in Cartesian frame.

$\kappa$	Scaling factor for standard deviance of measured towline tension.
$\lambda_i$	Scale of iceberg model.
$\lambda_s$	Scaling factor of model vessel.
$\nu_c = [u_c, v_c, 0]^\top$	Current velocity in BODY-frame
$\nu_i = [u_i, v_i]^\top$	Cartesian iceberg velocity.
$\nu_s = [u_s, v_s, r_s]^\top$	Velocity and angular velocity of towing vessel in BODY-frame.
$\nu_{r,i}$	Relative velocity between iceberg and ocean current.
$\nu_{r,s}$	Relative velocity between towing vessel and ocean current.
$\nu_{ref}$	Velocity reference for the towing vessel in BODY-frame.
$\bar{T}(t)$	Mean of measured towline tension.
$\sigma$	Tuning parameter for the LOS integral term.
$\sigma_T$	Standard deviance of measured towline tension.
$\sigma_{x,T}$	Standard deviance of the maximum tolerable tension for a failure mode. $x = \{b = rupture, slip, overturn\}$ .
$\tau_s = [\tau_u, \tau_v, \tau_r]^\top$	Control forces of the towing vessel.
$\tau_{pen}$	Penalized control forces for the towing vessel.
$\tilde{\eta}_s$	Towing vessel position estimation error.
$A$	Cross-sectional area of the towline.
$A_{ref}, B_{ref}, C_{ref}$	Reference model tuning matrices.
$atan2$	Computer function, calculating arctan, placing the answer in the correct quadrant, and within the set $[-\pi, \pi]$ .
$B_s$	Beam of model vessel.
$b_s$	Cartesian bias state for the towing vessel.
$D_i$	Linear damping matrix for the iceberg.
$D_s(\nu_{r,s})$	Sum of linear and nonlinear damping matrices for the towing vessel.
$E$	Young's modulus of the towline.

$e_{d,pos}$	Desired position measurement error percentage for HIL setup.
$e_{pos}$	Error signal from the position measurement system in the MC Lab.
$f_{act}$	Actuator forces.
$F_{TOW}$	The towline tension force.
$H_i$	Height of iceberg model.
$h_i$	Freeboard of iceberg model.
$K$	Linear tension constant for the towline.
$K_2, K_3, K_4$	Tuning matrices for the position estimation error of the towing vessel.
$K_c$	Gain matrix for thrust allocation.
$K_M$	Matrix converting towline tension into momentum on the towing vessel.
$K_p, K_d$	Proportional and Derivative tuning matrices for the backstepping controller.
$L$	Length of the towline.
$L_d$	Local distance between towing vessel position point, and towline fastening point.
$L_i$	Length/Diameter of cylindrical iceberg model.
$L_s$	Length of model vessel.
$L_{ext}$	Length of the extended towline.
$m_i$	Mass of iceberg model.
$m_s$	Mass of model vessel.
$M_{A,i}$	Added mass matrix of the iceberg.
$M_{A,s}$	Added mass matrix of the towing vessel.
$M_{RB,s}$	Rigid body mass matrix of the iceberg.
$M_{RB,s}$	Rigid body mass matrix of the towing vessel.
$N$	Number of sample instances for calculation of towline tension mean and standard deviation.

$p_k$	Penalty of sample $k$ .
$p_{k-1}$	Penalty of the previous sample.
$R^\top(\psi_s)$	Rotational matrix between BODY and Cartesian frame.
$r_{max}$	Maximum velocity in yaw for the towing vessel.
$T_b$	Tuning time constant matrix, for the bias estimation.
$T_c$	Thrust configuration matrix for thrust allocation.
$T_i$	Draught of iceberg model.
$T_s$	Simulation run time.
$T_{2DOF}$	Towline tension in 2 DOF.
$T_{3DOF}$	Towline tension in 3 DOF.
$T_{x,T}$	Mean of the maximum tolerable tension for a failure mode. $x = \{b = rupture, slip, overturn\}$ .
$u_{max}$	Maximum velocity in surge for the towing vessel.
$U_{ref,i,pen}$	Penalized velocity reference for the iceberg towing operation.
$U_{ref,i}$	Velocity reference for the iceberg towing operation.
$V_c^{3DOF}$	3 DOF Cartesian current velocity
$V_1, V_2$	Lyapunov functions for the backstepping controller.
$V_c = [\dot{x}_c, \dot{y}_c]^\top$	2 DOF Cartesian current velocity
$v_{max}$	Maximum velocity in sway for the towing vessel.
$waypoint(i)$	Cartesian coordinates of waypoint number $i$ .
$X_{TOW}$	X-component of the decomposed towline tension.
$y_{int} = [y_{int,x}, y_{int,y}]^\top$	Integral term for line-of-sight calculation.
$Y_{TOW}$	Y-component of the decomposed towline tension.
$z_1, z_2$	Error states for the backstepping controller.





# Chapter 1

## Introduction

According to Riska (2013, p.25), approximately 7.2% of the world oil reserves and 26.5% of the world gas reserves are present in the Arctic. The Arctic is on course for ice-free summers within a few decades, and had a record low ice extent during the summer of 2012, when the sea-ice extent dropped below 4 million square kilometers (NSIDC, 2012). This has increased the interest for petroleum resources north of the Arctic circle, where icebergs pose a serious threat to offshore structures, vessels, and operations.

The risk of iceberg impact motivates research into iceberg avoidance. All operations with the aim to avoid iceberg impact are collectively called an *iceberg management system*. When an iceberg is considered to be a threat, *iceberg handling* is required. According to Rudkin et al. (2005, p.16), single vessel towing is the typical method for physical iceberg management. Usually, this is done by laying a synthetic, floating towline around the iceberg.

Due to the small difference in density between glacial ice ( $\approx 920 \frac{kg}{m^3}$ ) and sea water ( $\approx 1025 \frac{kg}{m^3}$ ), only about 1/10 of the iceberg is above the waterline. This makes for several challenges during the towing operation. Firstly, the huge submerged volume leads to a large inertial force acting on the towline, making *towline rupture* a probable risk. Secondly, when using floating tows, the tow force acting on the iceberg in the waterline will create a momentum about the iceberg's center of gravity. Because an iceberg's submerged volume is of an unknown and often very asymmetric shape, there is a risk that even a small tow force can cause an overturning moment on the iceberg (*iceberg overturning*). Thirdly, when applying a tow force, there may be a risk of *towline slippage*, meaning that the towline slides off the iceberg. These challenges are denoted *failure modes* in iceberg towing.

### 1.1 Former work on iceberg towing

Iceberg management is already in operation in the Grand Banks area outside Newfoundland, Canada. Manual iceberg handling, where the entire operation is handled by the vessel captain and crew, has been performed for many years, and statistics covering the methodology and success rates for these operations have been presented by McClintock et al. (2007) and Rudkin et al. (2005).

Computer controlled towing of icebergs requires a mathematical model. The most notable work in this area has been performed by Aleksey Marchenko and Kenneth Johannessen Eik, most recently when Marchenko and Eik (2011) presented a scalar model of a set-up with an iceberg, a towline and a towing vessel.

This MSc thesis is a continuation on the work of Sundland (2013) on guidance and control of iceberg towing, with experimental tests conducted in the Marine Cybernetics Laboratory (MC Lab) (MC Lab, 2014) at the Norwegian University of Science and Technology (NTNU). Based on the scalar model of Marchenko and Eik (2011), Sundland developed a 3 degrees of freedom (DOF) model for iceberg towing.

## 1.2 Scope of work

The objective of towing an iceberg is to eliminate the threat it poses. The iceberg trajectory must be altered such that it no longer poses a threat to people, property, or operations.

As discussed above, using a towline and an applied tow force on the iceberg implicates the risk of towline rupture or slippage, or iceberg overturning. It is therefore important to apply a controlled amount of tow force such that the iceberg is towed safely. With that in mind, this thesis will look at automatic reliability-based control of iceberg towing in open waters.

With the goal in mind, the thesis will first focus on presenting previous work on iceberg towing, guidance control and reliability-based control. A mathematical model will be developed for iceberg towing. The mathematical model will be a basis for a Line-of-Sight (LOS) control method for towing an iceberg safely along a pre-defined path. For safe towing, reliability-based control is considered, with the end goal of combining reliability-based control with iceberg LOS control. Resulting control methods will be simulated and presented in the thesis, and experiments will be conducted in the MC Lab. Time in the MC Lab is allocated for weeks 10-11 and 17-18, 2014.

During the fall of 2013, the thesis author conducted a project report on the subject of *reliability-based control for towing of icebergs in open water* (Orsten, 2013). The report contained a list of relevant concepts within iceberg towing, and a literature review on icebergs, iceberg towing, reliability indices, and guidance and control of offshore vessels. The literature review in Part I of this thesis is based on this work, with some alterations. The report also contained some preparation for mathematical modelling of the towing operation, which is developed further in this thesis, and preliminary preparations for experiments in the MC Lab.

## 1.3 Thesis outline

As stated above, the first part of this thesis contains a literature review. The second part contains the complete setup for simulations and experiments of iceberg towing. The setup is separated into different chapters, presenting the mathematical model, a towing vessel observer, a Line-of-Sight (LOS) guidance algorithm, a backstepping controller, reliability-indices for the towline, and reliability-based control.

The third part of this thesis describes the experimental setup in the MC Lab, and contains simulation scenarios for iceberg towing, and experiments conducted with the model vessel CS Enterprise I (CSE1) and a model iceberg. The simulations are based on CSE1 and the iceberg model as well, and a Hardware-in-the-Loop (HIL) setup for towing experiments in the MC Lab is developed.

## 1.4 Publications

Previous algorithms on LOS maneuvering have succeeded in steering ships to and along pre-defined paths, even in the presence of environmental forces, such as ocean current, as is discussed in Chapter 5. In this thesis, the focus on LOS-guidance has been to extend this into steering an iceberg to, and along, a pre-defined straight-line path, using a towing vessel in the presence of constant and irrotational ocean current. A conference paper has been written on this subject, and has been accepted by the *22nd IAHR International Symposium on ICE 2014, 11-15 August, Singapore*. The publication is as follows:

- Orsten, A., Norgren, P., and Skjetne, R. (2014). LOS guidance for towing an iceberg along a straight-line path, *the 22nd IAHR International Symposium on ICE 2014, 11-15 August, Singapore*. **Accepted June 3<sup>rd</sup> 2014**.

The conference paper is included before the appendices at the end of the thesis.



# Part I

## Literature review



# Chapter 2

## Definitions

### **Failure mode**

When an item (either a part or a system) stops performing its intended function, it is called a fault. One or several faults may lead to a failure within a subsystem. A failure mode is the manifestation of some fault on the boundary of a component or system. In a stationkeeping operation, a dynamic positioning (DP) drift-off could be considered a failure mode with respect to the operation. For an iceberg towing operation, a failure mode could for instance be *towline slippage*.

### **First-year ice**

Sea water freezes to create sea ice. All sea ice that has not survived one summer's melt is called first-year ice.

### **Hawser**

A hawser is a thick and heavy cable or rope, used in mooring or towing operations. For towing operations, the hawser (usually made of steel) is used to submerge the floating towline in the fastening point, in order to create a slightly downwards, horizontal force on the iceberg. This slightly improves the system's stability with respect to *iceberg overturning* and *towline slippage*. The towing hawser also protects the vessel's stern in case of *towline rupture*.

### **Iceberg detection and monitoring**

Detection of icebergs in a relevant proximity to the protected operation, vessel or installation. The detected icebergs must be monitored continuously to evaluate the threat. Detection and monitoring is performed by visual observation, *marine radars*, aircraft radars and/or satellite (radar and images). Radars also work in bad weather and are essential for continuous monitoring.

### **Iceberg handling**

Iceberg handling, also called physical iceberg management, refers to forced change of an iceberg's drift direction in order to eliminate the threat it poses.

### **Iceberg management system**

The complete system with the aim to mitigate the risk of icebergs is called an iceberg management system. The system consists of *iceberg detection and monitoring* and evaluation of the potential threat. If the iceberg is considered a threat, physical iceberg management, or *iceberg handling*, is initiated.

**Iceberg overturning**

Iceberg overturning is when an iceberg loses stability, and either pitches or rolls to change its orientation in the water. As iceberg shapes are highly irregular, this could happen by ice calving off the iceberg, or when affected by a tow force. Overturning can endanger nearby operations, and would also end the tow attempt. If the tow rope does not loosen when the iceberg is overturning, this could cause a dangerous situation for the towing vessel.

**Iceberg targets**

When trying to detect icebergs using radar images, the radar filtering will pick out potential iceberg targets. They are not necessarily icebergs, and need to be confirmed. Thus, an iceberg target is a potential iceberg.

**Marine radar**

Radars installed on either marine vessels or marine installations.

**Multi-year ice**

When *first-year ice* does not melt during the summer season, second-, and multi-year ice is created. New layers of sea water freeze to create thicker and stronger sea ice. Since ice melting during summer expels salt from the sea-ice, multi-year ice is less porous and tougher to break than first-year ice.

**Single vessel towing**

Towing using only one towing vessel. This is mostly done using a *synthetic, floating towline*, but can also be done with a *tow-net*.

**Synthetic, floating towline**

Floating towline used for iceberg towing, encircling the iceberg in the waterline.

**Towline rupture**

If the towline tension reaches the rupture tension, the towline breaks. This would end the towing attempt, and there is also a risk that the ruptured towline snaps back at the towing vessel, endangering both the crew and the vessel.

**Towline slippage**

Icebergs are slippery. For some iceberg shapes, the towline could lose its grip and slip over the iceberg. This could be a result of applying tow force, especially when the iceberg pitches or rolls.

**Tow-net**

A tow-net could be used instead of a towline. The purpose is to apply the tow force at a certain depth and to counteract the overturning moment created by a floating towline working in the waterline.

**Towing hawser**

See *Hawser*.



# Chapter 3

## Iceberg statistics and operations

### 3.1 Introduction and motivation for towing of icebergs

Icebergs calve off glaciers and drift off with the currents, into Arctic and Antarctic regions, where they may be a threat to offshore installations, vessels, and operations. Thus, iceberg management must be considered when operating in areas where icebergs may occur.

When having detected an iceberg that must be handled, there are several different ways to do it. In the Grand Banks area outside Newfoundland, Canada, iceberg management has already been performed for many years.

#### 3.1.1 Iceberg handling

Different ways of iceberg handling that are already used in the Grand Banks (Rudkin et al., 2005) are:

- Iceberg towing using one vessel and tow rope.
- Iceberg towing using two vessels and tow rope.
- Iceberg towing using one vessel and tow net.
- Propeller-washing, using the vessel propeller to produce hydrodynamic force on the iceberg.
- Water cannon, firing water on the iceberg.
- Ramming, simply pushing the iceberg off track.

The last three alternatives are only applicable for smaller icebergs. According to Rudkin et al. (2005, p.16), single vessel towing is by far the preferred method of iceberg handling.

### 3.2 Areas of iceberg management

This report will only look at actual and potential iceberg management in the Grand Banks area and in the Barents Sea. In the Grand Banks area, iceberg management has already been going on for many years, due to there being offshore installations in the area since 1997 (McClintock et al., 2007, p.1). In the Barents Sea, this has not yet been necessary. However, some research has been made on towing icebergs in the Barents Sea (Marchenko and Ulrich, 2008).

### 3.2.1 Iceberg management in the Grand Banks area

Since 1997 there has been need for iceberg management in the ocean east of Newfoundland, Canada. This area is called the Grand Banks, and as of 2007 it consisted of three oil-producing fields; Hibernia, Terra Nova, and White Rose (McClintock et al., 2007, p.1). Hibernia is a gravity-based structure, whereas the other two are FPSO's (Floating Production, Storage and Offloading vessels).

A production facility alone is not enough to require iceberg management if icebergs are not a probability in the area. In the Grand Banks area, icebergs are a risk. Chunks of ice calve off the Greenland glaciers, creating icebergs in the ocean. These icebergs drift with the current, and as seen in Figure 3.1, the major ocean circulations force a large number of icebergs to follow along the Canadian coastline and into the Grand Banks. Icebergs usually spend one to three years of drifting, before arriving in the waters of Newfoundland (McClintock et al., 2007).

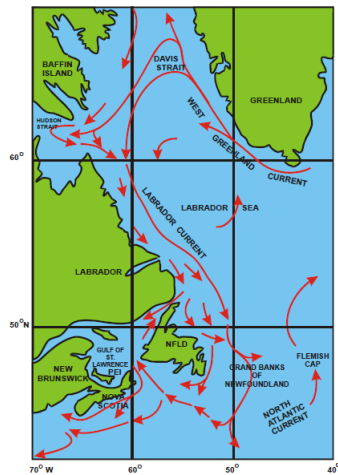


Figure 3.1: Major ocean circulation features (McClintock et al., 2007, p.5).

To avoid costly production shut-downs, not to mention personal, environmental and material damages, it is of vital importance to avoid iceberg impact. The operators were prepared for this, as attempts of iceberg management have been performed and documented since the early 1970's in East Canada. All of these data up until 2005 were presented by Rudkin et al. (2005). Table 3.1 contains key information on these iceberg management attempts:

As can be seen from Table 3.1, a total number of 1505 iceberg handling attempts were made, on 973 individual icebergs. With 86.6% of the total attempts, it is fair to conclude that single vessel tows are by far the most used management method in the Grand Banks.

### 3.2. Areas of iceberg management

Item	Value	%Total
Total number of individual management records	1505	100
Total number of individual icebergs	973	100
Types of management		
Total number of tows	1303	86.6
Total number of prop-washings	73	4.8
Total number of water cannon management	34	2.2
Total number of rammings	5	0.3
Total number two vessel tows	33	2.2
Total number of net tows	45	3.0
Total number other management techniques	8	0.5

Table 3.1: Overview of Grand Banks iceberg management statistics (Rudkin et al., 2005, p.16).

#### 3.2.2 Iceberg management in the Barents Sea



Figure 3.2: Limit for collision with icebergs with a probability of exceedance of  $10^{-2}$  (solid line) and  $10^{-4}$  (dotted line) (Standards Norway, 2007).

To decide where and when iceberg management is necessary in the Barents Sea, one must know where icebergs may occur. Where Greenland is the great producer of icebergs for the Grand Banks, the icebergs in the Barents Sea come from the glaciers of Svalbard, Novaya Zemlya, and Franz Josef Land. According to Petroleum Safety Authority Norway (2012), approximately 100 icebergs are afloat at any given time in the northern Barents Sea, between Svalbard and Bear Island.

These icebergs very rarely drift south to the Norwegian coast. Only twice, in 1881 and 1929, have there been documented sightings off the Norwegian coast (Petroleum

Safety Authority Norway, 2012). Standards Norway (2007) has established a rough estimation of 100-year and 1000-year probabilities of collision between icebergs and installations, depicted in Figure 3.2. As seen on Figure 3.2, the southern limit with a probability of  $10^{-2}$  and  $10^{-4}$  are on approximately 73 and 71.5 degrees north, respectively. Drawing these lines on a map showing Norwegian petroleum operations (Figure 3.3), it can be seen that iceberg management may be necessary in certain areas, depending on the acceptable risk for the operation.

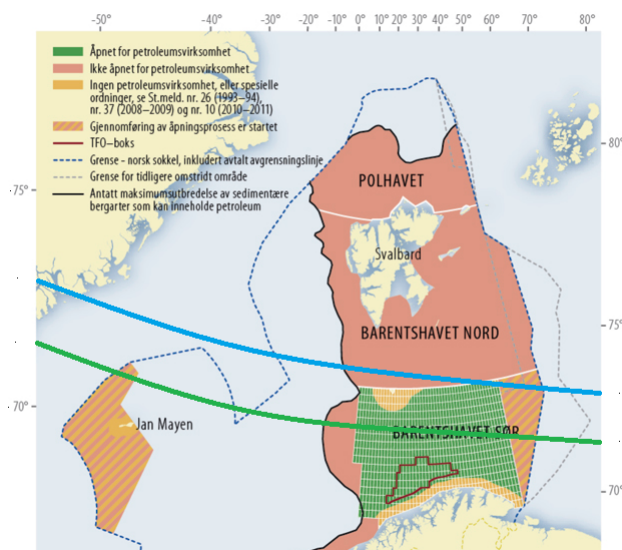


Figure 3.3: Iceberg limits drawn on a map showing Norwegian petroleum operations. 100-year (blue line) and 1000-year (green line) limits (Norwegian Ministry of Petroleum and Energy, 2011).

### 3.3 Detection of icebergs

When a vessel or an installation is placed in an area where icebergs may occur, it is vital that there is some system in place to detect incoming icebergs.

#### 3.3.1 Iceberg classification

Icebergs are typically classified according to size and shape. Every iceberg is different from the other, and the variations are large. They are oddly shaped, and the visible volume is generally much smaller than the submerged volume. In addition, they can vary in size from very small, to bergs the size of large islands.

### 3.3. Detection of icebergs

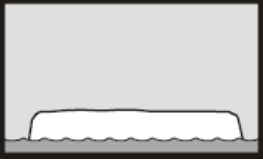

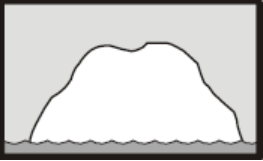
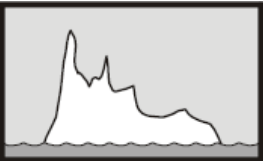
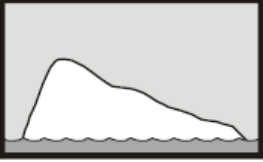
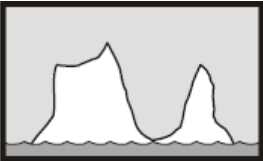
	<p><b>Tabular iceberg</b> Iceberg with a flat top, steep vertical sides and a length-to-height ratio above 5:1. They look like rectangular prisms.</p>
	<p><b>Blocky iceberg</b> Iceberg with a flat top and steep vertical sides, similar to a giant ice block. Length-to-height ratio between 3:1 and 5:1</p>
	<p><b>Dome iceberg</b> Iceberg with rounded top, resembling a dome.</p>
	<p><b>Pinnacle iceberg</b> Iceberg with one or more spires or peaks.</p>
	<p><b>Wedged iceberg</b> Iceberg with one steep vertical side, resembling a giant wedge.</p>
	<p><b>Dry-dock iceberg</b> Iceberg with an eroded center, with two or more separate sides above the water.</p>

Table 3.2: Iceberg shapes, illustrations and definitions (McClintock et al., 2007).

## Iceberg shapes

Iceberg shapes vary, but general classes have been made according to Table 3.2.

These shape classifications are based on the visible part of the iceberg. The submerged part also varies greatly with respect to shape. The result of odd shapes, is that icebergs are mostly unstable. The lack of stability makes iceberg overturning likely, thus complicating iceberg management even further. Both people and property should keep a safe distance to icebergs.

## Iceberg sizes

In addition to shape classifications, there are iceberg size and mass classifications in the following manner:

Type	Mass [T]	Height [m]	Length [m]
Growler	500	< 1	< 5
Bergy bit	1,400	1 - 5	5 - 15
Small berg	100,000	5 - 15	15 - 50
Medium berg	750,000	15 - 50	50 - 100
Large berg	5,000,000	50 - 100	100 - 200
Very large berg	> 5,000,000	> 100	> 200

Table 3.3: Iceberg sizes (McClintock et al., 2007).

### 3.3.2 Detecting icebergs

There are several ways of detecting icebergs in the ocean. The traditional way is by manual observation. This is possible from ships and installations, but has limited range and is rendered useless by fog and bad weather. Thus, other detection options must be considered, and several methods are already put into use.

McClintock et al. (2007, p.32) lists the following detection options already in use in the Grand Banks in 2007:

- Visual observation, from vessel, installation, aircraft or helicopter.
- Marine radar, installed on vessel or installation.
- Other radars, installed on aircraft.
- Satellite detection

Since visual observation is limited, detection during bad weather by radar is often the only feasible option (as it does not rely on weather). However, marine and

### 3.3. Detection of icebergs

---

satellite radars are only as good as their resolution. This means that large icebergs are more easily detected than small bergs, bergy bits, and growlers.

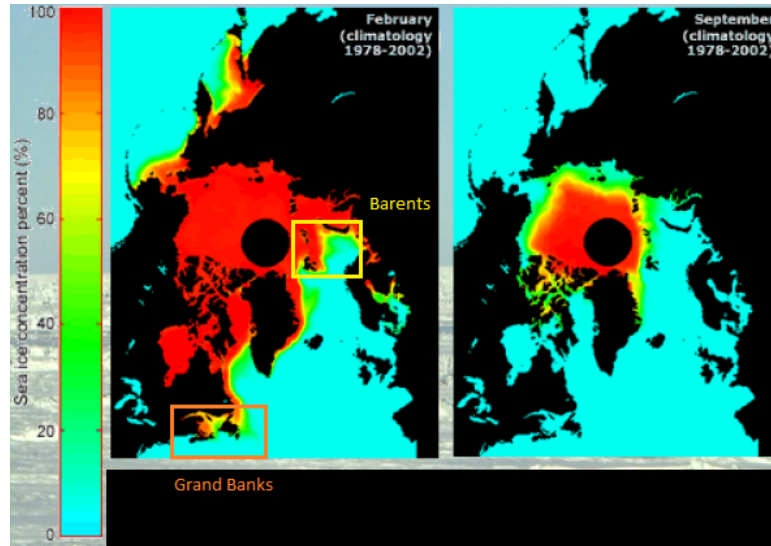


Figure 3.4: Arctic sea ice concentrations, 1978-2002 (Riska, 2013).

Another issue is detection of icebergs in sea-ice. As Figure 3.4 shows, there is somewhat more ice in the Barents than in the Grand Banks, making iceberg mitigation in sea-ice more probable and, thus, less convenient.

As for iceberg detection in sea-ice, Lane et al. (2004) concludes that detection is degraded. Their data show that detection is harder in *multi-year ice*, than in *first-year ice*. However, they also conclude that with proper use of the radar equipment, the performance degradation in sea ice is not significant, and icebergs can be properly detected.

#### 3.3.3 Threats of icebergs

It is obvious that ships have the ability to sail around floating objects, whereas stationary installations do not have that ability. Floating structures may disconnect, but it may be costly. This makes for different threats to the different vessels.

Stationary installations must either be dimensioned to handle iceberg impact, or have an iceberg management plan to reduce the design dimensions. Both larger and smaller icebergs may pose a threat to installations. Larger icebergs threaten the full structure, while small bergs, bergy bits, and even growlers may threaten risers and equipment.

Since ships can sail around icebergs, their biggest threat are icebergs they fail to detect. Larger icebergs are easier to detect, thus the bigger threat for ships are those small enough to evade detection. History is full of iceberg collision incidents, with the Titanic as the most well-known.

## Ship collisions with icebergs

Brian T. Hill. Institute for Ocean Technology (2000) has collected a database containing approximately 500 incidents of ships colliding with icebergs. The database focuses on the North Atlantic off Newfoundland and Labrador, but also includes a few incidents further north, nearby Greenland and Alaska.

The most notable incident is of course the RMS Titanic from 1912. However, what can be read from these incident reports, is that most of the incidents reporting iceberg size, report either growlers, bergy bits, or small bergs.

## 3.4 Limitations of iceberg towing

It is natural to assume that different factors may affect and reduce the probability of success when towing an iceberg. Obvious factors may be iceberg shapes, iceberg sizes, or sea state during tow operation.

Shape	Total number of records	Percentage of total	# Successful tows	Percentage
Wedge	81	5%	56	69%
Tabular	178	12%	145	81%
Non-tabular	10	0.7%	8	80%
Dome	257	17%	188	73%
Pinnacle	385	26%	278	72%
Dry-dock	368	24%	304	83%
Blocky	71	5%	57	80%
Unknown	155	10%	117	75%

Table 3.4: Grand Banks iceberg management: Shape vs. success statistics (Rudkin et al., 2005, p.45).

### 3.4.1 Iceberg shape limitations

Rudkin et al. (2005) collected data on 1505 iceberg management attempts, of which 86.6% were single vessel tows. The report with respect to iceberg shape is listed in Table 3.4.

From these results it seems that the shapes with steep sides are more easily managed, with dry-dock, blocky and tabular exceeding 80%, each with a fair amount



### 3.4. Limitations of iceberg towing

---

of attempts. Those with less steep sides, such as dome, pinnacle and wedge shaped icebergs have a towing success of around 70%.

#### 3.4.2 Iceberg size limitations

Not much difference between iceberg sizes can be found in Table 3.5 with respect to the success rate. However, it can be seen that most tows have been on small, medium or large bergs, probably based on necessity. Bergy bits and growlers may not be necessary to tow, and the very large bergs are perhaps rarer and/or somewhat unmanageable. For larger icebergs the objective of towing is mainly to deflect the iceberg heading a few degrees in order to mitigate the threat it poses (McClintock et al., 2007).

Size	Total number of records	Percentage of total	# Successful tows	Percentage
Very large	5	0.3%	4	80%
Large	309	21%	236	76%
Medium	460	31%	359	78%
Small	497	33%	361	73%
Bergy bit	110	7%	86	78%
Growler	41	3%	31	76%
Unknown	83	5%	67	81%

Table 3.5: Grand Banks iceberg management: Size vs. success statistics (Rudkin et al., 2005, p.46).

Height range (m)	# Records	# Successful tows	Percentage
0.1-1.0	347	266	77%
1.1-2.0	490	380	78%
2.1-3.0	275	189	69%
3.1-4.0	72	60	83%
4.1-5.0	26	22	85%
5.1-6.0	5	3	60%

Table 3.6: Grand Banks iceberg management: Sea state vs. success statistics (Rudkin et al., 2005, p.46).

### 3.4.3 Sea state limitations

Rudkin et al. (2005) also made a table showing success versus sea state, as shown in Table 3.6. These results show no sign of a significant drop before 5 meter significant wave height. Surprisingly, there is an increase of success between 3 and 5 meters. Whether there is some actual reason for this, or if it is just a statistical coincidence as a result of fewer records, is inconclusive.

### 3.4.4 Towing limitations during the Fylla exploration drilling program

McClintock et al. (2002) reviews Iceberg Management for the Fylla exploration drilling program, for operator Statoil, in West Greenland. The dynamically positioned drill-ship West Navion was used, and 228 *iceberg targets* were tracked during the ten-week period. A total of 168 icebergs were confirmed, and 64 were deflected, with a tow operation success rate of 91%.

A tow operation could consist of several tow attempts. Whereas several large to very large icebergs were towed with success, 22% of all tow attempts were ended due to towline slippage. Towline slippage was mostly attributed to smooth-surfaced, small to medium sized icebergs.

There were in total 7 unsuccessful tow operations. The reasons for these were:

- A sharp pinnacled berg where the towline slipped. Deemed untowable in mild wind and sea conditions.
- Three small to medium-sized icebergs were unsuccessful due to towline slippage.
- A 2.5 million tonnes large iceberg approached in a 4-5 meter significant wave height sea state. The operation was deemed unsafe due to the size and sea state. This was the only time West Navion disconnected during the period.
- A medium-sized dry-dock iceberg was towed twice successfully, but returned due to switches in drift direction. The third operation failed due to towline slippage and then iceberg overturning. It was eventually prop-washed away from the cite.
- A small dry-dock iceberg tow operation failed due to towline slippage. The berg later broke into two bergy bits.

# Chapter 4

## Single vessel iceberg towing operation

As discussed in Section 3.1.1, the most used method for iceberg handling is *single vessel towing*. This is typically performed using a synthetic, floating towline. The towline is laid encircling the iceberg, in order for a towing vessel to be able to tow it, as seen in Figure 4.1. The towline is normally fastened in a steel *towing hawser*. The hawser is heavy and submerges the towline in the fastening point. This is to achieve a more horizontal, slightly downwards directed force on the iceberg to counteract iceberg overturning and towline slippage. It also works to protect the towing vessel's stern in case of *towline rupture* (McClintock et al., 2007; Marchenko and Eik, 2011).

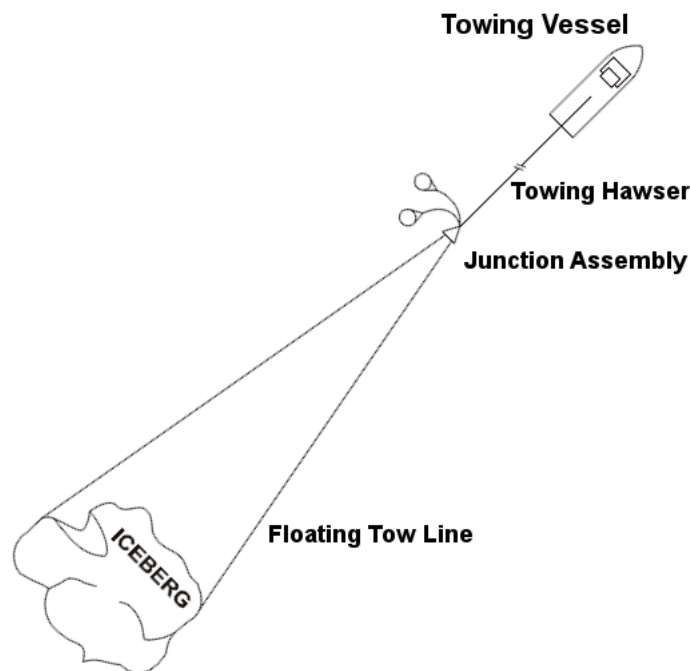


Figure 4.1: Towing vessel with steel hawser, towline, and iceberg (McClintock et al., 2007).

## 4.1 Current tow operations

Tow operations these days are performed manually, using a practical approach. McClintock et al. (2002) describes a lot of tow operations, all performed manually by the vessel crews. The towing vessel is usually an offshore supply vessel (OSV), with a bollard pull between 70-140 tonnes, a towing winch, a steel towing hawser of 100-400 meters and a towline of 1200 meters. The common towline is made of braided polypropylene (McClintock et al., 2007).

Another way of performing a single vessel tow is to use a *tow net*. As discussed in Section 3.4.4, floating towlines are least effective on small to medium-sized icebergs, where towline slippage is the main issue. The tow-net is intended to prevent slippage, and also to provide a tow force placed further down on the iceberg, reducing the risk of iceberg overturning. Sea trials found the net useful. However, some issues also arose with the net, such as net entanglement, and that it is harder to release the iceberg with a net than with the floating towline (McClintock et al., 2007).

Sensor equipment in tow operations today are mostly used for iceberg detection and monitoring, in addition to the normal sensors on the vessels included in the operation. In the reports from McClintock et al. (2002), McClintock et al. (2007) and Rudkin et al. (2005), no tow operation specific sensors were found, such as towline tension measurements, GPS tracking of the iceberg or measurements of the submerged volume of the iceberg. Iceberg detection is discussed in Section 3.3.2. Information on the towed icebergs are generally found from satellite radar and images, marine radars, and regular observations. When towing, especially in high sea states, wind sensors are used to decide towline deployment strategy (McClintock et al., 2007, p.26).

## 4.2 Mathematical model

Within mathematical modelling of the iceberg towing scenario, the most notable work has been done by Aleksey Marchenko, most recently in Marchenko and Eik (2011), an article presenting a scalar model on iceberg, towline and towing vessel.

Sundland (2013) wrote his MSc thesis on guidance and control of iceberg towing, with experimental tests conducted in the Marine Cybernetics Laboratory (MC Lab) at the Norwegian University of Science and Technology (NTNU). He proposed an extended model based on that of Marchenko and Eik (2011).

### 4.2.1 Towing method

Marchenko and Eik (2011) considers two methods of towing icebergs. Both methods loop a towline around the iceberg in the waterline and tows it using a single vessel. The two methods are depicted in Figure 4.2. In method (a) the towline ends are

fastened in the stern of the vessel, either flowing or hanging above the water surface. In method (b), however, the towline is fastened in a steel hawser shown in the figure by the thick line  $W$ . In both figures the towline floats until points  $O_1, O_2$ , and then either (a) hangs, or (b) is submerged. The practical reason for the steel hawser in method (b) is discussed above.

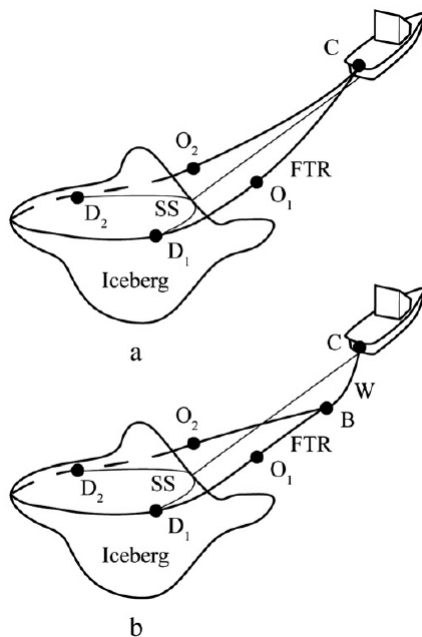


Figure 4.2: Schematics of towing icebergs (a) with and (b) without a steel hawser (Marchenko and Eik, 2011).

### 4.2.2 Model by Marchenko and Eik

Marchenko and Eik (2011) proposes a system balancing the momentum between the vessel and iceberg, which are connected by a towline. It assumes that the tow tension  $T$  is the same for the vessel and the iceberg, neglecting hydrodynamic forces on the towline. This model can be expressed as:

$$M_s \frac{dv_s}{dt} + M_{add,s} \frac{d(v_s - u)}{dt} = -D_s - T + \tau_s \quad (4.2.1)$$

$$M_i \frac{dv_i}{dt} + M_{add,i} \frac{d(v_i - u)}{dt} = -D_i + T \quad (4.2.2)$$

Here,  $M_s$  and  $M_i$  are due to hydrodynamic forces of the vessel and the iceberg respectively, whereas the  $M_{add}$  values are added mass.  $v_s$ ,  $v_i$ , and  $u$  are the vessel velocity, iceberg velocity, and current velocity in the towing direction, respectively.

$\tau_s$  denotes the vessel's propulsion force. In addition, the resistances  $D_s$  and  $D_i$ , of the vessel and iceberg respectively, are:

$$D_s = \rho_w C_{w,s} S_s |v_s - u| (v_s - u) \quad (4.2.3)$$

$$D_i = \rho_w C_{w,i} S_i |v_i - u| (v_i - u) \quad (4.2.4)$$

Here,  $S_{s/i}$  is the wet surface area of vessel and iceberg,  $\rho_w$  is the density of water, and the drag coefficients  $C_{w,s}$  and  $C_{w,i}$  of vessel and iceberg are estimated as:

- $C_{w,s} = 0.003$  (Voitkunsky, 1988)
- $C_{w,i} \in (0.5, 1)$  (Robe, 1980)

### 4.2.3 Model by Sundland

As the model by Marchenko and Eik (2011) only includes surge motion, an extension of the model is proposed by Sundland (2013).

Ship dynamics include 6 degrees of freedom (DOF):

1. Surge
2. Sway
3. Heave
4. Roll
5. Pitch
6. Yaw

For a ship maneuvering problem, it is normal to reduce the system to 3 DOF: Surge, sway, and yaw, since it is generally not possible to control the remaining DOFs. To control the heading of a ship, the yaw angle must be changed - as a ship is built to achieve the highest performance in pure surge motion.

Sundland (2013) then proposes the following model, incorporating the work of Marchenko and Eik (2011) into Fossen notation (Fossen, 2011):

#### Vessel model by Sundland

$$\dot{\eta}_s = R(\psi_s) \nu_s \quad (4.2.5)$$

$$\dot{b}_s = -T_{b,s}^{-1} b_s + w \quad (4.2.6)$$

$$M_s \dot{\nu}_s + D_s(\nu_s) \nu_s = \tau_s - R^T(\psi_s) T + R(\psi_s)^T b_s \quad (4.2.7)$$

## Iceberg model by Sundland

$$\dot{\eta}_i = R(\psi_i)\nu_i \quad (4.2.8)$$

$$\dot{b}_i = -T_{b,i}^{-1}b_i + w \quad (4.2.9)$$

$$M_i\dot{\nu}_i + D_i(\nu_i)\nu_i = R^T(\psi_i)T + R(\psi_i)^T b_i \quad (4.2.10)$$

Sundland's model is a 3 DOF model for both the vessel and the iceberg. These models take into account slowly-varying environmental forces via the  $b$  vector. The Fossen notation introduces mass and damping matrices. The matrices in the equations above can be expressed as:

$$M_x = M_{rigidbody} + M_{addedmass} \quad (4.2.11)$$

$$M_x = \begin{bmatrix} m & 0 & 0 \\ 0 & m & 0 \\ 0 & 0 & I_z \end{bmatrix} + \begin{bmatrix} -X_{\dot{u}} & 0 & 0 \\ 0 & -Y_{\dot{v}} & -Y_{\dot{r}} \\ 0 & -Y_{\dot{r}} & -N_{\dot{r}} \end{bmatrix} \quad (4.2.12)$$

$$D(\nu) = D_n(\nu) + D \quad (4.2.13)$$

$$D(\nu) = \begin{bmatrix} -X_{|u|u}|u| & 0 & 0 \\ 0 & -Y_{|v|v}|v| & Y_{|r|r}|r| \\ 0 & N_{|v|v}|v| & N_{|r|r}|r| \end{bmatrix} \quad (4.2.14)$$

$$+ \begin{bmatrix} -X_u & 0 & 0 \\ 0 & -Y_v & -Y_r \\ 0 & -N_v & -N_r \end{bmatrix}$$

The diagonal part in the first matrix of (4.2.14) is recognized as the resistance part from Marchenko's model.

The notation used in equations 4.2.12 - 4.2.14 is the SNAME notation (Fossen, 2011, p.16). Here,  $X_{\dot{u}}$  is the added mass in surge due to an acceleration in surge. It is always negative, as it counteracts the surge motion.  $Y_{\dot{v}}$  and  $N_{\dot{r}}$  are similar, only in sway and yaw respectively. The remaining  $Y_{\dot{r}}$  terms are added mass in sway due to acceleration in yaw.





# Chapter 5

## LOS-based guidance of ships

The guidance and control systems of offshore vessels are large systems, containing more than just the control and guidance algorithms. The complete system consists of numerous sensors, power generation, power management, and thrusters, to name a few of the main components. There are several ways to design the guidance system, and different control system objectives require different solutions. One such way is Line-of-Sight (LOS) guidance, where the objective is to make the vessel's position converge to and along a pre-defined path.

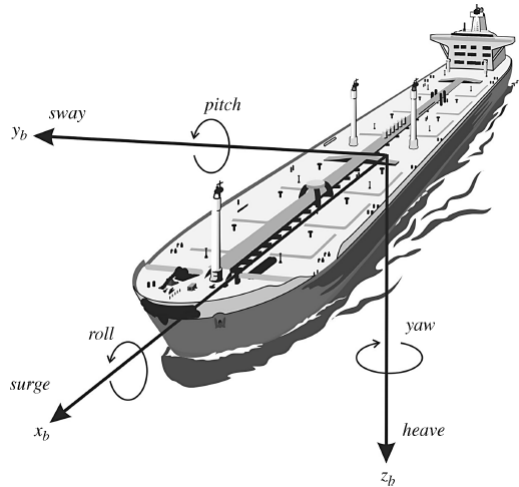


Figure 5.1: Motion of a vessel in 6 DOF (Fossen, 2011).

### 5.1 Modelling of offshore vessels

As discussed in Section 4.2.3, a 3 DOF model is usually used for the purpose of ship maneuvering. The following is a 3 DOF model for a surface vessel (Fossen, 2011):

$$J(\eta) \stackrel{3 \text{ DOF}}{=} R(\psi) = \begin{bmatrix} \cos(\psi) & -\sin(\psi) & 0 \\ \sin(\psi) & \cos(\psi) & 0 \\ 0 & 0 & 1 \end{bmatrix} \quad (5.1.1)$$

$$\eta = [x, y, \psi]^T \quad (5.1.2)$$

$$\nu = [u, v, r]^T \quad (5.1.3)$$

$$\dot{\eta} = R(\psi)\nu \quad (5.1.4)$$

$$M\dot{\nu} + C(\nu)\nu + D(\nu)\nu = \tau \quad (5.1.5)$$

For the purpose of adding constant ocean current into the equation, Børhaug et al. (2008) proposes:

$$\nu_r = \nu - \nu_c \quad (5.1.6)$$

$$M_{RB}\dot{\nu} + M_A\dot{\nu}_r + C_{RB}(\nu)\nu + C_A(\nu_r)\nu_r + D\nu_r = Bf \quad (5.1.7)$$

Comparing (5.1.7) and (5.1.5), it can be seen that  $\tau = Bf$ . Also, (5.1.7) assumes lower speeds for the vessel, making the nonlinear term  $D(\nu) = [D + D_n(\nu)] \approx D$ . For lower speeds, one can also assume that the Coriolis term  $C(\nu) = 0$ . The mass matrices  $M_{RB}$  and  $M_A$  are found as in (4.2.12).

## 5.2 LOS guidance

There are several ways to perform LOS guidance for ships. Fossen et al. (2003) and Børhaug et al. (2008) present LOS path-following using waypoints to define straight-line segments, whereas Breivik (2010) and Skjetne et al. (2011) present LOS path-following along regularly parametrized curves. According to McClintock et al. (2002) icebergs are difficult to control when the tow path is curved, thus this thesis will focus on straight-line LOS guidance.

### 5.2.1 Traditional LOS guidance

LOS guidance is a method to perform path following. It has been used to solve the geometric task of the maneuvering problem (Skjetne et al., 2011). Fossen et al. (2003) and Børhaug et al. (2008) have both presented the traditional LOS angle, but in two different ways.

Børhaug et al. (2008) describes the LOS angle in a path-fixed coordinate system (Figure 5.2) using the equation:

$$\psi_{LOS} \triangleq -\tan^{-1}\left(\frac{y}{\Delta}\right) \quad (5.2.1)$$

Fossen et al. (2003), on the other hand, describes the LOS angle in a Cartesian coordinate system (Figure 5.3), where the goal is to make the vessel yaw angle  $\psi$  converge to the LOS angle:

$$\psi_{LOS} = \text{atan2}(y_{LOS} - y, x_{LOS} - x), \quad (5.2.2)$$

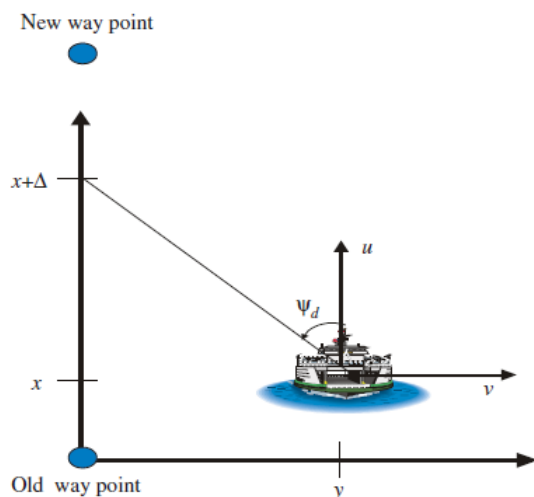


Figure 5.2: An interpretation of  $\psi_d$  and  $\Delta$ , in a path-fixed coordinate system (Fredrikson and Pettersen, 2006).

where  $x_{LOS}$  and  $y_{LOS}$  are the Cartesian coordinates of the intersection point  $p_{LOS}$  between the straight-line path and a circle around the vessel, as shown in Figure 5.3.

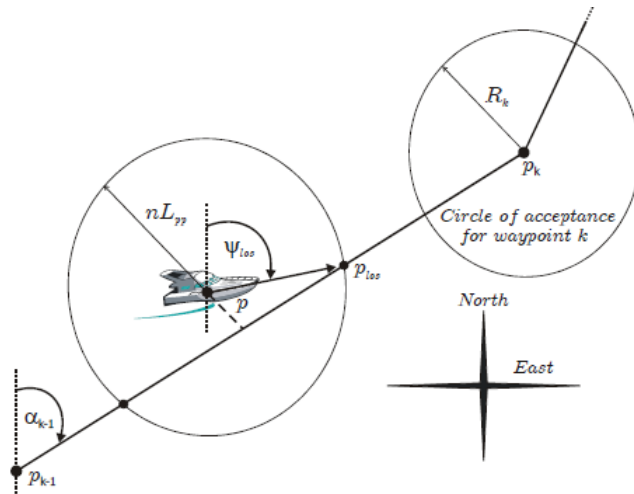


Figure 5.3: An interpretation of the desired path in a Cartesian coordinate system (Fossen et al., 2003).

For further LOS guidance, the Cartesian coordinate representation of Fossen et al. (2003) will be in focus.

The desired path of the vessel is a collection of waypoints in a table. The LOS position is located somewhere on the straight line connecting the previous ( $p_{k-1}$ ) and

the current waypoint ( $p_k$ ), where  $p_k = [x_k, y_k]^T$ . Let the vessel's current position  $p$  be the center of a circle with a radius of  $n$  vessel lengths ( $L_{pp}$ ). This circle will intersect the straight line at two points where  $p_{LOS}$  is selected as the point closest to the next waypoint. To calculate  $p_{LOS}$ , the following two equations must be solved online:

$$(y_{LOS} - y(t))^2 + (x_{LOS} - x(t))^2 = (nL_{pp})^2 \quad (5.2.3)$$

$$\frac{y_{LOS} - y_{k-1}}{x_{LOS} - x_{k-1}} = \frac{y_k - y_{k-1}}{x_k - x_{k-1}} = \tan(\alpha_{k-1}) \quad (5.2.4)$$

Equation (5.2.3) is the *Pythagoras* theorem, whereas (5.2.4) ensures that the slope of the path is constant between the two waypoints.

In order for the waypoint guidance to work, there must be a way to switch to the next waypoint in the waypoint table. This is naturally done when the vessel position is close enough to the current waypoint to accept a switch to the next waypoint. Hence, when the vessel position  $p$  satisfies the inequality

$$(x_k - x(t))^2 + (y_k - y(t))^2 \leq R_k^2, \quad (5.2.5)$$

the next waypoint is selected.  $R_k$  is the radius of the *circle of acceptance* for the current waypoint. It is required that  $(nL_i) \geq R_k$ , meaning that the circle enclosing the vessel is large enough to ensure that solutions to (5.2.5) exist.

### Implementation of the traditional LOS equations

To get the LOS path, (5.2.3) and (5.2.4) must be solved. Breivik (2003, pp.33-35) introduces the notation:

$$\Delta x = x_k - x_{k-1} \quad (5.2.6)$$

$$\Delta y = y_k - y_{k-1} \quad (5.2.7)$$

$$d = \left( \frac{\Delta y}{\Delta x} \right) \quad (5.2.8)$$

$$e = x_{k-1} \quad (5.2.9)$$

$$f = y_{k-1} \quad (5.2.10)$$

$$g = f - de \quad (5.2.11)$$

There are two cases when solving the equations, when  $|\Delta x| > 0$  and when  $\Delta x = 0$ .

**When**  $|\Delta x| > 0$ , the following quadratic equation is obtained:

$$(1 + d^2)x_{LOS}^2 + 2(dg - dy - x)x_{LOS} + (x^2 + y^2 + g^2 - (nL_i)^2 - 2gy) = 0 \quad (5.2.12)$$

This quadratic equation is solved:

$$a = 1 + d^2 \quad (5.2.13)$$

$$b = 2(dg - dy - x) \quad (5.2.14)$$

$$c = x^2 + y^2 + g^2 - (nL_i)^2 - 2gy \quad (5.2.15)$$

$$x_{LOS} = \frac{-b \pm \sqrt{b^2 - 4ac}}{2a} \quad (5.2.16)$$

To decide whether to add or subtract in the quadratic solution, the following criteria is used:

- When  $\Delta x > 0$ , add.
- When  $\Delta x < 0$ , subtract.

Having solved  $x_{LOS}$ , then  $y_{LOS}$  is easily obtained by (5.2.3).

**When**  $\Delta x = 0$ ,  $y_{LOS}$  is obtained from (5.2.3),

$$y_{LOS} = y \pm nL_i. \quad (5.2.17)$$

Again, to decide whether to add or subtract in the quadratic solution, the following criteria is used:

- When  $\Delta y > 0$ , add.
- When  $\Delta y < 0$ , subtract.

In this special case,  $x_{LOS}$  is obtained from  $x_{LOS} = x_{k-1} = x_k$ .

### 5.2.2 LOS method with constant ocean current

The traditional LOS method does not take into account ocean currents. Børhaug et al. (2008) builds on the path-fixed coordinate system (Figure 5.2), and suggests the following guidance law, using integral action, to achieve the current-modified LOS angle:

$$\psi^m_{LOS} \triangleq -\tan^{-1}\left(\frac{y' + \sigma y'_{int}}{\Delta}\right), \Delta > 0 \quad (5.2.18)$$

$$\dot{y}'_{int} = \frac{\Delta * y'}{(y' + \sigma y'_{int})^2 + \Delta^2} \quad (5.2.19)$$

These equations are explained in Figure 5.4, where  $y' = y$ , and  $\sigma$  is the integral gain - a design parameter.

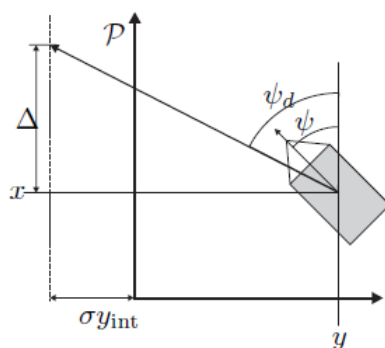


Figure 5.4: Illustration of modified LOS guidance, using Path-fixed coordinates (Børhaug et al., 2008).

# Chapter 6

## Reliability-based control

### 6.1 Reliability-based control of risers

Leira et al. (2004) presents a reliability-based control algorithm for dynamic positioning of floating vessels. An important design issue with floating production vessels is to protect the riser system. The risers are the vertical pipelines between the surface vessels and the sea floor. A typical floating production vessel has several risers and mooring cables. It is important that these vertical structures do not damage each other in any way. In addition, it is important that the vessel is well positioned to avoid huge stresses on the risers. Thus, a way to implement risers into the control algorithm is suggested.

A typical way to control the riser attitude is to control the riser angles. This is possible by using a Finite Element Method (FEM) model to estimate and apply top tensions to the risers (Rustad, 2007). The measured values of the risers are typically the riser angles.

When applying the measured riser angles, one should not include the instantaneous values. This is due to their rapid changes. A smoothed curve is a better alternative, and could be estimated by the mean of the measured values over a recent time interval. This would, however, remove the system's sensibility towards maximum responses. To also take into account the extreme values, the variance of the measured values over the same time interval is proposed (Leira et al., 2004, p.10).

A representation containing the mean value and variance is provided by the *Reliability Index*. Leira et al. (2004) states that, for a stochastic process, reliability is generally formulated by extreme values. With a known distribution function for extreme values  $F_{Reextr}(r_{extr})$ , and a given permissible response threshold value  $r_{\text{threshold}}$ , the reliability-index can be written as:

$$\beta = -\Phi^{-1}(p_f) = -\Phi^{-1}(1 - F_{Reextr}(r_{\text{threshold}})) \quad (6.1.1)$$

Where  $\Phi$  is the normal cumulative distribution function, and  $p_f$  is the probability of failure. Computation of the reliability index as defined in (6.1.1) introduces certain complexities (Leira et al., 2004, p.11):

1. Offshore structures generally have non-stationary response, due to time-varying environmental conditions. Because of this, it is convenient to use smaller time durations in which the response is considered stationary.

2. It is difficult to estimate the parameters of the extreme-value distribution ( $F_{Reextr}$ ).
3. To solve the equation online, the software used must be able to calculate the inverse normal cumulative distribution function.

As a consequence of a these complexities, Leira et al. (2004) introduces the simplified reliability index:

$$\beta = \frac{r_{\text{threshold}} - E[r]}{\sigma_r} \quad (6.1.2)$$

Here,  $r_{\text{threshold}}$  is a set response threshold and  $E[r]$  is the mean and  $\sigma_r$  the variance of the response.

## 6.2 Reliability-based control of mooring lines

More in line with the focus on towlines in this report, Berntsen (2008) proposes a reliability index for mooring lines with respect to their breaking strength.

The maximum load a structure is able to withstand is defined as  $R$ . The loads acting on the structure are defined as  $S$ . Assuming these are independent Gaussian random variables with mean values  $\mu_R$  and  $\mu_S$  and variances  $\sigma_R^2$  and  $\sigma_S^2$ , and defining  $Z = R - S < 0$  as the breaking condition, the following relationships are obtained:

$$\mu_Z = \mu_R - \mu_S \quad (6.2.1)$$

$$\sigma_Z^2 = \sigma_R^2 + \sigma_S^2 \quad (6.2.2)$$

The probability of failure for the system is then:

$$p_f = P(R - S \leq 0) = P(Z \leq 0) = \Phi\left(\frac{0 - \mu_Z}{\sigma_Z}\right) \quad (6.2.3)$$

Inserting equations (6.2.1) and (6.2.2) into (6.2.3) gives the safety index  $\beta$ :

$$p_f = \Phi\left(\frac{-(\mu_R - \mu_S)}{\sqrt{\sigma_R^2 + \sigma_S^2}}\right) = \Phi(-\beta) \quad (6.2.4)$$

$$\beta = \frac{\mu_Z}{\sigma_Z} = \frac{\mu_R - \mu_S}{\sqrt{\sigma_R^2 + \sigma_S^2}} \quad (6.2.5)$$

In Berntsen (2008), the main concern is the integrity of a mooring system. Using the measured tension values for mooring line  $k$ , which are filtered through a low-pass filter, the following relationship is established:



$$T_k(t) \leq T_{k,lf}(t) + \kappa\sigma_k, \quad (6.2.6)$$

where  $T_k(t)$  is a time-varying tension signal.  $T_{k,lf}(t)$  is the filtered low-frequency signal.  $\sigma_k$  is the standard deviation of  $T_k$  amplified by a scaling factor  $\kappa$ . When using filtered results, the extreme values due to 1. order variations may be lost. The term  $\kappa\sigma_k$  will compensate for the missing 1. order variations in the filtered measurements.

The standard deviation (6.2.7) is found by using the mean value of  $T_k$  (6.2.8):

$$\sigma_k = \sqrt{\frac{1}{N} \sum_{i=1}^N (T_{k,i} - \bar{T}_k)^2} \quad (6.2.7)$$

$$\bar{T}_k = \frac{1}{N} \sum_{i=1}^N T_{k,i} \quad (6.2.8)$$

Finally, Berntsen (2008) proposes a reliability index  $\delta$ , as a reformulation of  $\beta$ :

$$\delta_k(t) = \frac{T_{b,k} - (T_{k,lf}(t) + \kappa\sigma_k)}{\sigma_{b,k}}, \quad (6.2.9)$$

where  $T_{b,k}$  is the mean, and  $\sigma_{b,k}$  the standard deviation of the breaking strength for mooring line  $k$ .

## 6.3 Application of reliability index in control

Leira et al. (2004) introduces three different ways of how reliability indices can enter the control loop:

### Reliability-index monitoring

Monitoring the reliability index, actions can be made based on whether the index goes below a set limit.

### Reliability-index weighting

Similar to monitoring, actions are assigned to whether certain indices go below set limits. Based on how much the indices satisfy given criteria for different actions, weighted combinations of these actions are performed.

### Control actions based directly on reliability indices

Control laws are designed with the reliability index in them. For instance, a

control objective for controller design could be that the reliability index ( $\delta_i$ ) never goes below the threshold index ( $\delta_{i,t}$ ):

$$\delta_i \geq \delta_{i,t} \tag{6.3.1}$$

## Part II

### Simulation setup for iceberg towing



# Chapter 7

## Mathematical model for iceberg towing

In order to simulate a feasible towing scenario, a mathematical model must be developed. Through this chapter, a model containing a 3 DOF towing vessel model in the BODY-frame, and a 2 DOF iceberg model in Cartesian coordinates, will be presented. The model incorporates forces from a towline, and a constant, irrotational ocean current. The towline is modelled by a linear tension observer.

### 7.1 Ocean current model

Both the towing vessel and the iceberg are affected by ocean current. To implement this into the mathematical model, an ocean current velocity is introduced. The ocean current is assumed constant and irrotational in the inertial frame. To account for this in the BODY-frame, a transformation is required (Børhaug et al., 2008):

$$V_c^{3DOF} = \begin{bmatrix} V_c \\ 0 \end{bmatrix}, V_c = \begin{bmatrix} \dot{x}_c \\ \dot{y}_c \end{bmatrix} \quad (7.1.1)$$

$$\nu_c = R^\top(\psi_s) V_c^{3DOF} = \begin{bmatrix} u_c \\ v_c \\ 0 \end{bmatrix} \quad (7.1.2)$$

$$\dot{\nu}_c = \frac{d}{dt}(R^\top(\psi_s) V_c^{3DOF}) = \begin{bmatrix} r_s v_c \\ -r_s u_c \\ 0 \end{bmatrix}, \quad (7.1.3)$$

where  $r_s$  is the rotational velocity of the towing vessel in BODY-frame,  $V_c$  the Cartesian current velocity, and  $\nu_c$  the current velocity in BODY-frame, respectively.

### 7.2 Towline tension observer

As both the towing vessel and the iceberg are affected by the towline, a combined towline estimate must be developed to be implemented into the mathematical model.

This has been done by creating a tension observer. In order to calculate the tension of a towline, certain assumptions are necessary (Sørensen, 2012):

**Assumption 1.**

1. *When working with cables there is no bending stiffness and no torsional stiffness.*
2. *Axial tension in the cable is small enough to allow operation within the linear range of the stress/strain relationship.*
3. *The towline is assumed isotropic, meaning its' material properties are independent of direction.*
4. *The cross-sectional area of the towline will not change significantly due to axial deformation.*

When in accordance with Assumption 1, the following physical relationships are valid for the tension in a towline:

$$F_{TOW} = \sigma A \quad (7.2.1)$$

$$\sigma = E\epsilon \quad (7.2.2)$$

$$\epsilon = \frac{\Delta L}{L} \quad (7.2.3)$$

$$F_{TOW} = \frac{EA}{L}\Delta L, \Delta L \geq 0, \quad (7.2.4)$$

where  $F_{TOW}$  is the tension force,  $\sigma$  the stress,  $A$  the cross-sectional area,  $E$  the Young's modulus,  $\epsilon$  the strain,  $L$  the initial length, and  $\Delta L$  the deformation of the towline, respectively. The condition on  $\Delta L$  in (7.2.4) is added because the towline only resists stretching force, not pushing force.

For simulation purposes, the deformation  $\Delta L$  must be found. One way to find this, is using the difference in position between towing vessel and iceberg, and comparing it to the zero-tension length between them. For practical purposes, the position measurement noise may be too large for this to be a decent estimate, but it could work in simulations studies.

The calculation can be done by knowing where on the vessel the position is measured, and where on the vessel the towline is fastened, and assuming the iceberg position is the same geometrically in which ever direction it is towed. See Figure 7.2 for global positions. The distance  $L_d$  between vessel position and towline fastening point can then be calculated (local positions are shown in Figure 7.1):

$$L_d = \sqrt{(x_{vp} - x_{fp})^2 + (y_{vp} - y_{fp})^2} \quad (7.2.5)$$

Furthermore, the global, Cartesian towline fastening point can be found, with explanations in Figure 7.2:

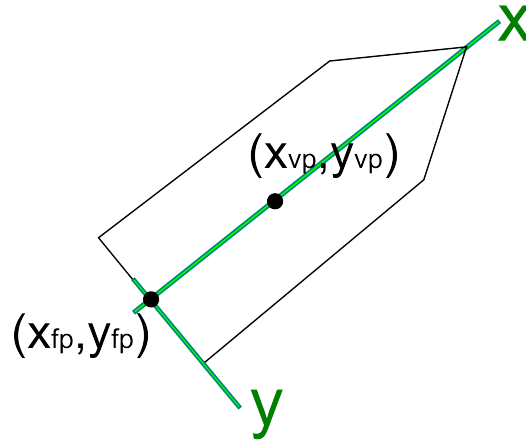


Figure 7.1: Local calculation of distance between vessel position center and towline fastening point on vessel.

$$x_{tl} = x_s - L_d \cos(\psi_s) \quad (7.2.6)$$

$$y_{tl} = y_s - L_d \sin(\psi_s) \quad (7.2.7)$$

Knowing the positions of the fastening point and the iceberg globally, the distance  $L_{ext}$  (extended length) between them can be found:

$$L_{ext} = \sqrt{(x_{tl} - x_i)^2 + (y_{tl} - y_i)^2} \quad (7.2.8)$$

Then it remains to check if the calculated distance  $L_{ext}$  exceeds the zero-tension towline length ( $L$ ). If the length is exceeded, the tension  $F_{TOW}$  is calculated to be:

$$K = \frac{EA}{L} \quad (7.2.9)$$

$$\Delta L = L_{ext} - L \quad (7.2.10)$$

$$F_{TOW} = K * \Delta L \quad (7.2.11)$$

To create the  $T$  vectors found in (7.3.7) and (7.4.4), the tension must be transformed into Cartesian coordinates. This is done by calculating the towline angle ( $\beta_{tl}$ ) and using these equations:

$$\beta_{tl} = \text{atan2}(y_{tl} - y_i, x_{tl} - x_i) \quad (7.2.12)$$

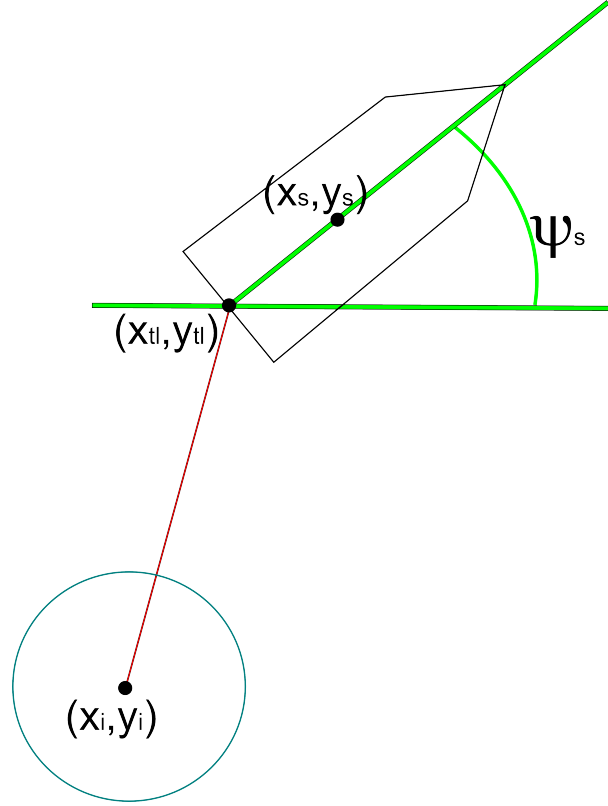


Figure 7.2: Tension trigonometry, relevant points in Cartesian coordinates to calculate the towline length and deformation using vessel and iceberg positions.

$$X_{TOW} = F_{TOW} \cos(\beta_{tl}) \quad (7.2.13)$$

$$Y_{TOW} = F_{TOW} \sin(\beta_{tl}) \quad (7.2.14)$$

### 7.3 Towing vessel model

Inspired by the model of Sundland (2013), this thesis uses the Fossen notation (Fossen, 2011) for modelling a marine craft. It is important to separate which physical effects are affected by the ocean current, and thus by the relative velocity. The rigid body dynamics are not affected, whereas the added mass phenomenon and the hydrodynamical damping are affected.

External forces acting on the system are the vessel's actuator forces  $\tau_s$ , and the towline forces  $T_{3DOF}$ . This produces the towing vessel model:

$$\eta_s = [x_s, y_s, \psi_s]^T \quad (7.3.1)$$

$$\nu_s = [u_s, v_s, r_s]^T \quad (7.3.2)$$



$$\dot{\eta}_s = R(\psi_s)\nu_s \quad (7.3.3)$$

$$M_{RB,s}\dot{\nu}_s + M_{A,s}\dot{\nu}_{r,s} + D_s(\nu_{r,s})\nu_{r,s} = \tau_s - K_M R^\top(\psi_s) T_{3DOF} \quad (7.3.4)$$

$$\nu_{r,s} = \nu_s - \nu_c \quad (7.3.5)$$

$$R(\psi_s) = \begin{bmatrix} \cos(\psi_s) & -\sin(\psi_s) & 0 \\ \sin(\psi_s) & \cos(\psi_s) & 0 \\ 0 & 0 & 1 \end{bmatrix} \quad (7.3.6)$$

$$T_{3DOF} = \begin{bmatrix} X_{TOW} \\ Y_{TOW} \\ 0 \end{bmatrix} \quad (7.3.7)$$

$$K_M = \begin{bmatrix} 1 & 0 & 0 \\ 0 & 1 & 0 \\ 0 & -L_d & 0 \end{bmatrix}, \quad (7.3.8)$$

where the matrix  $K_M$  is a matrix causing momentum on the vessel from the towline tension. In this version of  $K_M$  it is assumed that both the towline fastening point, and the vessel position are placed in the vessel's Center Line.

## 7.4 Iceberg model

The model by Sundland (2013) is developed in 3 DOF. When towing the iceberg, the towline is laid floating in the waterline, encircling the iceberg (Figure 4.2). When moving the towing vessel around the iceberg, the towline will rotate around the iceberg.

**Assumption 2.** *In order to develop an iceberg model of sufficient fidelity for a model-based guidance and control design, some simplifying assumptions are made as follows:*

1. *Iceberg shapes come in all variations, especially below water. This makes the iceberg's hydrodynamic behavior difficult to predict without advanced underwater measurement tools. For the sake of simplicity it is then fair to assume the iceberg is symmetric and cylinder-shaped.*
2. *There is practically no iceberg yaw force from rotating the towline around the iceberg, and there is no response on the towline when the iceberg rotates due to hydrodynamical or environmental forces. This is due to that the towline is floating around the iceberg, and that there is little friction between towline and iceberg.*
3. *The towline force is assumed to act directly through the center of gravity (CoG) and center of buoyancy (CoB) of the iceberg. This is fair for a stable iceberg*

with small roll/pitch motions. In reality most icebergs are unstable due to their asymmetric shapes, and roll and pitch motion would move CoG or CoB away from the towline force. However, due to assumptions 2.1 and 2.2, this is ignored.

4. According to Fossen (2011, p.174), for low-speed applications, when roll and pitch angles are assumed small, it implies that the Coriolis term and the non-linear damping term can be linearized about  $\nu = 0$ . Since  $C(0) = 0$  and  $D_{nl}(0) = 0$ , and since tow velocities are small, the Coriolis effect and non-linear damping terms are disregarded.

Thus, the simplified iceberg model is a linear, 2 DOF model:

$$\dot{\eta}_i = \begin{bmatrix} \dot{x}_i \\ \dot{y}_i \end{bmatrix} = \begin{bmatrix} u_i \\ v_i \end{bmatrix} = \nu_i \quad (7.4.1)$$

$$\nu_{r,i} = \nu_i - V_c \quad (7.4.2)$$

$$(M_{RB,i} + M_{A,i})\dot{\nu}_i + D_i\nu_{r,i} = T_{2DOF} \quad (7.4.3)$$

$$T_{2DOF} = \begin{bmatrix} X_{TOW} \\ Y_{TOW} \end{bmatrix}, \quad (7.4.4)$$

# Chapter 8

## Towing vessel observer

An observer is, within control system design, a model-based filter. Observers may have multiple purposes (Sørensen, 2012):

### **Filtering of measurement noise.**

Sensor signals are usually contaminated by noise. By filtering the measurements to get rid of the measurement noise, the measurements will become more accurate and stable.

### **Reconstruction of unmeasured data.**

Some unmeasured states can be estimated from the measured states and the mathematical model of the system, assuming some conditions on the model are fulfilled. For instance, position sensors only measure positions, whereas the system might need velocities, or even accelerations. This can be reconstructed using observers.

### **Dead reckoning.**

Should the measurement equipment fail at some time, estimated values of these measurements could replace the measured values. This could, if tuned correctly, allow the control system not to lose its function due to loss of signals, for a certain amount of time.

## 8.1 Nonlinear passive observer (NPO)

In this thesis, a nonlinear passive observer (NPO) is developed for the towing vessel, with the aim to:

1. Estimate the velocities of the towing vessel ( $\nu_s$ ), for use in the guidance and control system.
2. Filter measurement noise from the position measurements.
3. Provide estimated position data when the position signals are lost (which is a common occurrence in the lab experiments in the MC Lab).
4. Estimate the bias state in 3 DOF, which the controller can use to overcome external forces, such as the ocean current and the force from the towline.

The simulation model is required to include an ocean current affecting the towing operation, but not waves. Thus, waves are not added to the simulations, and wave-filtering is not added to the observer. The equations in an NPO are comprehensible with clear references to the system model, and thereby easier to tune than for instance a Kalman filter. The NPO is also less computationally demanding, and it is straightforward to remove wave-filtering from it.

The NPO for the towing vessel then becomes (Sørensen, 2012, p.237):

$$\tilde{\eta}_s = \eta_s - \hat{\eta}_s \quad (8.1.1)$$

$$\dot{\hat{\eta}}_s = R(\psi_s)\hat{\nu}_s + K_2\tilde{\eta}_s \quad (8.1.2)$$

$$\dot{\hat{b}}_s = -T_b^{-1}\hat{b}_s + K_3\tilde{\eta}_s \quad (8.1.3)$$

$$(M_{RB,s} + M_{A,s})\dot{\hat{\nu}}_s = -D_S\hat{\nu}_s + R^\top(\psi_s)\hat{b}_s + R^\top(\psi_s)K_4\tilde{\eta}_s + \tau_s, \quad (8.1.4)$$

where  $\tilde{y}_s \triangleq \tilde{\eta}_s$ .  $\eta_s$  is the measured vessel position,  $\hat{\eta}_s$ ,  $\hat{b}_s$  and  $\hat{\nu}_s$  are the estimated states, and  $K_2$ ,  $K_3$ ,  $K_4$  and  $T_b$  are observer tuning matrices.

### 8.1.1 Dead reckoning

In the MC lab, where the experiments are conducted in this thesis, a common occurrence for the position measurement system is that the measurements fail. The system always sends an error signal  $e_{pos}$  indicating whether or not the signals are correct or if they failed. If  $e_{pos} \neq 0$ , then the measured state  $\eta_s$  is replaced by the estimated state  $\hat{\eta}_s$ , rendering the equations such that dead reckoning is achieved:

$$\tilde{\eta}_s = 0 \quad (8.1.5)$$

$$\dot{\hat{\eta}}_s = R(\hat{\psi}_s)\hat{\nu}_s \quad (8.1.6)$$

$$\dot{\hat{b}}_s = -T_b^{-1}\hat{b}_s \quad (8.1.7)$$

$$(M_{RB,s} + M_{A,s})\dot{\hat{\nu}}_s = -D_S\hat{\nu}_s + R^\top(\hat{\psi}_s)\hat{b}_s + \tau_s \quad (8.1.8)$$

# Chapter 9

## Iceberg LOS guidance and control

In this thesis, the LOS objective is to tow an iceberg to, and along, a pre-defined straight-line path. In order to achieve this, a four step guidance and control setup is developed:

1. A LOS algorithm is developed for the iceberg, calculating the *iceberg course* angle required to steer the iceberg to, and along, the desired iceberg path.
2. An *ideal towing vessel position* is calculated in order to tow the iceberg in the desired *iceberg course*.
3. A towing vessel reference model is developed, based on the *ideal vessel position*, the current vessel position, a velocity reference, and towing vessel dynamics. The reference model ensures a more feasible vessel trajectory in order to realistically tow the iceberg. The output from the reference model is then the *desired vessel position, velocity, and acceleration*.
4. A towing vessel controller is developed in order to force the vessel position, velocity, and acceleration to converge to the *desired vessel position, velocity, and acceleration*. This is achieved with a backstepping controller.

For the LOS method described in this chapter to work, iceberg position measurements are required. In real towing scenarios, this could perhaps be done by landing a small unmanned flying vessel on the iceberg with a global positioning system (GPS) installed.

### 9.1 LOS algorithm for an iceberg

The content of this section is presented in the attached conference paper, with simulation studies to show the performance of the stand-alone LOS algorithm.

The current-modified LOS angle is presented in equations 5.2.18 and 5.2.19. To avoid confusion, the yaw angle  $\psi_{LOS}^m$  is replaced with an iceberg towline angle,  $\alpha_{LOS}$ :

$$\alpha_{LOS} \triangleq -\arctan\left(\frac{y' + \sigma y'_{int}}{\Delta}\right), \Delta > 0 \quad (9.1.1)$$

$$\dot{y}'_{int} = \frac{y' \Delta}{(y' + \sigma y'_{int})^2 + \Delta^2} \quad (9.1.2)$$

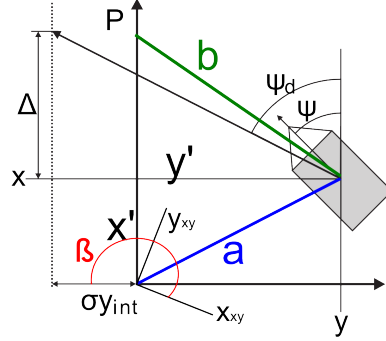


Figure 9.1: Notation for transforming between path-fixed and Cartesian coordinates. Original illustration is found in Børhaug et al. (2008).

In order to apply (9.1.1) to the iceberg model, it must be transformed into Cartesian coordinates. Using the notation from Figure 9.1, the following relationships hold:

$$a = \sqrt{(x(t) - x_{k-1})^2 + (y(t) - y_{k-1})^2} \quad (9.1.3)$$

$$b = \sqrt{(x_{LOS} - x(t))^2 + (y_{LOS} - y(t))^2} \quad (9.1.4)$$

$$c = \sqrt{(x_{LOS} - x_{k-1})^2 + (y_{LOS} - y_{k-1})^2} \quad (9.1.5)$$

$$x' = \frac{a^2 + c^2 - b^2}{2c} \quad (9.1.6)$$

$$y' = \pm \sqrt{a^2 - (x')^2} \quad (9.1.7)$$

$$\Delta = c - x' \quad (9.1.8)$$

If the path lies on the iceberg's port side,  $y'$  is positive. Otherwise,  $y'$  is negative. When having obtained all these values,  $\dot{y}_{int}$  is obtained and can be integrated. The integrated value  $y_{int}$  must then be transformed into Cartesian coordinates:

$$\beta = \text{atan2}(y_k - y_{k-1}, x_k - x_{k-1}) + \frac{\pi}{2} \quad (9.1.9)$$

$$y_{int,x} = y_{int} \cos(\beta) \quad (9.1.10)$$

$$y_{int,y} = y_{int} \sin(\beta) \quad (9.1.11)$$

The index  $k$  denotes the selected waypoint.  $\beta$  is perpendicular to the angle between the Cartesian and the path-fixed coordinate system. Then, finally the Cartesian LOS angle can be calculated:

$$\Delta y_{LOS} = y_{LOS} - y \quad (9.1.12)$$

## 9.2. Ideal towing vessel position

---

$$\Delta x_{LOS} = x_{LOS} - x \quad (9.1.13)$$

$$\alpha_{LOS}^{xy} = \text{atan2}(\Delta y_{LOS} + \sigma y_{int,y}, \Delta x_{LOS} + \sigma y_{int,x}), \quad (9.1.14)$$

where the use of  $\text{atan2}$ , as opposed to  $\text{arctan}$ , ensures that the LOS angle is placed in the correct quadrant and within the set  $(-\pi, \pi]$ .

## 9.2 Ideal towing vessel position

The output from the LOS algorithm in Step 1 is a Cartesian LOS iceberg course angle, denoted  $\alpha_{LOS}^{xy}$ . In order to achieve the iceberg course, the idea is to place the towing vessel such that the towline applies force in that direction. The ideal towing vessel position is denoted  $\eta_{ref}$ , and is calculated as such (see Figure 9.2 for definitions):

$$\eta_{ref} = [x_{ref}, y_{ref}, \psi_{ref}]^T \quad (9.2.1)$$

$$\begin{bmatrix} x_{ref} \\ y_{ref} \end{bmatrix} = \eta_i + (L + L_d) \begin{bmatrix} \cos(\alpha_{LOS}^{xy}) \\ \sin(\alpha_{LOS}^{xy}) \end{bmatrix} \quad (9.2.2)$$

$$\psi_{ref} = \alpha_{LOS}^{xy}, \quad (9.2.3)$$

where  $\eta_i$  is the iceberg position vector,  $L$  is the towline length, and  $L_d$  is described in (7.2.5).

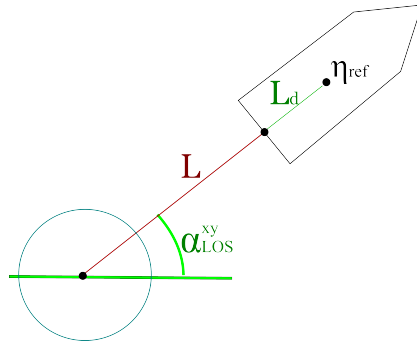


Figure 9.2: Calculation of the ideal ship position  $\eta_{ref}$ , based on the LOS iceberg course angle  $\alpha_{LOS}^{xy}$ .

### 9.3 Towing vessel reference model

In order to achieve a feasible towing vessel position, velocity and acceleration, a reference model is developed. It is created as a marine craft simulator, and is chosen to be of third order to properly filter the reference input (Fossen, 2011). The reference model is inspired by Fossen (2011, p.250), and contains both a position reference and a velocity reference:

$$R(\psi_{ref}) = \begin{bmatrix} \cos(\psi_{ref}) & -\sin(\psi_{ref}) & 0 \\ \sin(\psi_{ref}) & \cos(\psi_{ref}) & 0 \\ 0 & 0 & 1 \end{bmatrix} \quad (9.3.1)$$

$$\eta_d^{(3)} + A_{ref}\ddot{\eta}_d + B_{ref}\dot{\eta}_d + C_{ref}\eta_d = C_{ref}\eta_{ref} + B_{ref}R(\psi_{ref})\nu_{ref}, \quad (9.3.2)$$

where  $\eta_d$ ,  $\dot{\eta}_d$  and  $\ddot{\eta}_d$  are the filtered, desired vessel position, velocity and acceleration, respectively, whereas  $\eta_d^{(3)}$  is the third order filtering state. The matrices  $A_{ref}$ ,  $B_{ref}$  and  $C_{ref}$  are for tuning the reference model.

The input position  $\eta_{ref} = [x_{ref}, y_{ref}, \psi_{ref}]^\top$  is the ideal vessel position obtained from (9.2.1).

#### Velocity reference

The dynamic assignment in the maneuvering problem (Skjetne, 2005) is solved by defining a user-defined forward ship velocity reference  $U_{ref,i}$ . It is then transformed into the BODY-frame for the towing vessel:

$$u_{ref} = U_{ref,i} \cos(\alpha_{LOS}^{xy} - \psi_s) \quad (9.3.3)$$

$$v_{ref} = U_{ref,i} \sin(\alpha_{LOS}^{xy} - \psi_s), \quad (9.3.4)$$

which is then implemented into the reference model as:

$$\nu_{ref} = \begin{bmatrix} u_{ref} \\ v_{ref} \\ r_{ref} = 0 \end{bmatrix} \quad (9.3.5)$$

#### 9.3.1 Saturation

To ensure that the reference model does not allow unrealistic vessel behavior, such as too high velocities and accelerations, saturating elements can be added (Fossen, 2011).



The idea is that when a signal is created, for instance the desired towing vessel velocities  $\nu_d = R^\top(\psi_d)\dot{\eta}_d$ , a check for unrealistic values is added, typically by checking whether the signal exceeds a maximum value. Here is an example for the desired surge velocity:

$$\text{sat}(u_d) = \begin{cases} \text{sgn}(u_d)u_{max}, & \text{if } |u_d| \geq u_{max} \\ u_d, & \text{else} \end{cases} \quad (9.3.6)$$

In order to disallow unrealistic towing vessel velocities, saturation elements are added in the reference model for velocities in surge, sway and yaw.

## 9.4 Backstepping controller

Having developed the model for calculating the desired position and velocity set-points, a controller must be developed to calculate the necessary thrust forces for the towing vessel. During initiation of towing, the towline tension fluctuates, making it suboptimal to feedback the tension measurements to the controller. Thus, a bias state  $b_s$  is chosen to compensate the tow force. Assuming all states ( $\eta_s$ ,  $\nu_s$ , and  $b_s$ ) are known, the control plant model (CPM) becomes:

$$\dot{\eta}_s = R(\psi_s)\nu_s \quad (9.4.1)$$

$$M_s\dot{\nu}_s + D_s\nu_s = \tau_s + R^\top(\psi_s)b_s \quad (9.4.2)$$

A robust, nonlinear controller able to perform tracking design is needed. Therefore, a backstepping controller is chosen. The control objective for the backstepping controller is tracking, ensuring that the error states  $z_1$  and  $z_2$  converge to zero:

$$z_1 = R^\top(\psi_s)(\eta_s - \eta_d) \quad (9.4.3)$$

$$z_2 = \nu_s - \alpha_1, \quad (9.4.4)$$

where  $\alpha_1$  is a stabilizing function to be determined later, which will be designed to make the controller stable.

Using the facts that:

$$R^{-1}(\psi_s) = R^\top(\psi_s) \quad (9.4.5)$$

$$\dot{R}(\psi_s) = -R(\psi_s)S r_s \quad (9.4.6)$$

$$S = \begin{bmatrix} 0 & -1 & 0 \\ 1 & 0 & 0 \\ 0 & 0 & 0 \end{bmatrix} = -S^\top \quad (9.4.7)$$

$$z_1^\top r_s S z_1 = 0, \quad (9.4.8)$$

the following is obtained, where  $V_1$  and  $V_2$  are Lyapunov functions:

$$\dot{z}_1 = -r_s S z_1 + z_2 + \alpha_1 - R^\top(\psi_s) \dot{\eta}_d \quad (9.4.9)$$

$$V_1 = \frac{1}{2} z_1^\top z_1 \quad (9.4.10)$$

$$\dot{V}_1 = z_1^\top z_2 + z_1^\top (\alpha_1 - R^\top(\psi_s) \dot{\eta}_d) \quad (9.4.11)$$

The stabilizing function  $\alpha_1$  is then designed:

$$\alpha_1 = -K_P z_1 + R^\top(\psi_s) \dot{\eta}_d \quad (9.4.12)$$

$$\dot{\alpha}_1 = -K_p \dot{z}_1 - r_s S R^\top(\psi_s) \dot{\eta}_d + R^\top(\psi_s) \ddot{\eta}_d \quad (9.4.13)$$

$$\dot{V}_1 = z_1^\top z_2 - z_1^\top K_p z_1 \quad (9.4.14)$$

$$M_s \dot{z}_2 = -D_s \nu_s + \tau_s + R^\top(\psi_s) b - M_s \dot{\alpha}_1 \quad (9.4.15)$$

$$V_2 = V_1 + \frac{1}{2} z_2^\top M_s z_2 \quad (9.4.16)$$

$$\dot{V}_2 = -z_1^\top K_p z_1 + z_2^\top (z_1 - D_s \nu_s + \tau_s + R^\top(\psi_s) b - M_s \dot{\alpha}_1) \quad (9.4.17)$$

Hence, the control law can be chosen as:

$$\tau_s = -z_1 + D_s \nu_s - R^\top(\psi_s) b + M_s \dot{\alpha}_1 - K_d z_2, \quad (9.4.18)$$

where  $K_p = K_p^\top > 0$ ,  $K_d = K_d^\top > 0$ , and  $M_s$  is a positive, semi-definite matrix. This results in:

$$V_2 = \frac{1}{2} z_1^\top z_1 + \frac{1}{2} z_2^\top M_s z_2 = \frac{1}{2} z^\top \begin{bmatrix} \mathbb{I} & 0 \\ 0 & M_s \end{bmatrix} z \quad (9.4.19)$$

$$\dot{V}_2 = -z_1^\top K_p z_1 - z_2^\top K_d z_2 = -z^\top \begin{bmatrix} K_p & 0 \\ 0 & K_d \end{bmatrix} z \quad (9.4.20)$$

According to Skjetne (2005, Definition A.9), the smooth Lyapunov function  $V_2$  should satisfy:

1. there exist two  $\mathcal{K}_\infty$ -functions  $\chi_1$  and  $\chi_2$  such that for any  $x \in \mathcal{R}^n$ ,

$$\chi_1(|x|) \leq V(x) \leq \chi_2(|x|), \quad (9.4.21)$$

2. there exists a continuous and, at least, positive semi-definite function  $\chi_3$  such that for any  $x \in \mathcal{R}^n$ ,

$$V^x(x)f(x) \leq -\chi_3(|x|). \quad (9.4.22)$$

In the case of this backstepping controller, the following is achieved:

$$\chi_1 = \min\left(\frac{1}{2}, \frac{1}{2}\lambda_{\min}(M_s)\right)|z|^2 = C_1|z|^2 \quad (9.4.23)$$

$$\chi_2 = \max\left(\frac{1}{2}, \frac{1}{2}\lambda_{\max}(M_s)\right)|z|^2 = C_2|z|^2 \quad (9.4.24)$$

$$\chi_3 = \lambda_{\min}(K_p, K_d)|z|^2 = C_3|z|^2 \quad (9.4.25)$$

Then, according to Skjetne (2005, Theorem A.10), since there exists a smooth Lyapunov function for the system  $\dot{z} = [\dot{z}_1, \dot{z}_2]^\top$ , then the controller is uniformly globally stable (UGS). Furthermore, since  $\chi_3$  is positive-definite, and  $\chi_i(|z|) = c_i|z|^2$  for  $i = 1, 2, 3$ , where  $c_1, c_2, c_3$  are strictly positive reals, then the controller is uniformly globally exponentially stable (UGES).

It is proven, for the nonlinear observer class discussed in Chapter 8, that the observer is UGES and that the separation principle holds (Fossen and Strand, 1999; Loria et al., 2000). When the separation principle holds, the observer and controller stability may be analysed separately, and since both are UGES, the complete system is UGES.



# Chapter 10

## Reliability-index for the towline

Inspired by Berntsen (2008), a reliability index for the towline tension has been developed, based on the reliability index in (6.2.9):

$$\delta_T(t) = \frac{T_{b,T} - (\bar{T}(t) + \kappa\sigma_T)}{\sigma_{b,T}} \quad (10.0.1)$$

The main requirement for this index, is that real-time tension measurements are available, either from a towline tension observer, or actual real-time measurements during towing. Also required are the mean  $T_{b,T}$ , and standard deviation  $\sigma_{b,T}$ , of the towline breaking strength. These values are usually tested or known by mooring line manufacturers (Berntsen, 2008), and are thus assumed known for towlines as well. Using the tension measurements and equations (6.2.7) and (6.2.8), the mean tension  $\bar{T}(t)$  and standard deviation  $\sigma_T$  are found.

Using the idea from Section 6.3 on control actions based directly on reliability indices, the following control objective is proposed for  $\delta_T(t)$ :

$$\delta_T(t) \geq \delta_{T,limit} \quad (10.0.2)$$

### 10.1 Failure mode implementation

In the interest of avoiding failure modes for the towing operation, such as iceberg overturning, towline rupture, and towline slippage, it is desirable to implement these in the simulation model. To be able to implement the failure modes, indicators of when they are happening must be added.

For towline rupture this indicator is already created as the reliability index for towline rupture in equations (10.0.1) and (10.0.2).

Monitoring towline slippage is difficult, especially in simulations where it can not even be observed. By placing 6-DOF position and movement sensors on the iceberg, and combining these with tension measurements, it could possibly provide a model for monitoring slippage. However, in the simulation model, it is assumed that a certain tow force would cause the towline to slip. With such an assumption, a reliability index for towline slippage can be created:

$$\delta_{slip}(t) = \frac{T_{slip,T} - (\bar{T}(t) + \kappa\sigma_T)}{\sigma_{slip,T}} \quad (10.1.1)$$

$$\delta_{slip}(t) \geq \delta_{slip,limit} \quad (10.1.2)$$

where  $T_{slip,T}$  and  $\sigma_{slip,T}$  correspond to the mean and standard deviation of the tow force causing towline slippage, respectively.

Similarly to towline slippage, iceberg overturning is difficult to monitor directly. By placing 6-DOF position and movement sensors on the iceberg, and combining these with the tension measurements, it could perhaps be possible to roughly estimate the iceberg stability using online system identification methods. This has not been within the scope of this thesis. In addition, to identify 6-DOF movements of the iceberg in the simulation model, a 6-DOF iceberg model would be required.

Limited to a 2-DOF iceberg model, it can be assumed that a certain tow force would cause the iceberg to overturn. Then, such as with towline rupture and slippage, a reliability index for iceberg overturning can be created:

$$\delta_{overturn}(t) = \frac{T_{overturn,T} - (\bar{T}(t) + \kappa\sigma_T)}{\sigma_{overturn,T}} \quad (10.1.3)$$

$$\delta_{overturn}(t) \geq \delta_{overturn,limit} \quad (10.1.4)$$

It could be argued that a simple implementation of the breaking strength  $T_{b,T}$  would be a good failure mode implementation of towline rupture. This has not been chosen, since it does not take into account the variance  $\sigma_{b,T}$  of the towline breaking strength.

### 10.1.1 Combined implementation

The three indicators of the different failure modes are calculated from the towline measurements. In addition the three limits are initialized prior to the simulations and experiments.

Simple if-tests are then run, checking if either of the limitations in equations (10.0.2), (10.1.2) and (10.1.4) are false. If one is false, an alert is printed during the simulation, and the towline is disconnected. In the simulation model, disconnection of the towline is performed by setting the output from the towline observer (Section 7.2) to zero:

$$X_{TOW} = Y_{TOW} = 0, \quad (10.1.5)$$

which causes the towing vessel and iceberg to drift separately.

# Chapter 11

## Reliability-based control

The objective of this chapter is to develop a controller for the tow operation based on the reliability indices developed in Chapter 10. Towline tension will increase when deforming the towline, which, in a towing scenario, is achieved by propagating the towing vessel away from the iceberg. This produces increased tow force and increased towing velocity, and a decreased reliability-index. The target in this chapter is to ensure that none of the reliability indices go below a set limit, as described in (10.0.2). This is possible by decreasing the tow force when the reliability index is near the limit. Too little tow force is not desired either, as it would cause slack on the towline, which will cause transient loads when re-tightening the towline. This could probably be avoided by using a tow winch, but this is not investigated in this thesis.

### 11.1 Thrust penalty control

One way of decreasing the tow force can be by detecting when the reliability index is near the set limit, and then penalizing the commanded thrust. To do this, a  $\delta_{near}$  value is determined. This is a reliability index value higher than  $\delta_{limit}$ , where the penalty kicks in. A linear penalty scheme for the reliability-index for towline rupture  $\delta_T$  is proposed, but could easily be replaced with the index for other failure modes. The penalized thrust  $\tau_{pen}$  is:

$$\tau_{pen} = \begin{cases} \tau_s, & \text{if } \delta_T > \delta_{near} \\ \tau_s(a_\delta\delta_T + b_\delta), & \text{if } \delta_{near} \geq \delta_T > \delta_{limit} \\ 0, & \text{otherwise,} \end{cases} \quad (11.1.1)$$

where:

$$\delta_{near} > \delta_{limit} \quad (11.1.2)$$

$$a_\delta = \frac{1}{\delta_{limit} - \delta_{near}} \quad (11.1.3)$$

$$b_\delta = -a_\delta * \delta_{near}. \quad (11.1.4)$$

It is important that  $\delta_{near}$  is sufficiently larger than  $\delta_{limit}$ , such that the system has time to compensate before  $\delta_{limit}$  is reached, otherwise the reliability index might skip past both limits with one sudden tension rise.

When dealing with several reliability-indices, such as in this thesis, index weighting should be performed, meaning that a penalty should be calculated for each index, and the index with the highest penalty (resulting in smallest  $\tau_{pen}$ ) is to be used.

As shown in Section 13.4, the thrust penalty scheme is seen to delay the failure mode, but not to secure completely against it. Therefore, the thrust penalty scheme is deemed ineffective.

## 11.2 Velocity reference penalty control

A penalty scheme for the iceberg velocity reference (Section 9.3) is developed. The same theory is applied as with the thrust penalty, where the penalized iceberg velocity reference  $U_{ref,i,pen}$  is:

$$U_{ref,i,pen} = \begin{cases} U_{ref,i}, & \text{if } \delta_T > \delta_{near} \\ U_{ref,i}(a_\delta \delta_T + b_\delta), & \text{if } \delta_{near} \geq \delta_T > \delta_{limit} \\ 0, & \text{otherwise.} \end{cases} \quad (11.2.1)$$

The penalty  $p_k$  of sample  $k$  is defined as:

$$p_k = \frac{1}{U_{ref,i}} U_{ref,i,pen}, \quad (11.2.2)$$

where when  $p_k = 1$ , the velocity reference is not penalized, whereas when  $p_k = 0$ , it is fully penalized.

However, as is shown in Section 13.4.2, there is need to limit the rate of change  $\dot{p}_k$  when it increases in order to avoid unstable behavior of  $U_{ref,i,pen}$ . During the work of this thesis there has not been enough time to find an optimal way of limiting  $\dot{p}_k$ . However, a linear rate of change scheme is proposed.

The linear rate of change assumes that at  $p_k = 0$ , the desired positive rate of change  $\dot{p}_k^+$  is very small, because this is very close to the failure mode occurring. However, for  $p_k = 1$  it may be a little faster, because then the failure mode is further away from occurring. Then, by defining the allowable positive rate of change at  $p_k = 0$  to be  $\dot{p}_{min}^+$ , and at  $p_k = 1$  to be  $\dot{p}_{max}^+$ , the following linear relationship is found:

$$\dot{p}_k^+ = \frac{\dot{p}_{max}^+ - \dot{p}_{min}^+}{1} p_k + \dot{p}_{min}^+ \quad (11.2.3)$$

This is implemented by checking whether the current penalty is higher than the previous penalty, and if so by applying the rate of change:



## 11.2. Velocity reference penalty control

---

$$\text{if } p_k > p_{k-1}, \quad (11.2.4)$$

$$\text{then } p_k = \min(p_k, p_{k-1} + \dot{p}_k^+), \quad (11.2.5)$$

$$\text{else } p_k = p_k, \quad (11.2.6)$$

for systems with a sample rate of 1s. For other sample rates it must be modified accordingly.



## Part III

# Simulations and experiments in the MC Lab



# Chapter 12

## MC Lab overview

Model experiments of iceberg towing have been conducted in the Marine Cybernetics Lab (MC Lab) at NTNU (MC Lab, 2014). In order to properly conduct experiments in the MC Lab, an understanding of the lab, and the experiments to be conducted, must be gained. Prior to the experiments, the mathematical model and the proposed control setup were simulated numerically using MatLab<sup>TM</sup> and SimuLink<sup>TM</sup>. These simulations can not identify practical challenges in the experimental setup of the MC Lab. Thus, in addition to conducting model experiments, a Hardware-in-the-Loop (HIL) setup was developed.

HIL is a setup where software is tested by connecting it to a hardware simulator. The hardware simulator contains the behavior of the model, in addition to as many as possible of the different failures that can occur. The software is therefore tested to see how it reacts to the different failures, and to check if it is still able to perform after the failure has occurred.

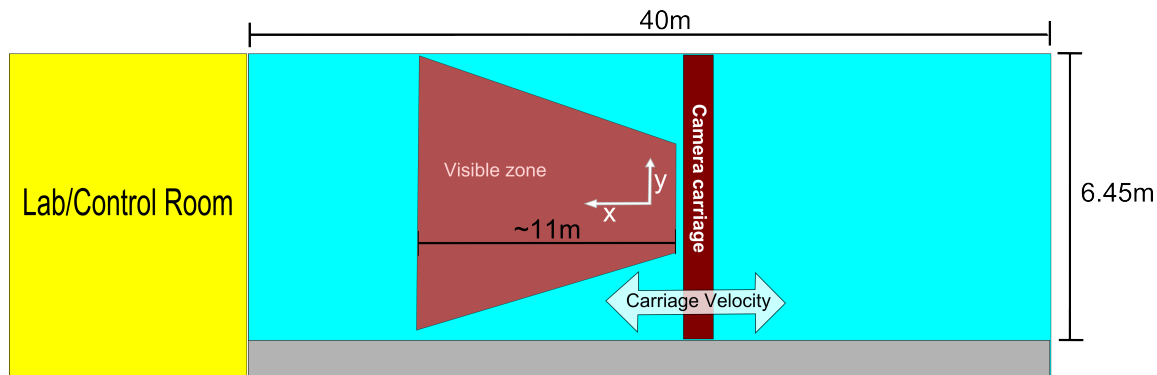


Figure 12.1: Overview drawing of the MC Lab.

### 12.1 MC Lab setup

An overview of the MC Lab is shown in Figure 12.1. The tank dimensions are  $L \times B \times D = 40m \times 6.45m \times 1.5m$ . The laboratory is equipped with a carriage, which carries a positioning system able to measure 6 DOF.

The positioning system is delivered by Qualisys, using Oqus cameras (Qualisys, 2014). It is placed on the carriage, which is able to move in the x-direction, as shown in Figure 12.1. The position measurements are calculated by three cameras mounted on the carriage, viewing reflectors on the object to be measured. At least two cameras must see a minimum of three reflectors on an object in order to calculate its position.

This creates a *visible zone* for the positioning system, reaching approximately 11m from the carriage, as shown in Figure 12.1.

In addition to the measurements, a residual of the position measurements for each object is calculated. If the residual is deemed too high by the Qualisys system, the measurement is deemed erroneous. Thus, measurements may drop out also within the *visible zone*. This effect is enhanced if the reflectors are slightly moved from their initial positions on the object. It is required that all objects (in this thesis the towing vessel and the iceberg) are found by the cameras in order to send position signals to the computer, which means that if one object is outside the visible zone or has a too high residual, neither objects are found on the computer.

The coordinate system is relative to the camera positions along the x-direction. This means that if the carriage moves, the towing vessel and the iceberg (if standing still in the water) will be moving in the relative coordinate system. This is used to simulate ocean current, making the carriage velocity equal to the ocean current.

The experiments were conducted using the software LabVIEW™. It handles the communication between the real-time controller, the lab computer and the position measurements. The model vessel, CS Enterprise I (Section 12.2), has a compact RIO (cRIO) installed in order to perform its real-time control functions (National Instruments, 2014). In order to create the mathematical model, and decide inputs to, and outputs from the experiments, MatLab™ and Simulink™ is used. The Simulink™ model is then built in two versions, one for LabVIEW™ and one for the cRIO, in order for them to communicate.

## 12.2 CS Enterprise I

The mathematical model from Section 7.3 is used to model CS Enterprise I (CSE1). CSE1 is a model vessel (depicted in Figure 12.2), based on the anchor-handling tug Aziz (Model Slipway, 2014). It is for use in the MC Lab at NTNU, and has the following main dimensions:

**Length overall:**  $L_s = 1.105m$

**Beam:**  $B_s = 0.248m$

**Scale:**  $\lambda_s = 1 : 50$

**Mass:**  $m_s = 17.6kg$

In order to be seen by the positioning system, 5 reflectors are attached to CSE1, seen as round balls on poles in Figure 12.2.

Skåtun (2011) equipped CSE1 with a bow thruster and two Voith-Schneider propellers, making it a fully actuated model vessel in surge, sway, and yaw. A cRIO was also installed and placed in a water-tight container on deck, and is used as a real-time controller for CSE1 (National Instruments, 2014). In addition, functionality was added such that CSE1 could be controlled using a Sony Dualshock3 controller.



Figure 12.2: CS Enterprise I, model vessel at NTNU.

Tran (2014) has performed system identification on CS Enterprise I, and has found most of the values to use in  $M_{RB,s}$ ,  $M_{A,s}$ ,  $D_s(\nu_{r,s})$  and  $K_M$ . Some values were not found, however, and were taken from Cybership II, a slightly larger model ship at NTNU (Cybership II is  $1.255m$  long and  $0.29m$  wide) (Skjetne, 2005).

Since the iceberg towing simulations and experiments are to be conducted in low velocities, the nonlinear damping term is assumed very small and therefore negligible, leaving only the linear term. The matrices for CS Enterprise I are (using SNAME notation for coefficients):

$$M_{RB,s} = \begin{bmatrix} m & 0 & 0 \\ 0 & m & mx_g \\ 0 & mx_g & I_z \end{bmatrix} = \begin{bmatrix} 17.6 & 0 & 0 \\ 0 & 17.6 & 0.528 \\ 0 & 0.528 & 1.76 \end{bmatrix} \quad (12.2.1)$$

$$M_{A,s} = - \begin{bmatrix} X_{\dot{u}} & 0 & 0 \\ 0 & Y_{\dot{v}} & Y_{\dot{r}} \\ 0 & Y_{\dot{r}} & N_{\dot{r}} \end{bmatrix} = \begin{bmatrix} 2 & 0 & 0 \\ 0 & 10 & 0 \\ 0 & 0 & 1 \end{bmatrix} \quad (12.2.2)$$

$$D_s = - \begin{bmatrix} X_u & 0 & 0 \\ 0 & Y_v & N_v \\ 0 & Y_r & N_r \end{bmatrix} = \begin{bmatrix} 0.5974 & 0 & 0 \\ 0 & 3.5063 & -0.1814 \\ 0 & 7.25 & 1.9 \end{bmatrix} \quad (12.2.3)$$

$$K_M = \begin{bmatrix} 1 & 0 & 0 \\ 0 & 1 & 0 \\ 0 & -0.555 & 0 \end{bmatrix}, \quad (12.2.4)$$

where the values in  $M_{A,s}$  are retrieved from Cybership 2.

### 12.2.1 Thrust allocation

To control CSE1, the desired vessel forces  $\tau_s$  must be properly distributed between the actuators of the vessel. This is called *thrust allocation*. After thrust is allocated to each thruster, the thrusters must be controlled to actually deliver the desired force. This is done through the *thruster mapping*.

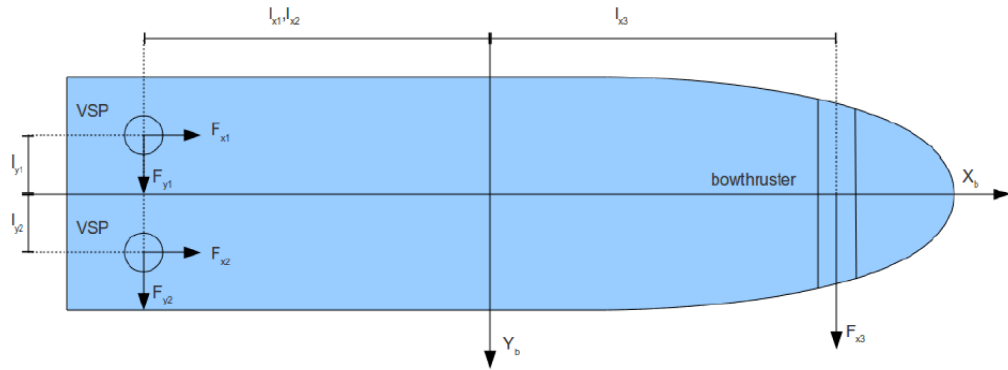


Figure 12.3: Thrust allocation of CSE1 (Skåtun, 2011).

Thrust allocation for CSE1 has already been addressed by Skåtun (2011). The Voith-Schneider propeller forces are decomposed into forward- and lateral force components, as can be seen in Figure 12.3. The extended thrust matrix is defined:

$$\tau_s = T_c K_c f_{act}, \quad (12.2.5)$$

where  $T_c$  is the thrust configuration matrix,  $K_c$  a gain matrix and  $f_{act}$  the control input vector for the actuators. For CSE1, using Figure 12.3, the following thrust configuration matrix is obtained (Skåtun, 2011):

$$T_c = \begin{bmatrix} 1 & 0 & 1 & 0 & 0 \\ 0 & 1 & 0 & 1 & 1 \\ l_{y1} & -l_{x1} & -l_{y2} & -l_{x2} & l_{x3} \end{bmatrix} = \begin{bmatrix} 1 & 0 & 1 & 0 & 0 \\ 0 & 1 & 0 & 1 & 1 \\ 0.055 & -0.45 & -0.055 & -0.45 & 0.385 \end{bmatrix}, \quad (12.2.6)$$

where  $K_c = \mathcal{I}$ , and the control input vector is:



$$f_{act} = \begin{bmatrix} f_1 \\ f_2 \\ f_3 \\ f_4 \\ f_5 \end{bmatrix} = \begin{bmatrix} F_{x1} \\ F_{y1} \\ F_{x2} \\ F_{y2} \\ F_{x3} \end{bmatrix}. \quad (12.2.7)$$

### 12.2.2 Thruster mapping

Having obtained the individual thrusters' desired force, *thruster mapping* is performed to ensure that the output force from the thruster corresponds to the desired force.

The thruster mapping used in the iceberg towing experiments have been determined by Skåtun (2011) and Tran (2014). The thruster mapping from Skåtun (2011) was used the first two weeks in the MC Lab. This proved not to work properly for the low velocities of the iceberg towing. The thruster mapping of Tran (2014) was finished between the two periods in the MC Lab. When implemented, the actuators performed relatively well, and much better than the previous thruster mapping, which is discussed in Section 14.2.1.

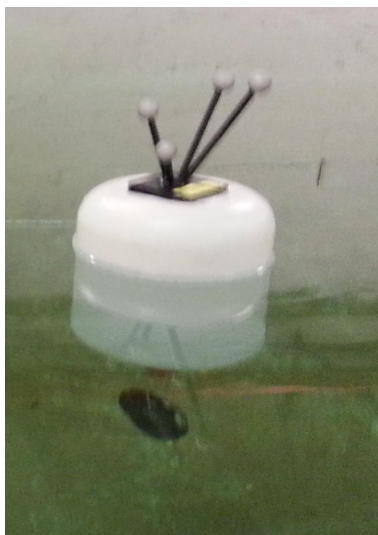


Figure 12.4: Iceberg modelled with a cylindrical 25 liter bottle, filled 22.8 liters and turned upside-down with a  $1kg$  mass hanging below to add stability.

## 12.3 Iceberg model

In order to model an iceberg in the MC Lab, a 25 liter cylindrical liquid bottle was used. Due to the density relation between glacial ice and water, 22.8 liters of fresh water were filled into the bottle, and a 1kg mass was attached in a rope hanging from the lid to add stability. The bottle was then laid in the water upside-down, with the mass hanging from the bottom, as seen in Figure 12.4. Four reflector balls were attached on top of the iceberg to be used by the positioning system.

The mathematical model from Section 7.4 is used to model the iceberg. The matrices  $M_{RB,i}$ ,  $M_{A,i}$ , and  $D_i$  in (7.4.3) must be determined. The iceberg is assumed to be a standing cylinder, with the following dimensions:

**Diameter:**  $L_i = 20cm$

**Height:**  $H_i = 80cm$

**Draught:**  $T_i = 72.85cm$

**Freeboard:**  $h_i = 7.15cm$

**Mass:**  $m_i = 23kg$

**Scale:**  $\lambda_i = 1 : 50$

According to Pettersen (2007), the added mass coefficient for a cylinder is 1. This gives the following mass matrices for the iceberg:

$$M_{RB,i} = M_{A,i} = \begin{bmatrix} 23 & 0 \\ 0 & 23 \end{bmatrix} \quad (12.3.1)$$

As seen in Section 4.2.2, a nonlinear term for iceberg damping is discussed. However, as discussed in Assumption 2 in Section 7.4, the nonlinear damping term is neglected. This leaves only linear viscous damping, a term which is difficult to calculate. According to Sundland (2013), such a calculation can be performed by using the software WAMIT (WAMIT, 2014).

Due to the complexity of determining linear damping, it has been treated as a tuning parameter. These were the final values in the simulations:

$$D_i = \begin{bmatrix} 50 & 0 \\ 0 & 50 \end{bmatrix} \quad (12.3.2)$$

## 12.4 Towline modelling and tension measurements

In the experiments, tension measurements are vital to the use of reliability indices, and must be real-time. The tension force is measured by a force ring attached between the aft of CSE1 and the towline, as seen in Figure 12.5.

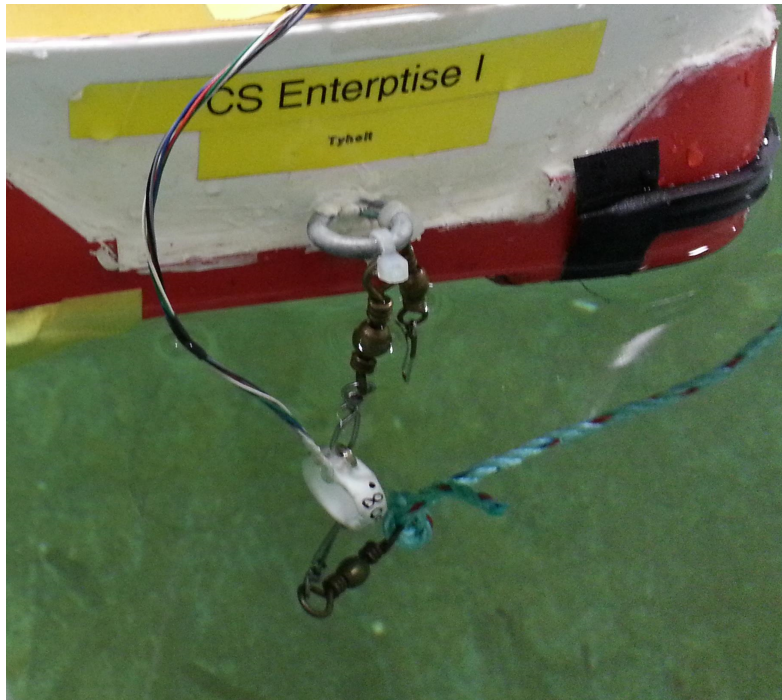


Figure 12.5: Force ring attached between aft of CSE1 and towline, for tension measurements.

The force ring uses strain gage technology for measuring, and a signal is sent through wire to the cRIO on CSE1. The signal is then sent wirelessly from the cRIO to the lab computer. The signal holds a linear relationship to actual tension. This relationship is unique for the force ring, and found via measurements to be:

$$F_{TOW} = mg = \frac{s - 0.00094}{-0.000077} \times 9.81, \quad (12.4.1)$$

where  $s$  is the signal, and  $g$  is the acceleration of gravity.

The towline is a floating rope, with a length of  $1.105m$ . As the model scale is  $1 : 50$ , this is far shorter than the towlines discussed in Section 4.1. This is due to the limited *visible zone* in the MC Lab, as discussed in Section 12.1.

## 12.5 HIL setup

A HIL setup for iceberg towing with CS Enterprise I in the MC Lab has been developed. The simulation setup described in Part II contains failure modes of the general iceberg towing operation. In addition, the HIL setup must include failures specific to the MC Lab setup. In this thesis, the following failures have been identified:

**Position measurement error:** The position measurements may fall out. Either due to being outside the reach of the camera system, or due to large residuals for measurements. Within the *visible zone* this appears to occur randomly, but is more likely to occur when the camera system is not recently calibrated, or if the reflectors on the vessel/iceberg are moved from the initialized positions, for instance by nudging them when physically handling the models. If the position is lost in one sample, it appears likely that the next samples also fail.

**Compact RIO crash:** The cRIO on board CSE1 may crash, making it impossible to control the vessel. No reasons for this were discovered. It appears to occur randomly, and can only be fixed by physically resetting the cRIO on board.

**Out of bounds:** The towing vessel and/or iceberg may crash into the borders of the model basin. This could be harmful to the models, and is best avoided. During experiments, this mainly happened during *cRIO crash*.

These failures have been identified through experience in the lab. As *cRIO crash* renders the entire system useless and uncontrollable, this has not been implemented into the HIL setup. Also, *out of bounds* detection is not implemented into the HIL simulations. During experiments, it is made sure that the desired area of movement is well within bounds.

The remaining failure to implement is *position measurement error*.

### 12.5.1 Position measurement error

When either the vessel or the iceberg experiences a position measurement error, the positioning system returns an error signal unequal to zero:  $e_{pos} \neq 0$ , and the position measurements of both the vessel and iceberg are set to be those of the previous non-erroneous sample.

This is reproduced in the HIL model by adding a measurement error block. Input to the error block is a *desired error percentage*  $e_{d,pos}$  for the simulation.

A random number  $n_r$  between 0 and 1 is generated. Then, if  $n_r \leq e_{d,pos}$ , an error is signalled by assigning  $e_{pos} = 1$ , and by assigning the position measurement sample equal to the previous measurement sample.

The measurements normally do not fail, meaning  $e_{d,pos}$  is low. However, when it fails, it often fails many samples in a row. Thus, a test is added to check if the previous sample failed. If so,  $e_{d,pos}$  is set to 0.95.

A tactic of overcoming position measurement errors is *dead reckoning*, discussed in Section 8.1.1.

# Chapter 13

## Simulation study

In this chapter, the different concepts and setups in the thesis are simulated. In total, nine scenarios are simulated, with the following objectives:

### **Scenarios 1 and 2: Mathematical model performance.**

These two scenarios confirm the behavior of the mathematical model, showing that the towing vessel, the iceberg and the towline move as expected, and are all affected by each other.

### **Scenario 3: Reliability index implementation.**

This scenario shows how the reliability indices are implemented into the model, and also shows how they are affected by transients in the towline tension.

### **Scenario 4: Failure mode implementation.**

This scenario investigates the failure mode implementation, and shows what happens to the model when the iceberg overturns and the towline is disconnected.

### **Scenarios 5 and 6: Thrust penalty control.**

These scenarios show the implementation of a thrust penalty control scheme, and demonstrate that this implementation is able to delay failure modes. However, if the system keeps pushing, the limit will eventually be reached. It is suggested to rather use a velocity reference penalty scheme.

### **Scenario 7: LOS guidance and control.**

This scenario shows the implementation of the iceberg LOS guidance and backstepping controller, and the observer producing the bias state for the controller. For three different ocean current angles it shows that the vessel is able to control the iceberg to and along the desired path.

### **Scenario 8: Combined strategy, LOS iceberg- and reliability-control.**

This scenario is a combination of scenario 7 and the proposed velocity reference penalty scheme. It shows the difference between not adding a penalty scheme and adding one, and it also shows the importance of limiting the penalty's rate of change.

### **Scenario 9: HIL test, with position measurement errors**

In this scenario, position measurement errors are added. The software's ability to function without position measurements is tested, which is why dead reckoning is implemented as in Section 8.1.1.

Simulation time is denoted  $T_s$  in all of the simulations. Ocean current is defined by magnitude  $|V_c|$  and direction  $\beta_c$ , with the following relationship to  $V_c$  from (7.1.1):

$$V_c = |V_c| \begin{bmatrix} \cos(\beta_c) \\ \sin(\beta_c) \end{bmatrix} \quad (13.0.1)$$

## 13.1 Mathematical model performance

To show the performance of the mathematical model, two scenarios have been simulated and run. Both scenarios are based on applying constant force and observing how the towing vessel, iceberg and towline tensions behave.

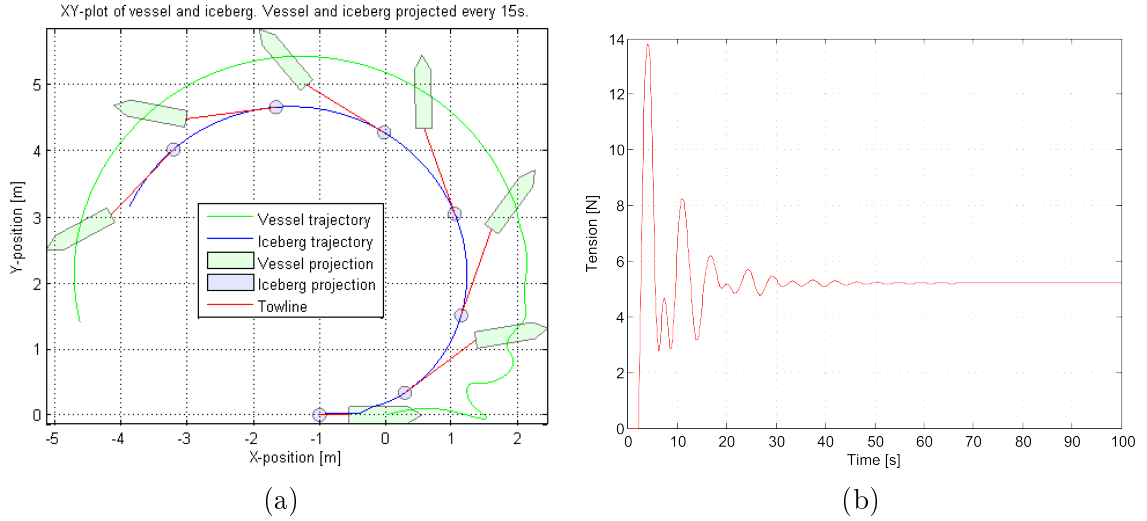


Figure 13.1: Scenario 1: (13.1a) XY-plot of the vessel and iceberg trajectories. (13.1b) Towline tension during the simulation.

### 13.1.1 Scenario 1

The vessel is fed a constant thrust force in surge and sway, while a current acts in the negative x-direction. The following conditions are tested:

$$T_s = 100s \quad (13.1.1)$$

$$\eta_s(0) = [0, 0, 0]^T \quad (13.1.2)$$

$$\eta_i(0) = [-1, 0]^T \quad (13.1.3)$$

$$|V_c| = 0.01 \frac{m}{s} \quad (13.1.4)$$

$$\beta_c = \pi \quad (13.1.5)$$

$$\tau_s = \begin{bmatrix} 5N \\ 2N \\ 0 \end{bmatrix} \quad (13.1.6)$$

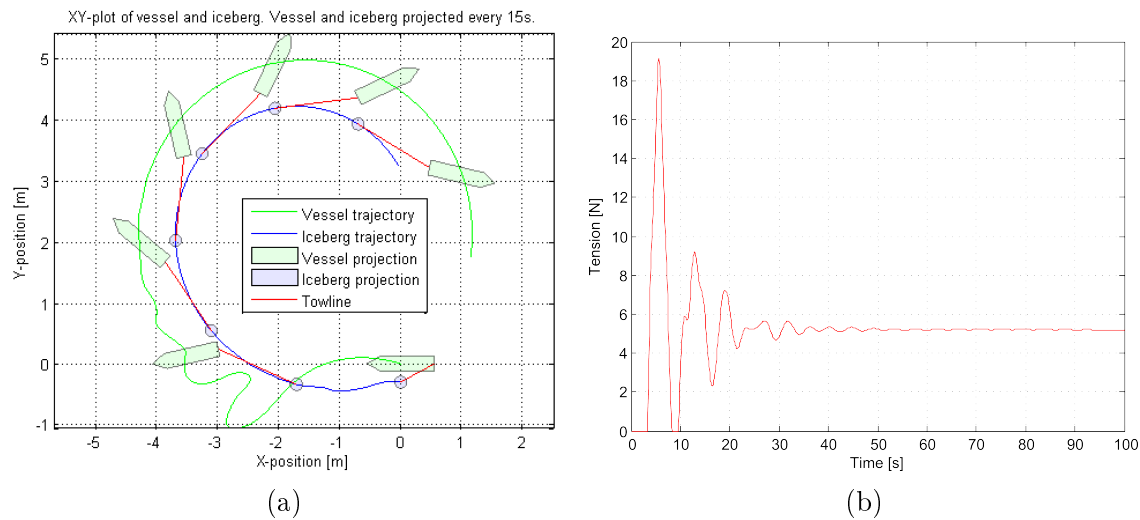


Figure 13.2: Scenario 2: (13.2a) XY-plot of the vessel and iceberg trajectories. (13.2b) Towline tension during the simulation.

### 13.1.2 Scenario 2

The vessel is fed a constant thrust force in surge and sway, while a current acts in the negative x-direction. This time, in order to show that the towline behaves properly, the vessel and iceberg are placed closer to each other and the vessel is rotated  $180^\circ$ . This is not a very realistic starting position, but is chosen to show how slack in the towline works. The following conditions are tested:

$$T_s = 100s \quad (13.1.7)$$

$$\eta_s(0) = [0, 0, \pi]^\top \quad (13.1.8)$$

$$\eta_i(0) = [0, -0.3]^\top \quad (13.1.9)$$

$$|V_c| = 0.01 \frac{m}{s} \quad (13.1.10)$$

$$\beta_c = \pi \quad (13.1.11)$$

$$\tau_s = \begin{bmatrix} 5N \\ -2N \\ 0 \end{bmatrix} \quad (13.1.12)$$

### 13.1.3 Discussions, mathematical model

The vessel and iceberg behaviours are reliant on each other, and it is shown that the vessel actually tows the iceberg. During the initiation phase, it is shown that there are transients in the towline tension, as can be seen in figures 13.1b and 13.2b. It is seen that the transients have a large effect on the towing vessel trajectory, whereas the iceberg trajectory is much less affected.

Comparing the two scenarios, the initial position of the vessel compared to the iceberg is such that in Scenario 2, it travels farther without experiencing towline tension. This is seen in Figure 13.2 to give larger tension transients and worse vessel behaviour initially.

## 13.2 Reliability index implementation

The reliability-indices for towline rupture, towline slippage and iceberg overturning are implemented as in Section 10.1.

### 13.2.1 Scenario 3

The same initialization as in Scenario 1 is run, with added information for the reliability indices for the three failure modes. The values used for the reliability indices are conceptual, and not mathematically based. The following values are used:

$$T_{b,T} = 160N \quad (13.2.1)$$

$$\delta_{b,limit} = 10 \quad (13.2.2)$$

$$T_{slip,T} = 140N \quad (13.2.3)$$

$$\delta_{slip,limit} = 10.5 \quad (13.2.4)$$

$$T_{overturn,T} = 70N \quad (13.2.5)$$

$$\delta_{overturn,limit} = 11 \quad (13.2.6)$$

To decide the standard deviation  $\sigma$  terms, they are assumed to have the relationship  $\sigma_{x,t} = 0.075T_{x,T}$ , where  $x = \{b, slip, overturn\}$  (Berntsen, 2008, p.86).

### 13.2.2 Discussions, reliability-index

The plots for Scenario 3 show that while applying a constant force, both the tension measurements and the reliability indices will reach steady-state after a while. Large transients can, however, be seen during tow initiation, which produce notable responses on the reliability indices.



### 13.3. Failure mode implementation

These transients are only based on the linear stretch transients of the towline. In reality, these transients will be even larger due to nonlinear tension effects. The reliability index will therefore not represent good approximations for the failure modes during these transients. The transients should therefore be avoided, which can be done by slowly applying thrust to the vessel, making the tow initiation smoother.

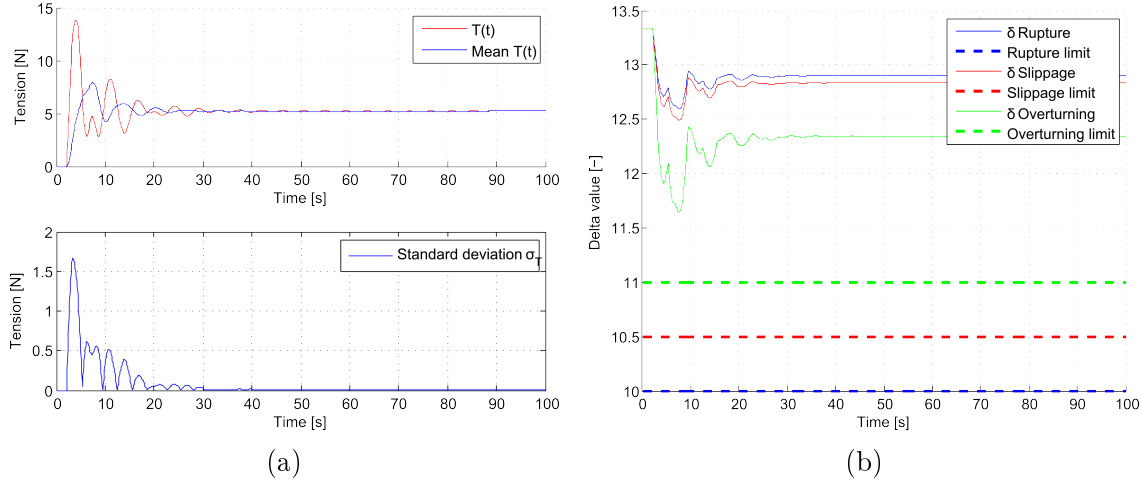


Figure 13.3: Scenario 3: (13.3a) Measurement, mean, and standard deviation of the towline tension. (13.3b) Reliability indices for the three failure modes, with corresponding lower limits.

## 13.3 Failure mode implementation

The different failure modes have been implemented using reliability indices. If the reliability index goes below a set limit, the failure mode is activated, and the towline is disconnected.

### 13.3.1 Scenario 4

In Scenario 4, the tow force is increasing linearly with respect to time. This is done for two reasons. Firstly, it is an attempt to reduce the transients in the towline tension, and secondly, in order to induce the failure mode of *iceberg overturning*. The reliability index data are conceptual, and are not based on mathematics. The following setup is used, where  $\sigma_{x,T} = 0.075T_{x,T}$ :

$$T_s = 20s \quad (13.3.1)$$

$$\eta_s(0) = [0, 0, \frac{\pi}{4}]^T \quad (13.3.2)$$

$$\eta_i(0) = [-0.7, -0, 7]^T \quad (13.3.3)$$

$$|V_c| = 0.1 \frac{m}{s} \quad (13.3.4)$$

$$\beta_c = \pi \quad (13.3.5)$$

$$\tau_s = \begin{bmatrix} 4tN \\ -tN \\ 0 \end{bmatrix} \quad (13.3.6)$$

$$T_{b,T} = 160N \quad (13.3.7)$$

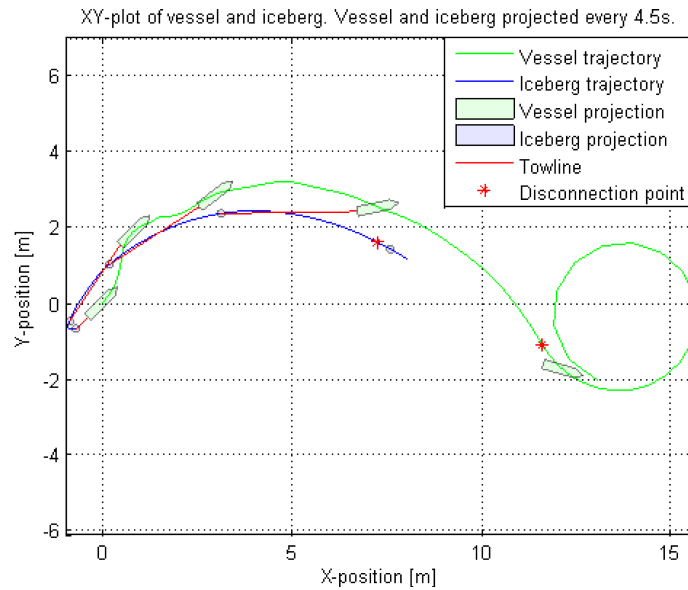
$$\delta_{b,limit} = 3 \quad (13.3.8)$$

$$T_{slip,T} = 140N \quad (13.3.9)$$

$$\delta_{slip,limit} = 5 \quad (13.3.10)$$

$$T_{overturn,T} = 130N \quad (13.3.11)$$

$$\delta_{overturn,limit} = 7 \quad (13.3.12)$$



(a)

```
theTime =
    17.5000
Iceberg has overturned, towline is disconnected.
```

(b)

Figure 13.4: Scenario 4: (13.4a) XY-plot for the vessel and iceberg trajectories, with disconnection point when iceberg overturns. (13.4b) Alert in MatLab command window when iceberg overturns.

## 13.4. Thrust penalty control

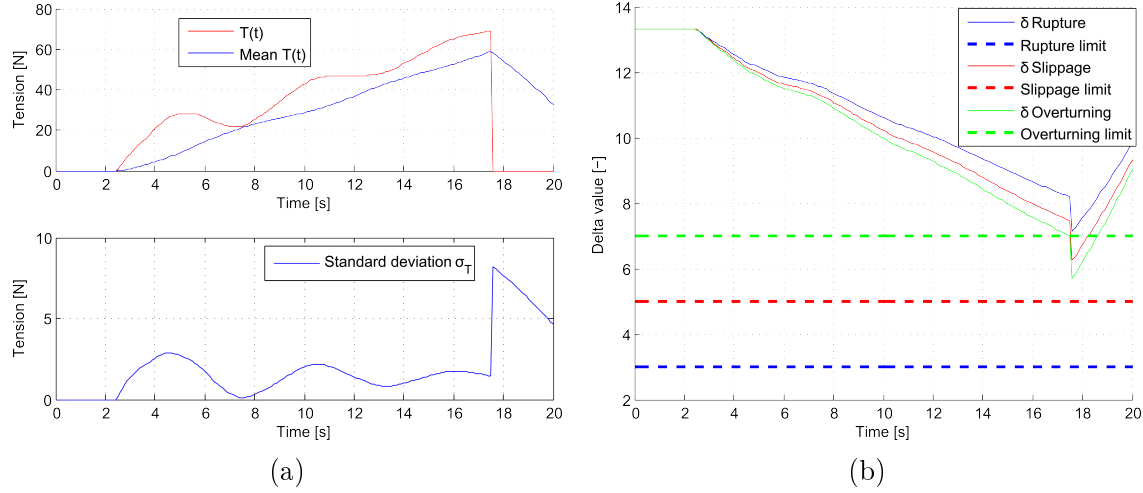


Figure 13.5: Scenario 4: (13.5a) Measurement, mean, and standard deviation of the towline tension. (13.5b) Reliability indices for the three failure modes, showing how  $\delta_{\text{overturn},T} < \delta_{\text{overturn},\text{limit}}$ .

### 13.3.2 Discussions, failure mode implementation

Figure 13.5 shows how the tension increases with time, and how the reliability index for iceberg overturning reaches its limit. As can be seen from Figure 13.4, the vessel and iceberg disconnect after the iceberg overturns, and an alert is printed in MatLab.

In the previous scenarios large transients were seen in the towline tension during the initiation phase. In this scenario, there is a slow rise of thrust, which has resulted in a stable rise of towline tension. Since there are no large transients, the tension is continuously valid for use in reliability-indices. This is recommended for iceberg towing, as it does not wear and tear the equipment as much, and it makes it easier to guarantee safe towing via reliability indices.

## 13.4 Thrust penalty control

As discussed in Section 11.1, a way to avoid going below the reliability index limit could be to penalize the thrust from the controller.

Note that the penalty  $p_k$  equals 1 at zero penalty, and 0 at full penalty. In retrospect, the penalty should rather have been implemented as  $(1 - p_k)$  in order to be more intuitive.

### 13.4.1 Scenario 5

In order to simulate thrust penalty control, a reference position and reference velocity is set. These are fed through the reference model described in Section 9.3. The new

desired values for position and velocities are then fed to the backstepping controller. The bias term in the controller is in this scenario set to zero. This is because the controller does not need to overcome any towline forces to follow an iceberg path, and also because the current magnitude  $|V_c| = 0$ . Tuning of the reference model and backstepping controller is discussed in Scenario 7.

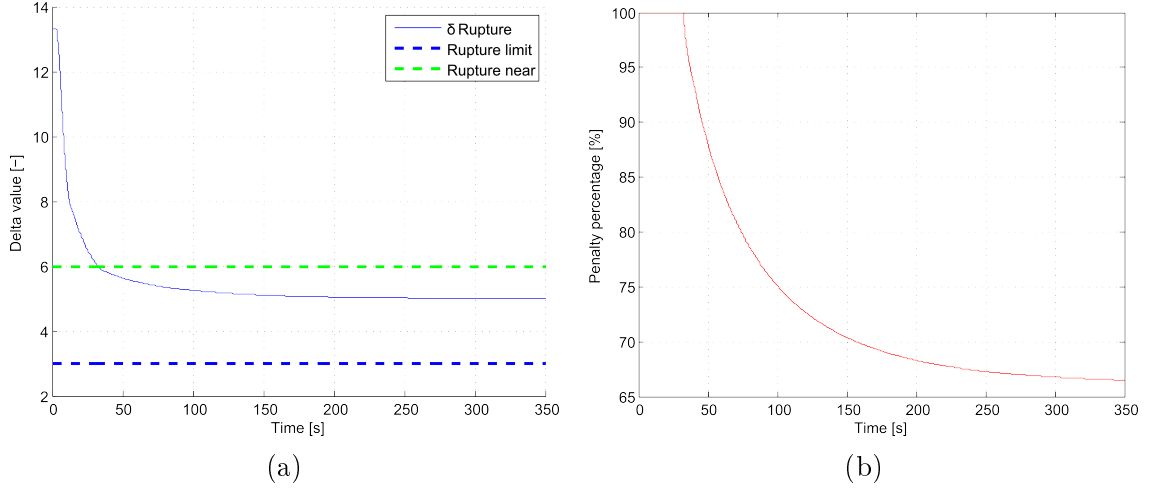


Figure 13.6: Scenario 5: (13.6a) Plot showing  $\delta_T$  over time, and the limits  $\delta_{near}$  and  $\delta_{limit}$ . (13.6b) Development of the penalty percentage. 100% means zero penalty, while 0% means full penalty.

For simplicity, only the reliability index for towline rupture  $\delta_T$  is used in this scenario. In order to avoid the initial transients and steadily decrease the reliability index, a linear time-increasing velocity reference is chosen. The following are the values for this simulation:

$$T_s = 350s \quad (13.4.1)$$

$$\eta_s(0) = [0, 0, 0]^T \quad (13.4.2)$$

$$\eta_i(0) = [-1, 0]^T \quad (13.4.3)$$

$$|V_c| = 0 \quad (13.4.4)$$

$$\eta_{ref} = [800, 0, 0]^T \quad (13.4.5)$$

$$\nu_{ref} = [0.01t, 0, 0]^T \quad (13.4.6)$$

$$T_{b,T} = 160N \quad (13.4.7)$$

$$\delta_{b,limit} = 3 \quad (13.4.8)$$

$$\delta_{b,near} = 6 \quad (13.4.9)$$

## 13.4. Thrust penalty control

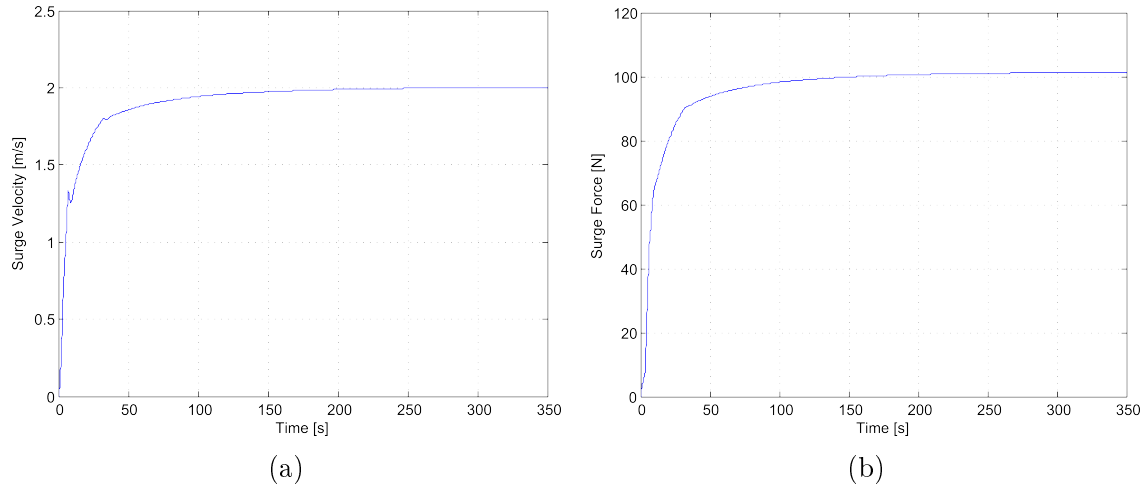


Figure 13.7: Scenario 5: (13.7a) Surge velocity is shown. Sway and yaw velocities are zero. Surge velocity is seen limited by saturation. (13.7b) The penalized force  $\tau_{pen}$  in surge. Sway and yaw forces are zero.

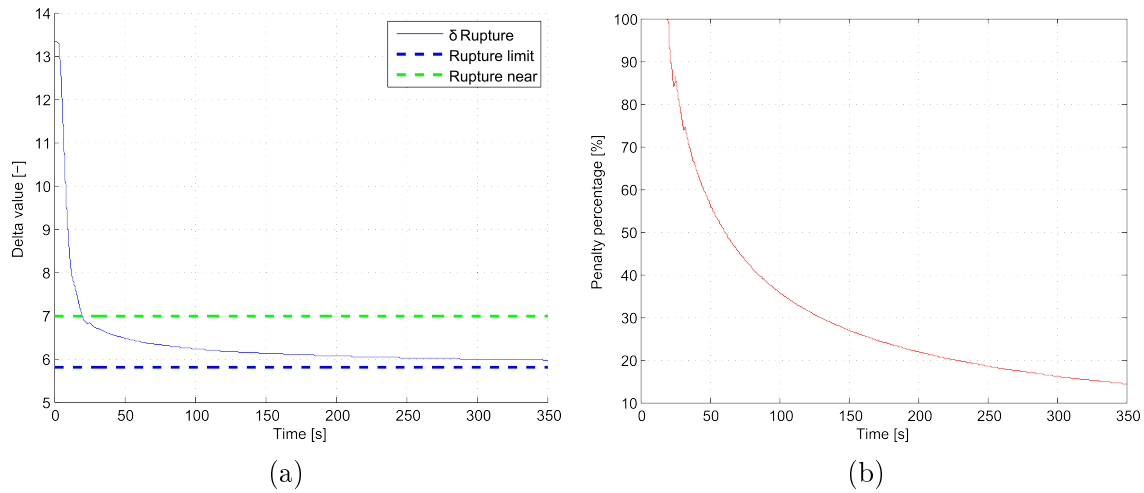


Figure 13.8: Scenario 6: (13.8a) Plot showing  $\delta_T$  over time, and the limits  $\delta_{near}$  and  $\delta_{limit}$ . (13.8b) Development of the penalty percentage. 100% means zero penalty, while 0% means full penalty.

### 13.4.2 Scenario 6

The same setup as in Scenario 5 is tested, only with changed values for:

$$\delta_{b,limit} = 5.8 \quad (13.4.10)$$

$$\delta_{b,near} = 7 \quad (13.4.11)$$

The aim with this scenario is to activate the penalty without help from the velocity saturation element which helped in Scenario 5.

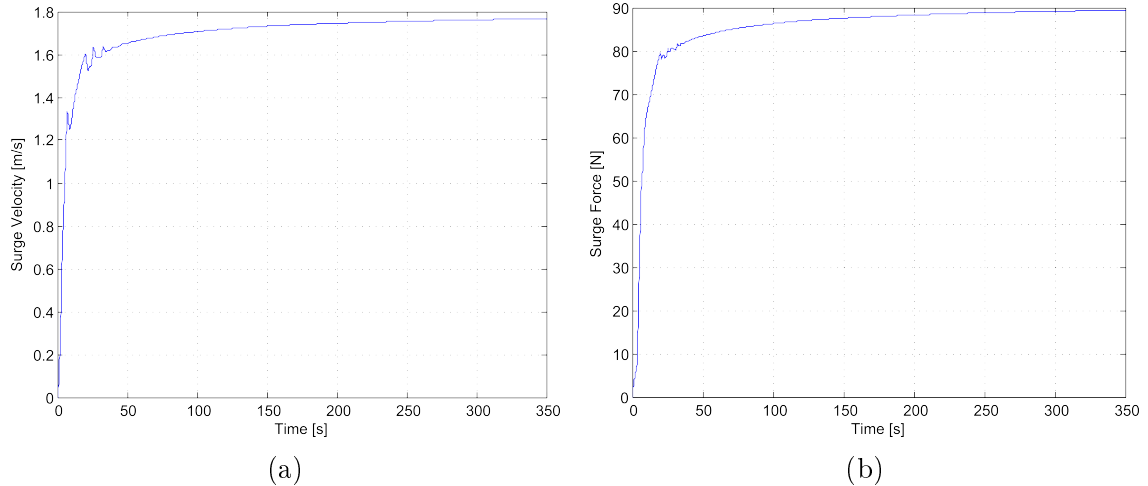


Figure 13.9: Scenario 6: (13.9a) Surge velocity, seen limited by penalty controller. (13.9b) The penalized force  $\tau_{pen}$  in surge.

### 13.4.3 Discussions, thrust penalty control

For Scenario 5, it is easily seen that the penalty control is activated after approximately 32s. At this point, surge velocity is at  $1.8\frac{m}{s}$ , and still rising a little while longer, letting the penalty increase. In the reference model, a velocity saturation element is added, which does not allow a higher surge velocity than  $2\frac{m}{s}$ . In Figure 13.7a it is seen that the velocity stops at  $2\frac{m}{s}$ , making it unclear whether the penalty controller would work without help from the velocity saturation.

Therefore, in Scenario 6, raised limits for the reliability index are simulated. It is now seen that the surge velocity is heavily reduced by the penalty control. However, the trends of  $\tau_{pen}$  and the penalty graph indicate that this scenario (which has a steadily increasing velocity reference) may eventually reach the limit for towline rupture.

```
Towline has ruptured, and is disconnected.
theTime =
    576.8000
```

Figure 13.10: Towline rupture alert for Scenario 6.

With that in mind, Scenario 6 is run a while longer, for 600s. The result is towline rupture, as seen in Figure 13.10. The conclusion from this is that direct thrust penalty, installed in this manner, may delay the failure mode, but is no guarantee if the velocity reference keeps commanding increased thrust. The immediate lesson

from this, is to set  $\delta_{limit}$  higher than the actual limit. If so, the tow force would be zero before it could actually happen. However, zero tow force would not be able to perform the tow. Because the method can not guarantee against failure modes occurring, it is deemed ineffective, and advised against using.

Another suggestion is to use velocity reference control instead, to make sure the commanded velocity does not keep increasing as it does in scenarios 5 and 6. This is further investigated in Scenario 8.

## 13.5 Iceberg LOS guidance and control

The LOS guidance and control scheme from Chapter 9 is implemented, using the observer from Chapter 8 to get position, velocity and bias data for use in the back-stepping controller.

In the process of setting up the simulations, tuning was needed. The resulting tuning for the observer matrices  $T_b$ ,  $K_2$ ,  $K_3$  and  $K_4$ , the reference model matrices  $A_{ref}$ ,  $B_{ref}$  and  $C_{ref}$ , and saturation elements, the controller matrices  $K_p$  and  $K_d$ , and the variables for the LOS guidance, are all found in Appendix A.

### 13.5.1 Scenario 7

In Scenario 7, the goal is to show the performance of the iceberg LOS control scheme in the presence of a constant, irrotational ocean current. This will be shown for three different relative angles between the desired path and the ocean current angle.

The following initialization is used, where the current direction  $\beta_c$  has three different values:

$$T_s = 400s \quad (13.5.1)$$

$$\eta_s(0) = [-2, -1, 0]^T \quad (13.5.2)$$

$$\eta_i(0) = [-1, -1]^T \quad (13.5.3)$$

$$|V_c| = 0.01 \frac{m}{s} \quad (13.5.4)$$

$$\beta_c = \left\{ \pi, 0, \frac{5\pi}{8} \right\} \quad (13.5.5)$$

$$waypoint(1) = (x = -5, y = -3) \quad (13.5.6)$$

$$waypoint(2) = (x = 7, y = 3) \quad (13.5.7)$$

$$U_{ref,i} = 0.03 \frac{m}{s} \quad (13.5.8)$$

Using the first current angle,  $\beta_c = \pi$ , the performance of the reference model and observer are shown in Appendix A, figures A.1 - A.4. As can be seen from the reference model plot,  $x_d$  is slightly ahead of  $x_{ref}$ . This is normal, since the

reference model is also fed a desired forward speed. The observed positions are very accurate. As for the velocities, there is a steady, small offset of approximately  $0.002 \frac{m}{s}$  in surge. This is so small that it is considered acceptable. When the position and velocity tuning is considered acceptable, the estimated bias is acceptable to use in the controller.

Furthermore, XY-plots, and the development of the integral term in the iceberg LOS algorithm, are shown for the three current angles  $\beta_c$  in figures 13.11, 13.12 and 13.13.

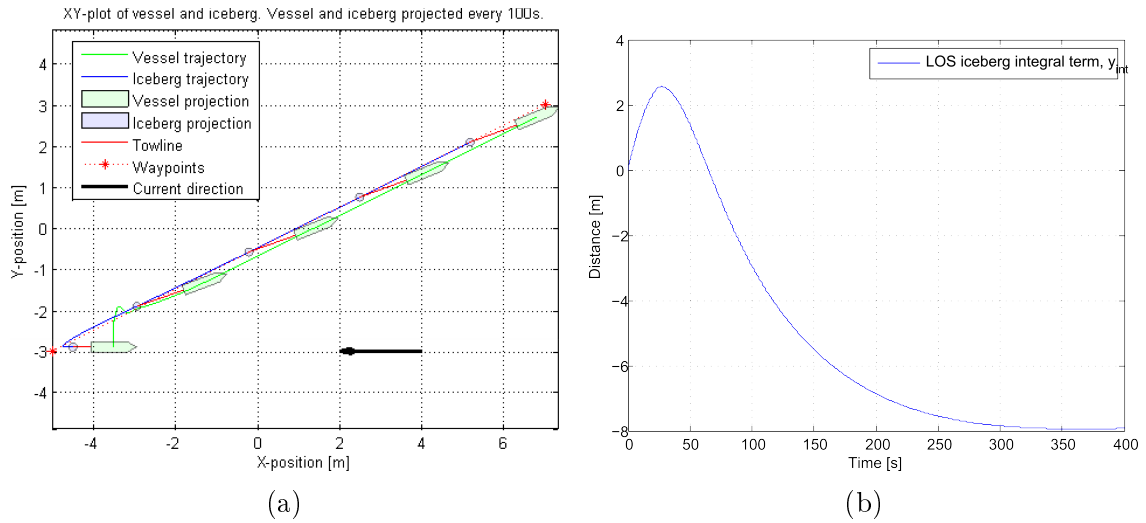


Figure 13.11: Scenario 7,  $\beta_c = \pi$ : (13.11a) XY-plot of the vessel and iceberg trajectories. (13.11b) The development of  $y_{int}$  in the iceberg LOS algorithm.

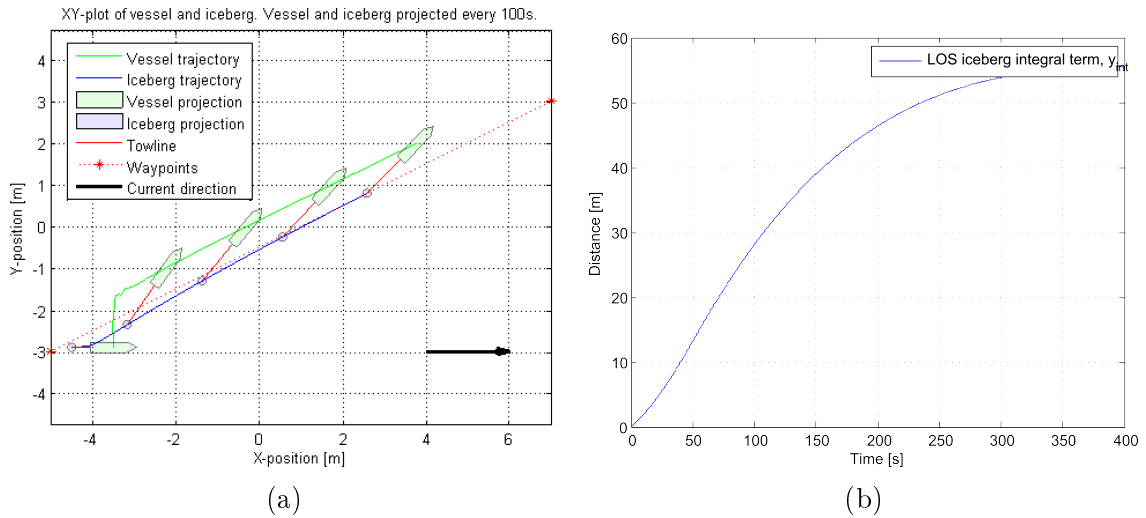


Figure 13.12: Scenario 7,  $\beta_c = 0$ : (13.12a) XY-plot of the vessel and iceberg trajectories. (13.12b) The development of  $y_{int}$  in the iceberg LOS algorithm.



## 13.6. Combined strategy, LOS iceberg- and reliability control

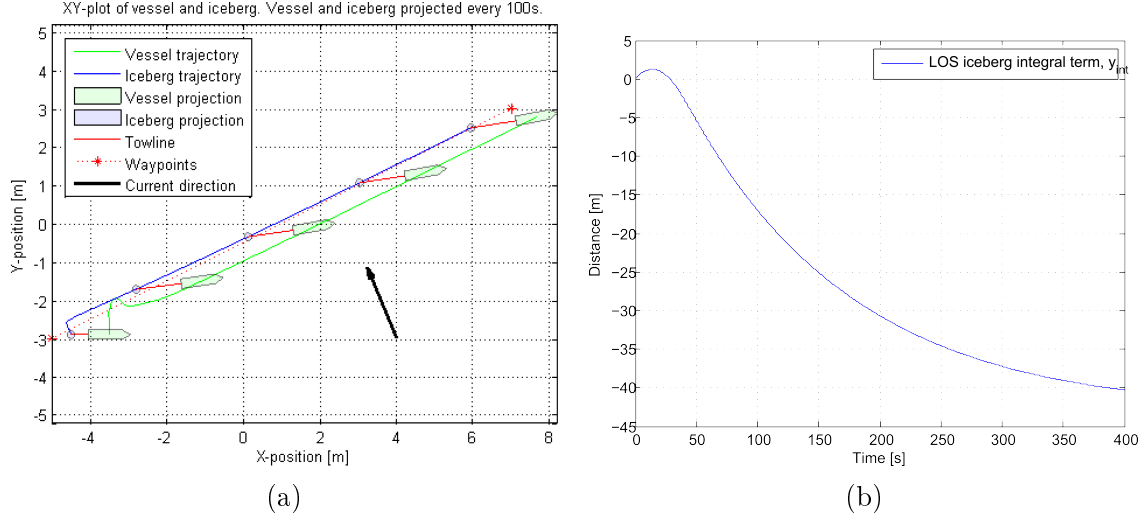


Figure 13.13: Scenario 7,  $\beta_c = \frac{5\pi}{8}$ : (13.13a) XY-plot of the vessel and iceberg trajectories. (13.13b) The development of  $y_{int}$  in the iceberg LOS algorithm.

### 13.5.2 Discussions, iceberg LOS control

The XY-plots and the development of the integral term from the iceberg LOS algorithm are seen in figures 13.11 - 13.13. In all three runs, the iceberg is seen to converge towards the waypoint-constructed path. It is also seen that the integral value  $y_{int}$  converges towards a certain value when the tow operation stabilizes on the desired path.

## 13.6 Combined strategy, LOS iceberg- and reliability control

In this simulation, the goal is to safely tow the iceberg along the desired path, while avoiding failure modes. This is implemented using the same setup as in Section 13.5, with an addition of the velocity reference penalty scheme from Section 11.2.

Note that the penalty  $p_k$  equals 1 at zero penalty, and 0 at full penalty.

### 13.6.1 Scenario 8

For simplicity, the only failure mode considered is towline rupture. To do this, three steps will be performed:

1. The scenario is run without velocity reference penalty, showing how  $\delta_T$  goes below  $\delta_{limit}$  - causing towline rupture.

2. The scenario is run with the penalty  $p_k$ , but without the limit on the positive rate of change  $\dot{p}_k^+$ .
3. The scenario is run with the penalty  $p_k$ , and with the limit on  $\dot{p}_k^+$ .

The data in these simulations are given below. It is seen that  $U_{ref,i}$  is steadily increasing until it reaches a maximum limit.

$$T_s = 1100s \quad (13.6.1)$$

$$\eta_s(0) = [-3.5, -2.9, 0]^\top \quad (13.6.2)$$

$$\eta_i(0) = [-4.5, -2.9]^\top \quad (13.6.3)$$

$$|V_c| = 0.01 \frac{m}{s} \quad (13.6.4)$$

$$\beta_c = \pi \quad (13.6.5)$$

$$waypoint(1) = (x = -5, y = -3) \quad (13.6.6)$$

$$waypoint(2) = (x = 17, y = 13) \quad (13.6.7)$$

$$U_{ref,i} = \min(0.03, \frac{0.03t}{200}) \frac{m}{s} \quad (13.6.8)$$

$$T_{b,T} = 6N \quad (13.6.9)$$

$$\delta_{b,near} = 9.5 \quad (13.6.10)$$

$$\delta_{b,limit} = 9 \quad (13.6.11)$$

$$\dot{p}_{min}^+ = \frac{1}{600000} \frac{1}{s} \quad (13.6.12)$$

$$\dot{p}_{max}^+ = \frac{1}{6000} \frac{1}{s} \quad (13.6.13)$$

The first run, where the velocity reference penalty control is not implemented, gives the  $\delta_T$  results as shown in Figure 13.15. The result is towline rupture, as seen in Figure 13.14.

```

theTime =
199.9000
Towline has ruptured, and is disconnected.

```

Figure 13.14: Towline rupture alert for Scenario 8, with no velocity reference penalty.

The second run, where the penalty control is added to the velocity reference, but without the limit on  $\dot{p}_k^+$ , is shown to bring the iceberg to and along the desired path without rupturing the towline, seen in Figure 13.17. However, as seen in Figure 13.18a, the penalty oscillates much, making both the velocity reference (Fig. 13.18b) and  $\delta_T$  (Fig. 13.16) oscillate largely.

### 13.6. Combined strategy, LOS iceberg- and reliability control

---

The third run, with the penalty, and the limiting elements to  $\dot{p}_k^+$  is simulated next, and is shown in figures 13.19 - 13.21. The iceberg is towed along the pre-defined path, and both the penalty and the velocity reference are seen to be relatively stable.

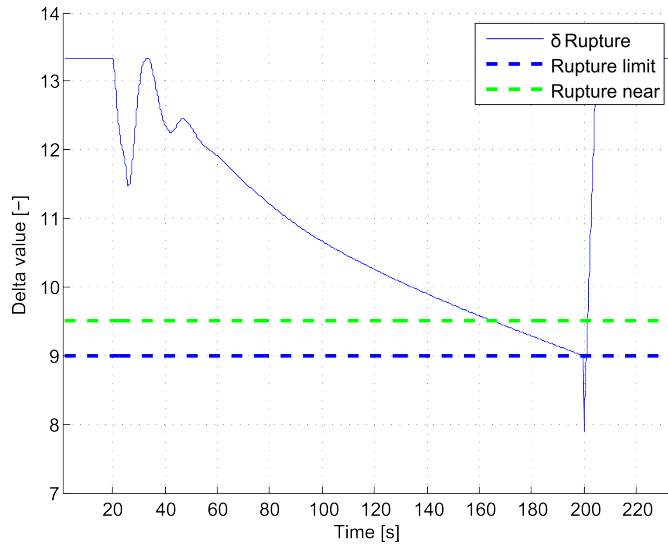


Figure 13.15: Scenario 8: No penalty added, plot showing  $\delta_T$  leading to towline rupture.

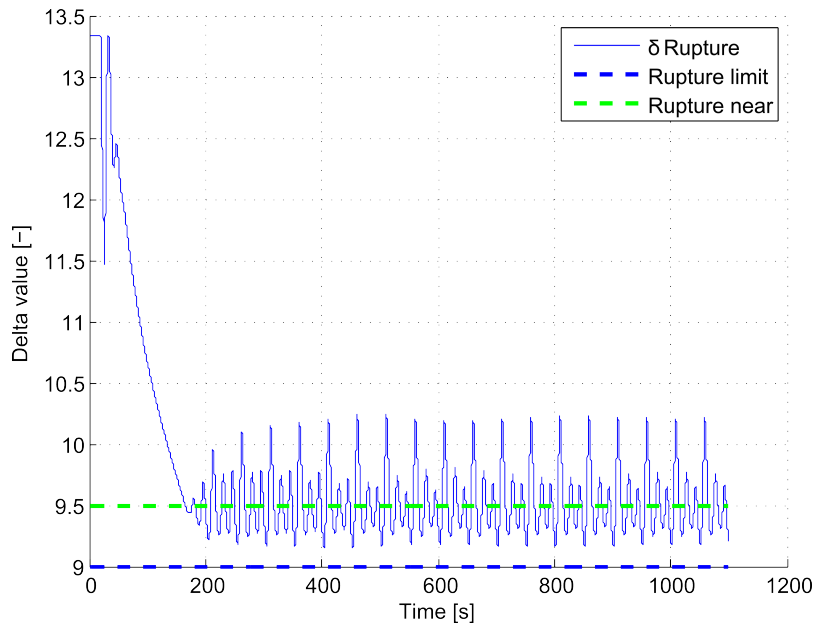


Figure 13.16: Scenario 8, penalty added, without  $\dot{p}_k^+$ : The development of  $\delta_T$  in the iceberg LOS algorithm, oscillating largely due to the penalty.

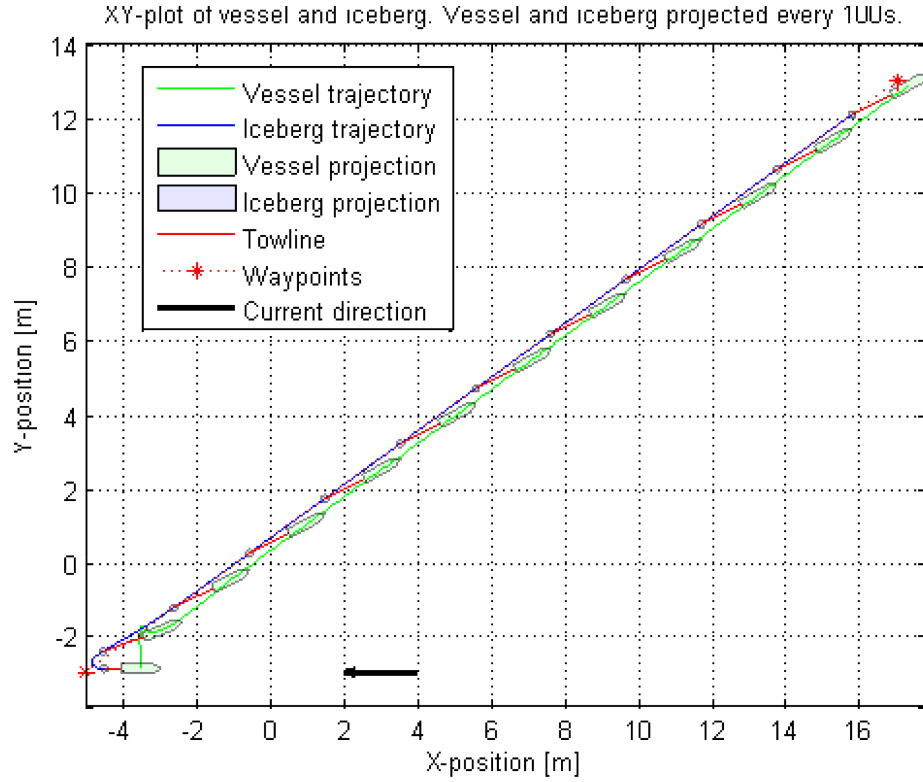


Figure 13.17: Scenario 8, penalty added, without  $\dot{p}_k^+$ : XY-plot of the vessel and iceberg trajectories.

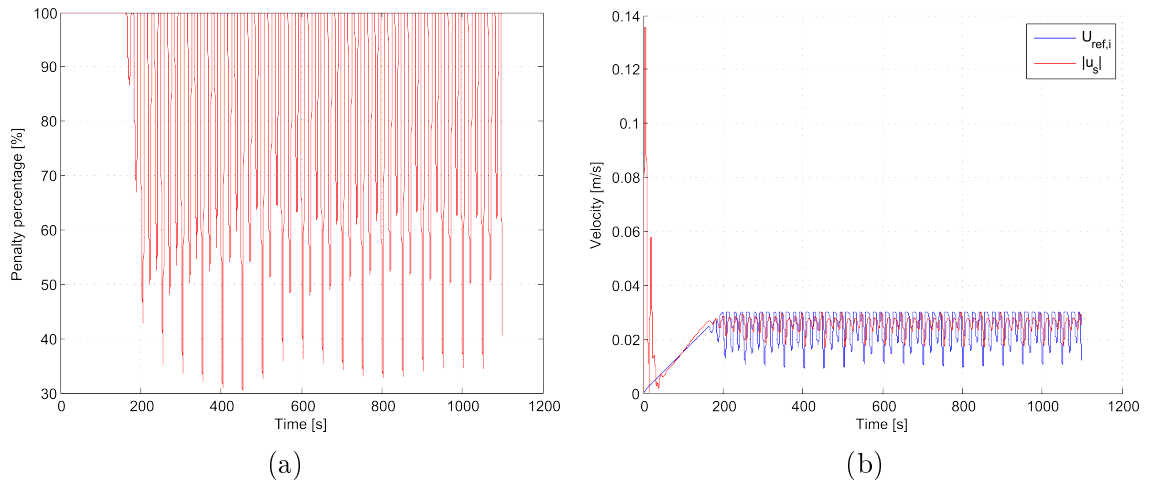


Figure 13.18: Scenario 8, penalty added, without  $\dot{p}_k^+$  (13.18a) The development of  $p_k$ , oscillating largely. (13.18b) The development of  $U_{ref,i}$  vs the absolute towing vessel velocity, showing oscillations in the reference velocity.

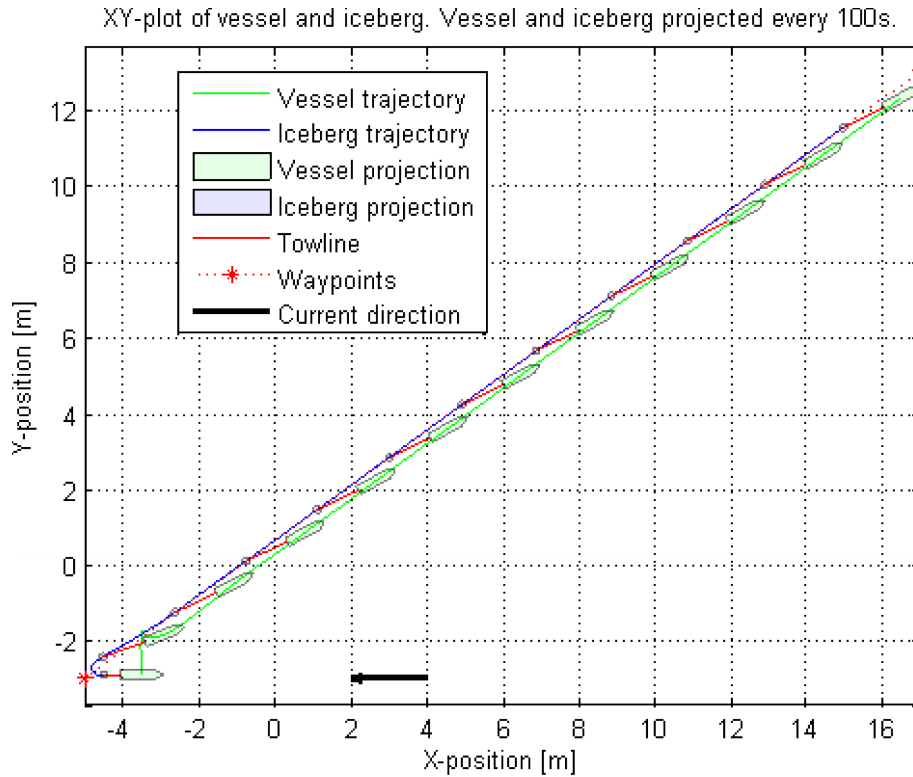


Figure 13.19: Scenario 8, penalty added, with  $\dot{p}_k^+$ : XY-plot of the vessel and iceberg trajectories.

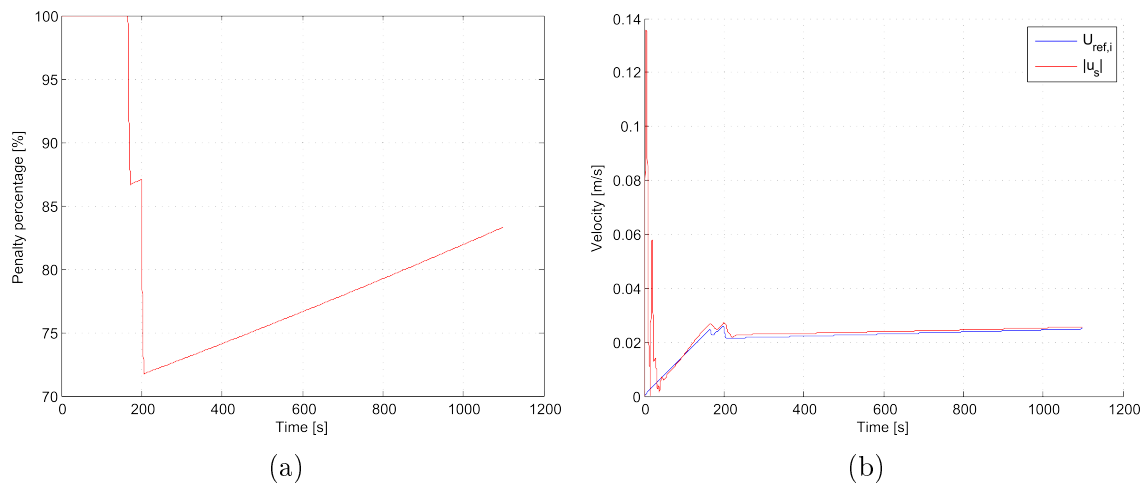


Figure 13.20: Scenario 8, penalty added, with  $\dot{p}_k^+$  (13.20a) The development of  $p_k$ , increasing slowly after being decreased. (13.20b) The development of  $U_{ref,i}$  vs the absolute towing vessel velocity, where  $U_{ref,i}$  increases slowly along with  $p_k$ .

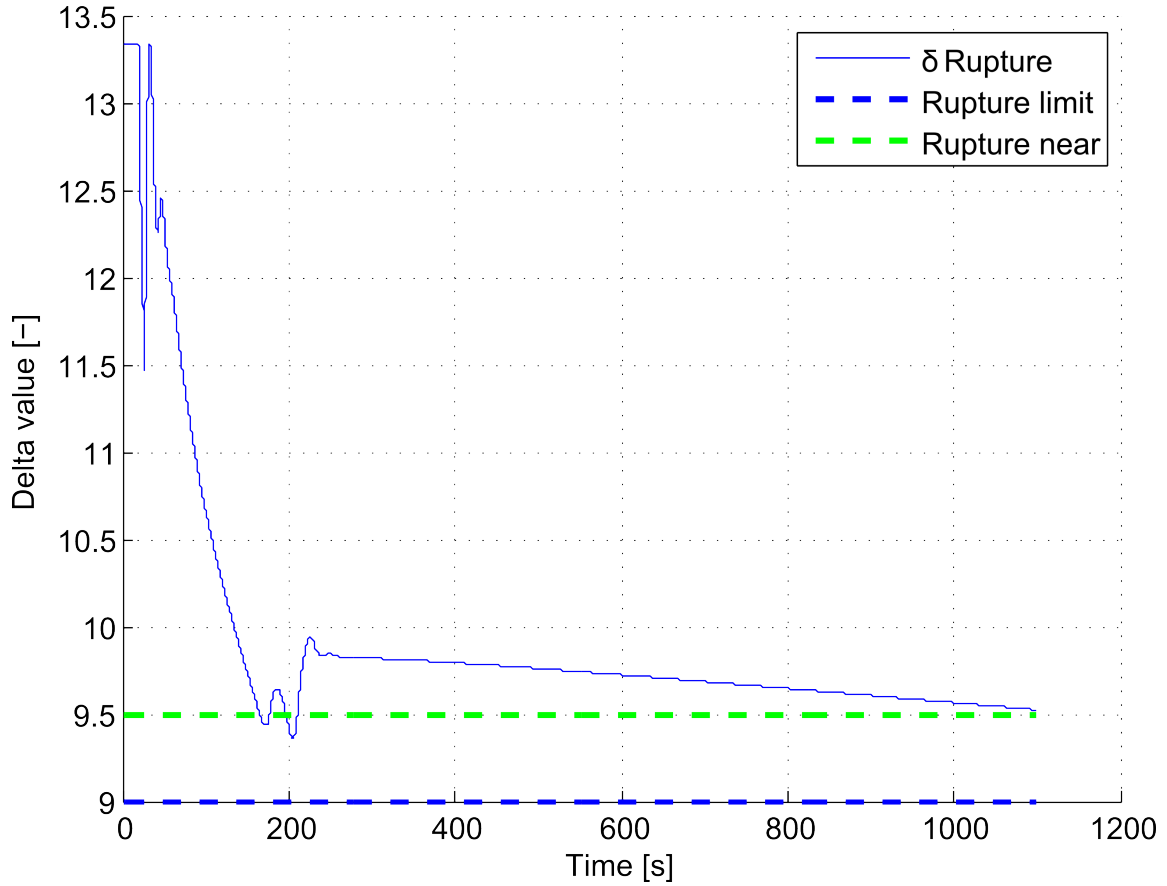


Figure 13.21: Scenario 8, penalty added, with  $\dot{p}_k^+$ : The development of  $\delta_T$  in the iceberg LOS algorithm, much more stable now then without the limitation to  $\dot{p}_k^+$ .

### 13.6.2 Discussions, combined LOS- and reliability-control

As seen in Figure 13.15, the vessel was not able to tow the iceberg along the desired path without rupturing the towline. By adding a penalty to the reference velocity, it is seen that the iceberg moves along the path without rupturing the towline. Comparing runs 2 (figures 13.16 - 13.18) and 3 (figures 13.19 - 13.21), the importance of stabilizing the penalty is illustrated. Penalty stabilization creates a more stable velocity reference, thus avoiding large oscillations in the towline tension and reliability index.

## 13.7 HIL test, with position measurement errors

Position measurement errors are implemented into the simulation model, as described in Section 12.5.1. By implementing these errors, it is possible to test how the system can handle them.

### 13.7.1 Scenario 9

In this scenario, the exact same setup as in Scenario 7 is tested, with the addition of random position measurement errors. Dead reckoning is implemented into the towing vessel observer according to Section 8.1.1, in order to compensate for the loss of positional information. Only the current angle of  $\beta_c = 0$  is tested. The only new variable in scenario 9 is the desired error percentage:

$$e_{d,pos} = 0.2\%, \quad (13.7.1)$$

meaning that 2 out of 1000 samples will experience a first fault, whereas there (as described in Section 12.5.1) is a 5% chance per sample of regaining measurements once they are lost.

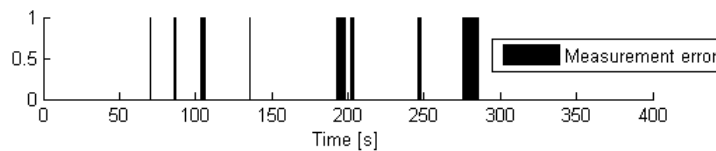


Figure 13.22: Plot showing when positioning errors  $\beta$  occur during the simulation.

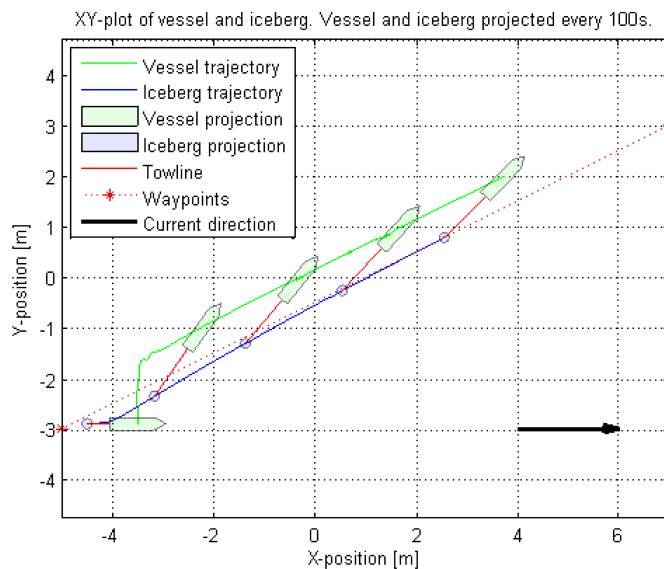


Figure 13.23: XY plot showing towing vessel and iceberg trajectories.

### 13.7.2 Discussions, position measurement errors

Figure 13.22 shows when there are measurement errors. The towing vessel is still able to tow the iceberg to and along the desired path, by applying dead reckoning

while the measurements are lacking, as seen in Figure 13.23. Figures 13.24 and 13.25 show the observer performance during the 10s of measurement loss, and show that the error between estimated and measured states is small. This means that the dead reckoning implementation works well in this example.

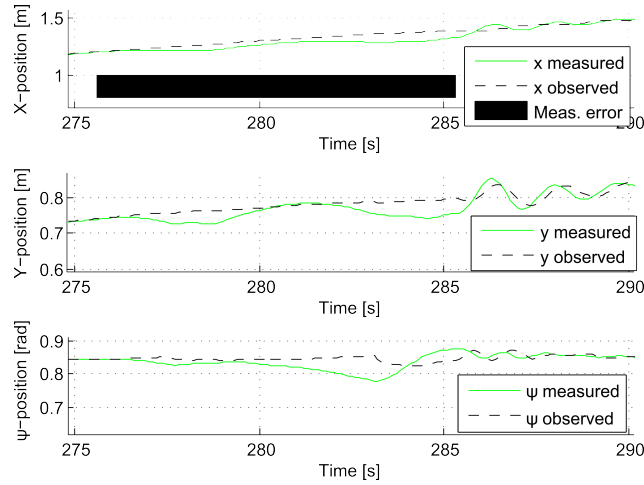


Figure 13.24: Scenario 9: Measured vs estimated positions during the period 275 – 290s. The error period is 275.6 – 285.3s.

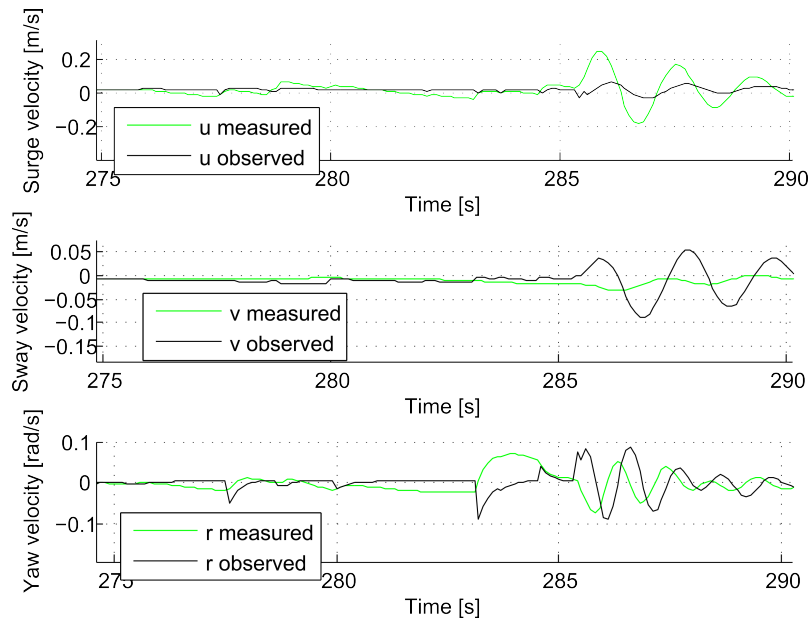


Figure 13.25: Scenario 9: Measured vs estimated velocities during the period 275 – 290s. The error period is 275.6 – 285.3s.



# Chapter 14

## Experiments

Weeks 10-11 and 17-18 of 2014 the MC Lab at NTNU was reserved for iceberg towing experiments. The objective during these weeks was to experimentally test the concepts of this thesis. Entering these weeks, the identified goals were:

1. To experimentally test a thrust penalty control scheme.
2. To experimentally test the iceberg LOS guidance and backstepping controller.

In all the experiments, the sampling period was set to 0.1s.

### 14.1 Thrust penalty control

The end goal of this experiment was to test the thrust penalty control scheme described in Section 11.1, based on a conceptual reliability index for towline rupture. Some sub-goals were defined in order to be able to test the penalty scheme:

1. To identify the relationship between velocity of the towing vessel and the measured towline tension.
2. To define feasible limits for  $\delta_{limit}$  and  $\delta_{near}$ .

Finding the tension-velocity relationship was a tuning process. CSE1 (Sec. 12.2), with the towed iceberg, was run at an approximately constant velocity until steady towing was achieved. Steady towing means that there were no visible transients in the vessel or iceberg motion, and that they moved smoothly together. During these periods, the velocity and tension were read. Due to noisy tension measurements, it was difficult to get an exact relationship, but what was definitely seen from the measurements was that for velocities below  $0.1 \frac{m}{s}$ , the steady tension was found to be below  $2N$ .

Having found an expected magnitude of the tension force, it was assumed that the mean tension required for towline rupture was  $T_{b,T} = 5N$ . The standard deviation for towline rupture was set to  $\sigma_{b,T} = 0.075T_{b,T}$  (Berntsen, 2008). In order to obtain feasible values for the mean and standard deviation of the tension measurements, it is important to get the right number of samples  $N$ . This was a tuning process, and it was decided to apply  $N = 50$ . With  $T_{b,T}$ ,  $\sigma_{b,T}$  and feasible mean and standard deviation of the measurements, the reliability index for towline rupture  $\delta_T$  could be calculated in real-time.

To find feasible limits for  $\delta_{limit}$  and  $\delta_{near}$ , CSE1 was run while measuring tensions and tow velocities and calculating  $\delta_T$ . A time-series with very few position measurement errors and relatively stable tow velocity, was chosen. Absolute velocity and mean towline tension are shown in Figure 14.2. The corresponding  $\delta_T$  is shown in Figure 14.1.

Using Figure 14.1, feasible limits were set to:

$$\delta_{near} = 6 \quad (14.1.1)$$

$$\delta_{limit} = 4 \quad (14.1.2)$$

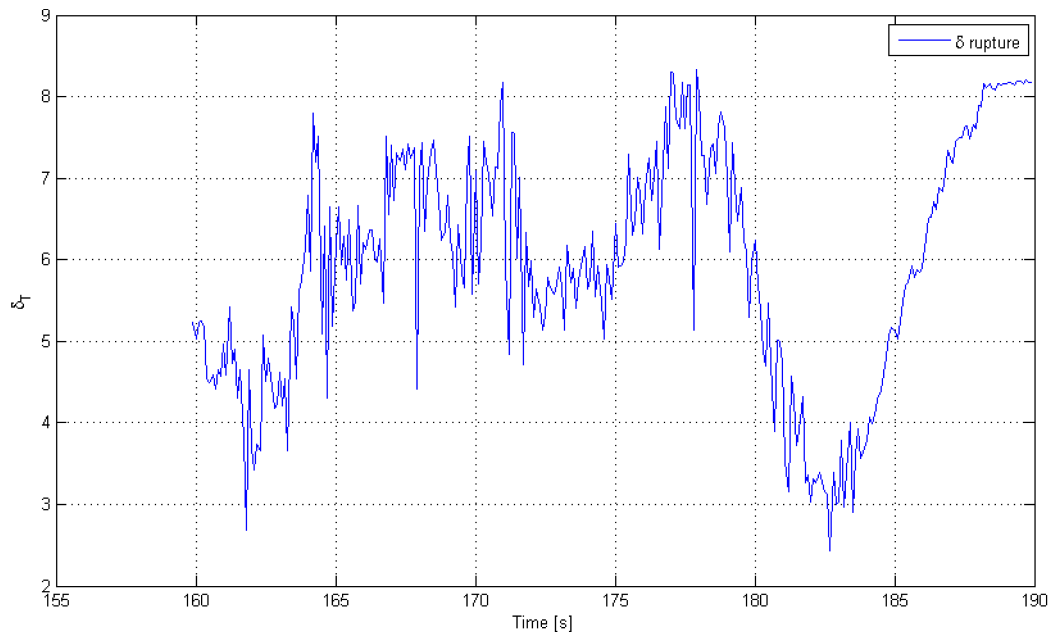


Figure 14.1:  $\delta_T$ , the reliability index for towline rupture during a time-series with mean tension and absolute velocities shown in Figure 14.2.

Having set the limits, a few attempts were made at towing the iceberg while applying the thrust penalty scheme. The penalty was applied when the reliability-index went below  $\delta_{near}$  as seen in figures 14.3 - 14.4. However, it is seen that  $\delta_T$  went below  $\delta_{limit}$  several times, indicating rupture of the towline. It was later found that the thruster mapping adopted from Skåtun (2011) did not work for the low velocities in the towing experiments. This is probably what caused the penalty attempts to fail, as the thrusters on CSE1 continuously kept producing more thrust than what was commanded of them. This means that when the penalty scheme demanded half thrust, CSE1 still produced more thrust than commanded, and  $\delta_T$  was bound to go below the limit.

## 14.1. Thrust penalty control

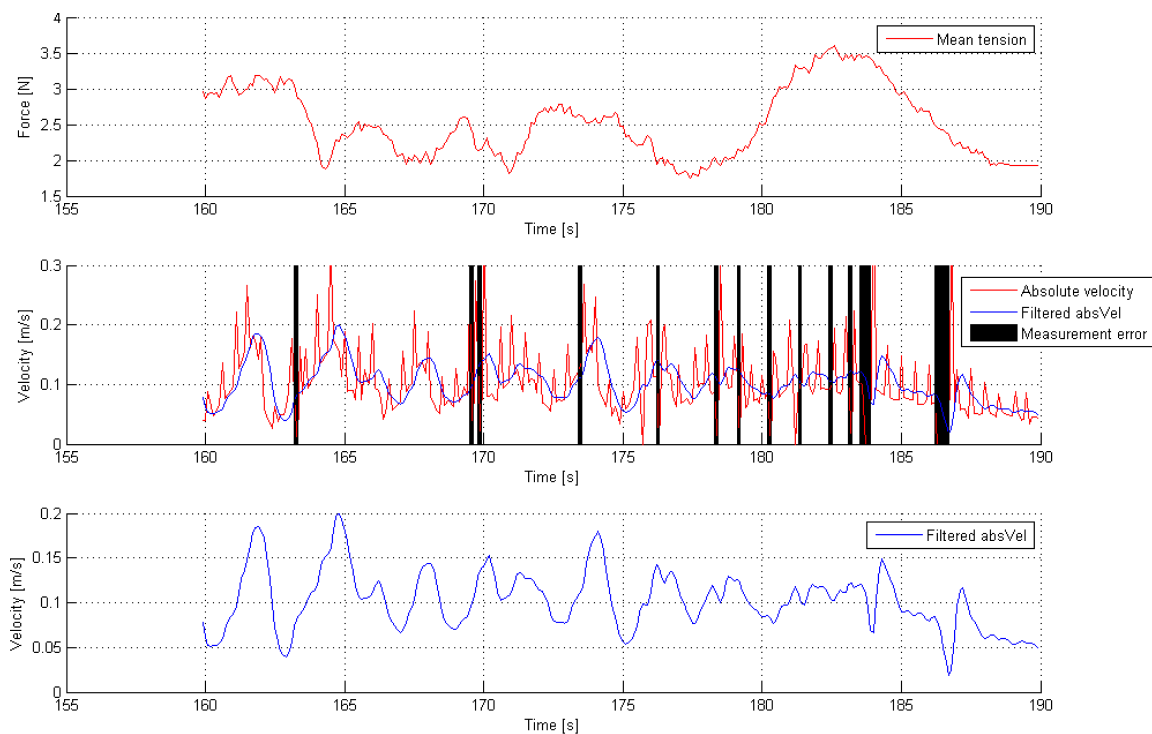


Figure 14.2: Mean tension and absolute velocity of a time-series. In the center plot, samples with measurement error are blacked out.

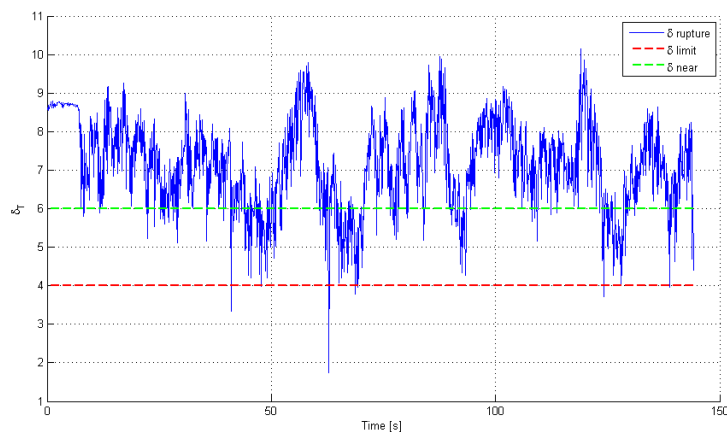


Figure 14.3:  $\delta_T$ , the reliability index for towline rupture, shown with the limits  $\delta_{near}$  and  $\delta_{limit}$ , during a thrust penalty control attempt.

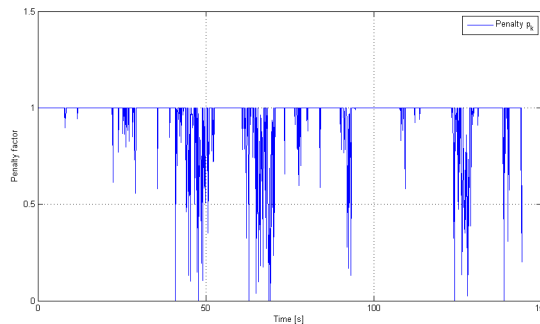


Figure 14.4: Development of the penalty applied to the thrust  $p_k$ , during a thrust penalty control attempt.

## 14.2 Iceberg LOS guidance and control

The end goal of this experiment was to test the iceberg LOS guidance and control scheme as described in Chapter 9. For a stepwise experimental procedure, the following sub-goals were determined:

1. Test iceberg LOS for a straight line pointing directly forward in the x-direction, without adding ocean current. The waypoints were:

$$\text{waypoint}(1) = (x = 0, y = 0) \quad (14.2.1)$$

$$\text{waypoint}(2) = (x = 7.5, y = 0) \quad (14.2.2)$$

2. Test iceberg LOS for a diagonal line, without adding ocean current. The waypoints were:

$$\text{waypoint}(1) = (x = 0, y = -1) \quad (14.2.3)$$

$$\text{waypoint}(2) = (x = 7.5, y = 1) \quad (14.2.4)$$

3. Test iceberg LOS for a diagonal line, adding ocean current by moving the carriage (Fig. 12.1) carrying the positioning system's cameras. The waypoints were the same as in (14.2.3) and (14.2.4).

During the second week in the MC Lab, the iceberg LOS guidance and control scheme was implemented, with a backstepping controller that used feedback of tension measurements to compensate the tow force affecting the towing vessel. After a few failed attempts on Sub-goal 1, two things became clear:

1. The tension measurement feedback was not successful in compensating the tow force.

2. Calibration of the positioning system’s cameras was very important, and needed to be recent in order to produce good measurements, otherwise measurement errors would be frequent.

In order to overcome these issues, a towing vessel observer was implemented, as described in Chapter 8. The backstepping controller was designed on the principle of a known bias state, which was estimated in the observer with the purpose of compensating both the tow force, and the external forces affecting the vessel. In addition, dead reckoning was implemented to compensate for lost position measurements, as described in Section 8.1.1.

Having implemented the observer and new backstepping controller, it was seen that the towing vessel and iceberg moved somewhat in the right direction. Still attempting to complete Sub-goal 1, the last tow attempt in week 2 is shown in Figure 14.5. It is seen that CSE1 is not able to tow the iceberg to the path. However, viewing the plot of the commanded sway thrust  $\tau_v$ , it is seen to constantly oscillate about  $-2N$ . This means that the controller is attempting to move the vessel in the negative y-direction. However, as seen in Figure 14.5a, CSE1 does not move in the negative y-direction. The conclusion from the experiments in week 2 was that there may have been something wrong with the observer, reference model and controller tuning, but the big issue was with the thrust allocation or the thruster mapping for the individual actuators. Thrust allocation was re-examined and no error was found, thus isolating the problem to the thruster mapping.

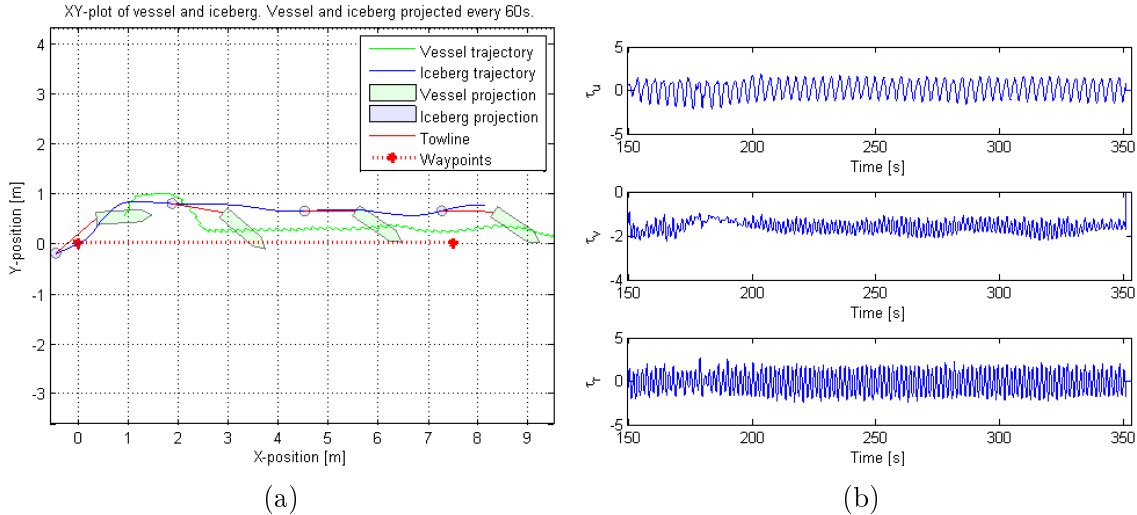


Figure 14.5: (14.5a) XY plot during LOS path following for the iceberg, without ocean current, last attempt week 2. (14.5b) Forces  $\tau_s$  fed to CSE1 during LOS path following for the iceberg, last attempt week 2.

### 14.2.1 Updated thruster mapping

For the last two weeks in the MC Lab, the thruster mapping of Skåtun (2011) was replaced with the new thruster mapping from Tran (2014), which was finished in between the second and third week in the MC Lab. In the first towing attempt after replacing the mapping, CSE1 behaved much better, but it appeared that the velocity reference of  $0.03 \frac{m}{s}$  was still a bit slow for the mapping. In the next attempt, an increase in velocity reference to  $0.06 \frac{m}{s}$  was tested with a much better result. The resulting trajectories are shown in Figure 14.6. It was seen that the iceberg was towed along the path, with some small fluctuations. Studying the position comparison plot in Figure 14.7, it is seen that the controller was not able to fully bring the measured position to the desired position, especially in the y-direction which is mostly affected by sway. This means that the controller tuning was suboptimal. However, it was deemed as good enough to continue with diagonal waypoints.

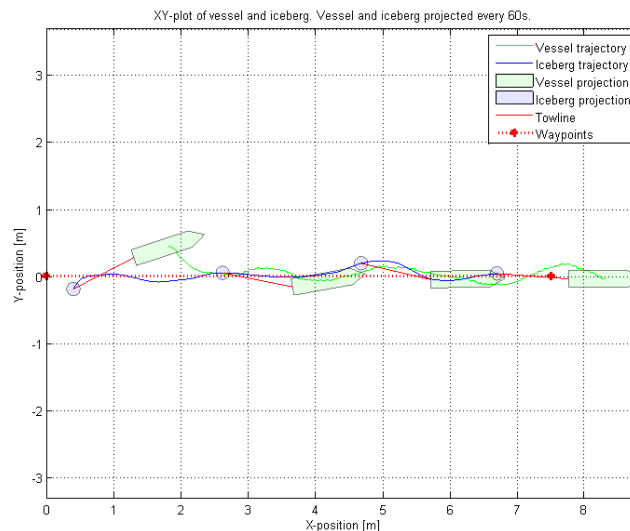


Figure 14.6: XY plot of CSE1 and iceberg trajectories during LOS iceberg path following, using straight-line waypoints in the positive x-direction.

When attempting LOS iceberg towing with diagonal waypoints, as in Sub-goal 2, similar results were achieved as with the straight x-direction waypoints in figures 14.6 - 14.7, and it was decided to tune the controller some more before adding ocean current. This was performed by running several attempts with diagonal towing, while altering  $K_p$  and  $K_d$  in the controller. After some attempts the tuning was satisfying, which resulted in the diagonal waypoints run seen in Figure 14.8. In Figure 14.9 it is seen that the measured y-position is quicker to converge to the desired y-position. It is not optimal though, as it overshoots and oscillates a little, but it is deemed good enough.

## 14.2. Iceberg LOS guidance and control

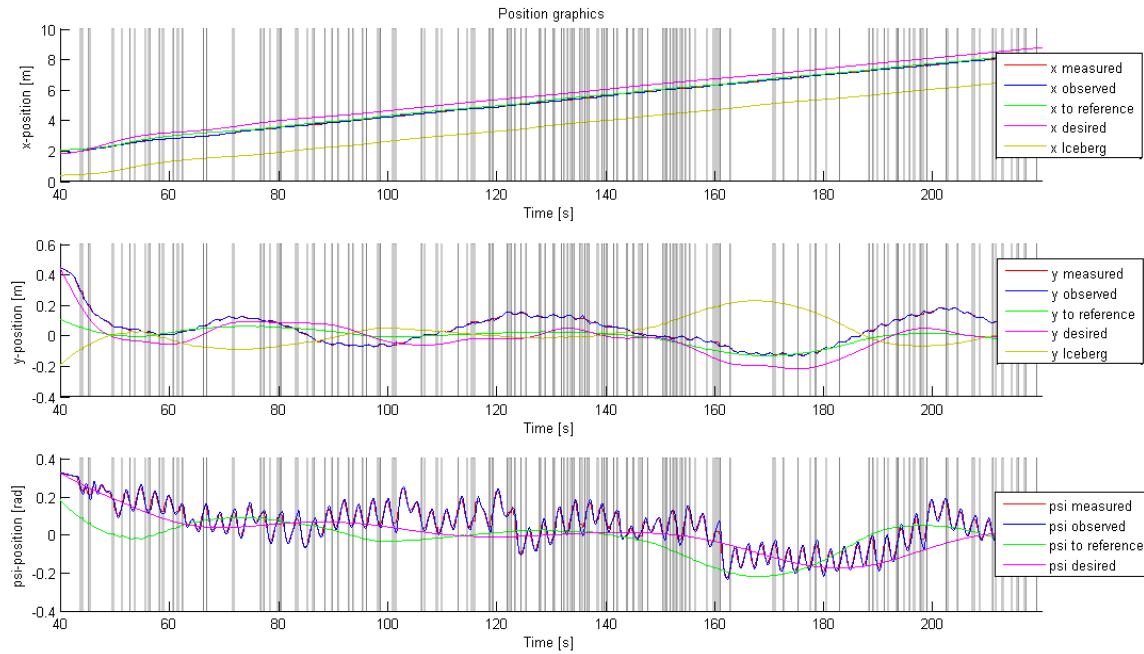


Figure 14.7: Positions in  $(x, y, \psi)$ , comparing measured, observed, pre-referenced and desired towing vessel positions, and showing iceberg position for the run in 14.6. Black stripes are samples with measurement errors.

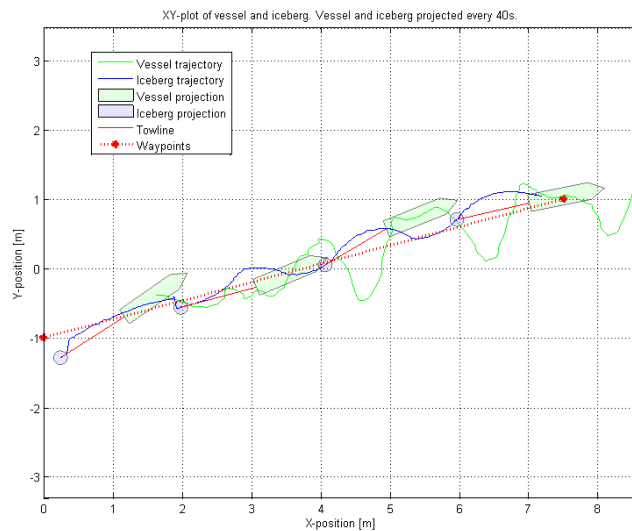


Figure 14.8: XY plot of CSE1 and iceberg trajectories during LOS iceberg path following, using diagonal waypoints in the positive x-direction.

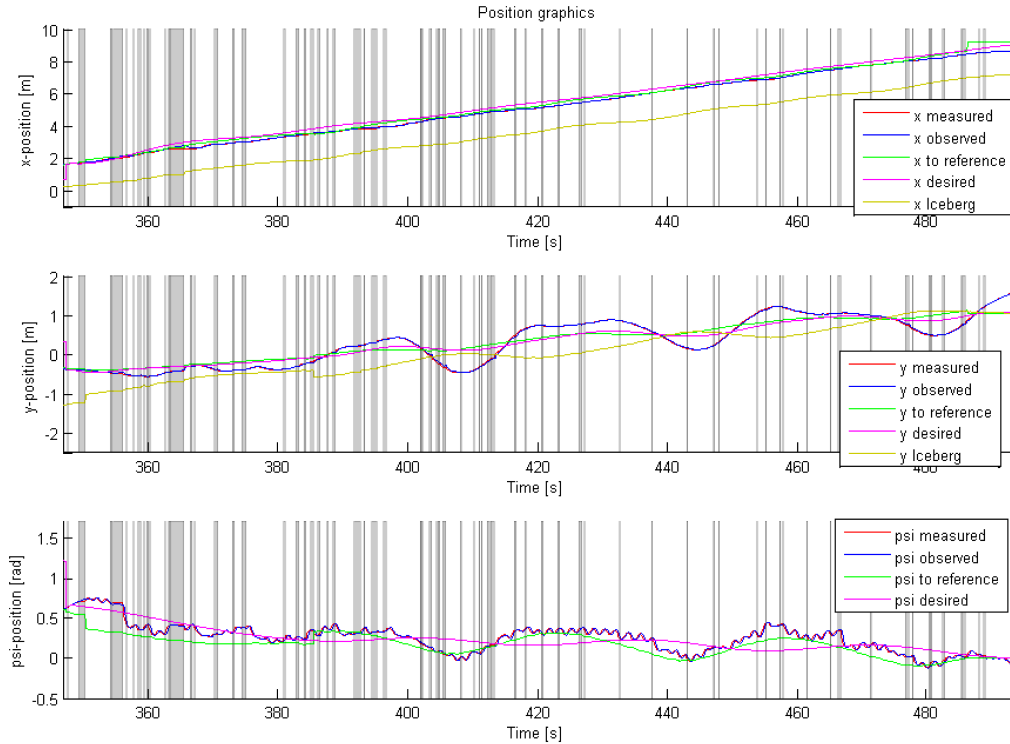


Figure 14.9: Positions in  $(x, y, \psi)$ , comparing measured, observed, pre-referenced and desired towing vessel positions, and showing iceberg position for the run in Figure 14.8. Black stripes are samples with measurement errors.

## 14.2.2 Iceberg LOS towing with ocean current

The last week in the MC Lab, experiments were conducted with an emulated ocean current, as in Sub-goal 3. It was emulated by moving the carriage (Fig. 12.1) with the cameras for the positioning system. It is possible to control the velocity of the carriage, which is the emulated current velocity,  $|V_c|$ .

The emulated current works only in the x-direction of the model basin. Thus, in order to test how CSE1 positions itself in lateral current, diagonal waypoints were used in the ocean current experiments.

The LOS towing with ocean current is presented by a run with a velocity reference of  $U_{ref,i} = 0.06 \frac{m}{s}$ , and a current velocity of  $|V_c| = 0.03 \frac{m}{s}$  in the negative x-direction. The results are presented in figures 14.10 and 14.11.

It is seen from Figure 14.10a that in the presence of ocean current, the iceberg trajectory moves along the desired path, with some small offsets along the way. Figure 14.10b, and especially the absolute velocity plot, shows that the tow operation is performed in a velocity oscillating about the velocity reference. The conclusion is that the iceberg LOS guidance and control scheme works in experiments, but that it ideally would need even more tuning. It would probably also be better if the



## 14.2. Iceberg LOS guidance and control

individual thruster mappings of CSE1 were perfectly tuned.

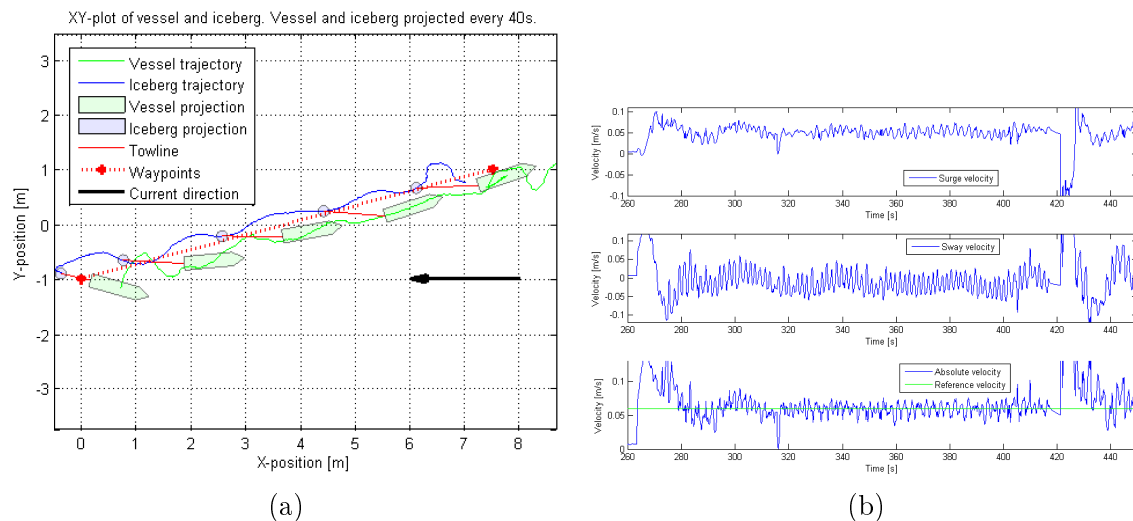


Figure 14.10: (14.10a) XY plot during LOS path following for the iceberg, with ocean current  $|V_c| = 0.03 \frac{m}{s}$ . (14.10b) Surge and sway velocities, and absolute velocity of CSE1 during the tow, plotted with the reference velocity.

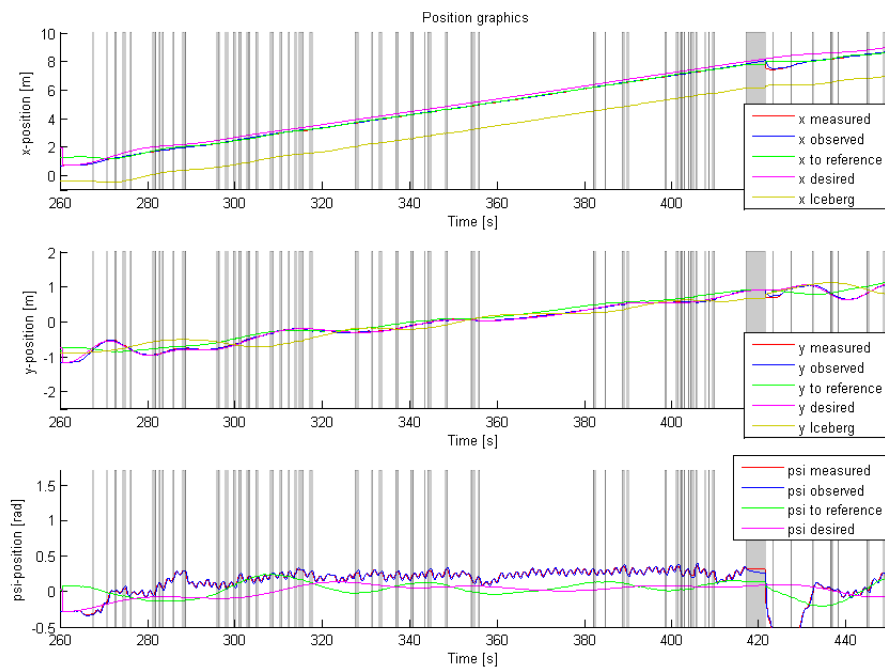


Figure 14.11: Positions in  $(x, y, \psi)$ , comparing measured, observed, pre-referenced and desired towing vessel positions, and showing iceberg position for the run in Figure 14.10a. Black stripes are samples with measurement errors.



# Conclusion

In this thesis, automatic reliability-based control of iceberg towing in open waters has been discussed, with emphasis on safely towing an iceberg along a pre-defined straight-line path in the presence of ocean current. When towing an iceberg, it is important to avoid towline rupture, towline slippage, and iceberg overturning. These have been denoted failure modes of the tow operation. Line-of-Sight- (LOS-) control has been discussed to tow the iceberg along the path, and reliability-based control was discussed to avoid the failure modes while towing. Simulations, and laboratory experiments in the Marine Cybernetics Laboratory (MC Lab) at the Norwegian University of Science and Technology (NTNU), have been performed to test the methods developed in this thesis.

A mathematical model has been developed for iceberg towing, using a 3 degrees of freedom (DOF) model for the towing vessel, and a 2 DOF model for the iceberg, both affected by an ocean current. A towline tension observer has been developed to calculate the tow force affecting both the vessel and the iceberg during simulations. The performance of the mathematical model has been tested in Section 13.1, and found to provide feasible behaviors of the vessel and iceberg. If the vessel force rises or falls too quickly, large transients will appear in the towline tension. This means that the tow operation should be initiated gradually in order to avoid these transients.

The model vessel CS Enterprise I (CSE1) was used for the experiments in the MC Lab. An iceberg model was created, and a floating towline was used. The towline was attached to CSE1 in a force ring able to measure the tow force, and was laid encircling the iceberg in the waterline. The setup proved effective for experimental iceberg towing, but the thruster mapping for CSE1 could have been better for the low velocities used in iceberg towing.

Reliability-indices for the failure modes have been developed, and minimum reliability-index limitations were implemented into the simulation model. If the reliability index goes below the set limit, the corresponding failure mode occurs. The reliability indices require steady towing in order to be valid, as they do not properly compensate for transients in the tow force.

A LOS guidance and control method has been developed, with the goal of towing an iceberg along a pre-defined straight-line path constructed by waypoints. The guidance algorithm calculates the desired course angle of the iceberg, using integral action to compensate for the ocean current. The ideal towing vessel position is calculated, in order to apply force in the desired iceberg course angle. A reference model is then used to calculate feasible trajectories for the towing vessel, based on the ideal vessel position, and an input velocity reference. The controller then places the towing vessel along the trajectory calculated by the reference model. A limitation to the LOS method is that it requires iceberg position measurements. This may not always be feasible in real iceberg towing attempts.

The LOS method is simulated in Section 13.5. The simulations show that the towing vessel is able to tow the iceberg to and along the desired path, for three different current directions. The method has also been experimentally tested in the MC Lab. The experiments provided satisfactory results, both with and without current. There were, however, some fluctuations from the path in the experiments, which may be fixed with better tuning of the control setup, or the thruster mappings for the individual thrusters.

A reliability index based penalty method *on commanded thrust* has been developed. The simulations show that the thrust penalty may delay failure modes, but is no guarantee against them if the velocity reference keeps commanding more thrust. Experiments were also conducted on this, but proved inconclusive due to issues with the thruster mapping at the time. It is advised against implementing thrust penalty in the manner discussed in the thesis, and focus should rather be on the velocity reference.

A reliability index based penalty *on the velocity reference* has been developed to replace the penalty on commanded thrust. An upper reliability index limit where the penalty controller should start penalizing is denoted  $\delta_{near}$ , whereas the minimum allowable limit is denoted  $\delta_{limit}$ . The penalty is linear, starting on 0% reduction at  $\delta_{near}$  and 100% reduction at  $\delta_{limit}$ . The simulation study in Section 13.6.1 shows that the rate of change of the penalty, when changing towards less penalty, should be limited in order to avoid large oscillations in the velocity reference and the commanded thrust. A limitation algorithm was proposed, and is shown in simulations to improve the performance of the penalty.

A combination of the LOS guidance and controller and the velocity reference penalty control has been investigated in Section 13.6.1, in order to tow the iceberg safely along a pre-defined straight-line path. The method is seen to tow the iceberg along the pre-described path with a nearly steady reliability index for towline rupture, staying well above the lower limit  $\delta_{limit}$ . It is important to keep the reliability index steady, in order to avoid large oscillations in the velocity reference, which in turn oscillates the commanded thrust and tow force.

Lastly, a hardware-in-the-loop (HIL) setup has been developed for iceberg towing using CSE1 in the MC Lab. This is described in Section 12.5. Within the HIL setup is a simulation of the position measurement errors in the MC Lab. The LOS path following method was tested with the HIL setup, and showed that the dead reckoning implemented in the observer performed well. Dead reckoning is also seen to work well in the lab experiments (figures 14.7, 14.9 and 14.11).

## Further work

In order to better prevent iceberg overturning, the stability of icebergs may be assessed. It could, for instance, be possible to use the tension measurements and the

---

motion measurements to roughly estimate the iceberg stability using online system identification methods. The iceberg shape could also possibly be scanned beneath the surface by a purpose-built underwater vehicle, in order to calculate its stability.

The limitation of the rate of change for the velocity reference penalty scheme, is probably suboptimal, since finding the optimal limitation was not investigated in this thesis. It could be improved to create even more stable reliability indices when close to the failure limit.

The towline estimate for simulations in this thesis is based on linear strain. A dynamic model for the towline could perhaps be developed, allowing the towline tensions to be modelled more accurately during transients. In addition, the towline in this thesis is not affected by the ocean current. Ocean current may influence the towline tension, especially for longer tows than those tested in this thesis. This could perhaps be assessed using a finite element method (FEM) model for the towline.

The iceberg LOS algorithm in this thesis is based on the assumption that the iceberg position is measured. If the iceberg position is not measured, the towline angle could be measured in the fastening point on the towing vessel. The iceberg position could possibly then be estimated by using the measured towline tension, the measured towline angle, and the known towline length, in addition to the towing vessel position and heading.



# Bibliography

- Berntsen, P. I. B. (2008). *Structural Reliability Based Position Mooring*. Ph. D. thesis, Department of Marine Technology, Norwegian University of Science and Technology, Trondheim, Norway.
- Breivik, M. (2003, June). Nonlinear maneuvering control of underactuated ships. Master's thesis, Department of Engineering Cybernetics, Norwegian University of Science and Technology, Trondheim, Norway.
- Breivik, M. (2010, June). *Topics in Guided Motion Control of Marine Vehicles*. Ph. D. thesis, Norwegian University of Science and Technology, Trondheim, Norway.
- Børhaug, E., A. Pavlov, and K. Y. Pettersen (2008). Integral los control for path following of underactuated marine surface vessels in the presence of constant ocean currents. *Proc. of the 47th IEEE Conference on Decision and Control, Cancun, Mexico*.
- Brian T. Hill. Institute for Ocean Technology (2000, December). Database of ship collisions with icebergs.
- Fossen, T. I. (2011). *Handbook of Marine Craft Hydrodynamics and Motion Control* (1 ed.). John Wiley & Sons Ltd.
- Fossen, T. I., M. Breivik, and R. Skjetne (2003). Line-of-sight path following of underactuated marine craft. *Proc. 6th IFAC Maneuvering and Control of Marine Craft, Girona, Spain*, pp. 244–249.
- Fossen, T. I. and J. P. Strand (1999). Passive nonlinear observer design for ships using lyapunov methods: full-scale experiments with a supply vessel. *Automatica* 35(1), 3–16.
- Fredriksen, E. and K. Y. Pettersen (2006). Global  $\kappa$ -exponential way-point maneuvering of ships: Theory and experiments. *Automatica* 42(4), pp.677–687.
- Lane, K., D. Power, J. Youden, and C. Randell (2004). Validation of synthetic aperture radar for iceberg detection in sea ice. *Geoscience and Remote Sensing Symposium*.
- Leira, B. J., A. J. Sørensen, and C. M. Larsen (2004). A reliability-based control algorithm for dynamic positioning of floating vessels. *Structural Safety* 26, pp. 1–28.
- Loria, A., T. I. Fossen, and E. Panteley (2000). A separation principle for dynamic positioning of ships: Theoretical and experimental results. *IEEE Trans. Contr. Sys. Tech.* 8(2), 332–343.

- Marchenko, A. and K. Eik (2011). Iceberg towing in open water: Mathematical modeling and analysis of model tests. *Cold Regions Science and Technology 73 (2012)*, pp. 12–31.
- Marchenko, A. and C. Ulrich (2008, May). Iceberg towing: Analysis of field experiments and numerical simulations. In *Proceedings. The International Workshop Celebrating Professor Alf Tørum's 75th Birthday. COASTAL TECHNOLOGY - Coast 2008.*, Trondheim, Norway, pp. 235–246. Iceberg towing: Analysis of field experiments and numerical simulations, NTNU.
- MC Lab (2014). NTNU marine cybernetics lab. <http://www.ntnu.no/imt/lab/kybernetikk>. Accessed: 2014-06-07.
- McClintock, J., T. Bullock, R. McKenna, F. Ralph, and R. Brown (2002, March). Greenland iceberg management: Implications for grand banks management systems. *PERD/CHC Report 20-65. Report prepared for PERD/CHC, National Research Council Canada, Ottawa, ON. Report prepared by AMEC Earth & Environmental, St. John's, NF, R.F. McKenna & Associates, Wakefield, QC, and CORE, St. John's, NF.*
- McClintock, J., R. McKenna, and C. Woodworth-Lynas (2007, May). Grand banks iceberg management. *PERD/CHC Report 20-84. Report prepared for PERD/CHC, National Research Council Canada, Ottawa, ON. Report prepared by AMEC Earth & Environmental, St. John's, NL, R.F. McKenna & Associates, Wakefield, QC, and PETRA International Ltd., Cupids, NL.*
- Model Slipway (2014). Anchor handling tug aziz / arif. <http://www.modelslipway.com/aziz.htm>. Accessed: 2014-05-25.
- National Instruments (2014). Ni crio-9024. <http://sine.ni.com/nips/cds/view/p/lang/no/nid/207371>. Accessed: 2014-06-07.
- Norwegian Ministry of Petroleum and Energy (2011). En næring for framtida – om petroleumsvirksomheten. <http://www.regjeringen.no/nb/dep/oed/dok/regpubl/stmeld/2010-2011/meld-st-28-2010-2011.html?id=649699>. Accessed: 2014-06-07.
- NSIDC (2012). National snow and ice data center: Arctic sea ice falls below 4 million square kilometers. <http://nsidc.org/arcticseaicenews/2012/09/arctic-sea-ice-falls-below-4-million-square-kilometers/>. Accessed: 2014-06-04.
- Orsten, A. (2013, December). Reliability-based control for towing of icebergs in open water. Project thesis, Department of Marine Technology, NTNU.



## BIBLIOGRAPHY

---

- Petroleum Safety Authority Norway (2012). Barents sea - cold facts. <http://www.ptil.no/news/barents-sea-cold-facts-article8353-878.html>. Accessed: 2014-06-07.
- Pettersen, B. (2007, January). *Marin teknikk 3 : hydrodynamikk*. Marine Technology Centre, Trondheim, Norway.: Department of Marine Technology, NTNU.
- Qualisys (2014, May). Oqus camera series. <http://www.qualisys.com/products/hardware/oqus/>. Accessed: 2014-05-29.
- Riska, K. (2013). Lecture 1, series of lectures on ice action on ships. Lecture notes distributed in Ship Design for Ice Operations at the Norwegian University of Science and Technology, Trondheim.
- Robe, R. Q. (1980). Iceberg drift and deterioration. *Colbeck, S. (Ed.), Dynamics of Snow and Ice Masses, Academic Press, New York*, pp. 211–259.
- Rudkin, P., C. Boldrick, and P. Barron Jr. (2005). Comprehensive iceberg management database. *PERD/CHC Report 20-72, Report prepared by Provincial Aerospace Environmental Services*.
- Rustad, A. M. (2007, November). *Modeling and Control of Top Tensioned Risers*. Ph. D. thesis, Department of Marine Technology, Norwegian University of Science and Technology, Trondheim, Norway.
- Skjetne, R. (2005). *The Maneuvering Problem*. Ph. D. thesis, Department of Engineering Cybernetics, Norwegian University of Science and Technology, Trondheim, Norway.
- Skjetne, R., U. Jørgensen, and A. R. Teel (2011). Line-of-sight path-following along regularly parametrized curves solved as a generic maneuvering problem. *50th IEEE Conference on Decision and Control and European Control Conference (CDC-ECC)*.
- Skåtun, H. N. (2011). Development of a DP System for CS Enterprise I with Voith Schneider Thrusters. Master's thesis, Department of Marine Technology, Norwegian University of Science and Technology., Trondheim, Norway.
- Sørensen, A. J. (2012). *Marine Control Systems - Propulsion and Motion Control of Ships and Ocean Structures*. Department of Marine Technology, NTNU.
- Standards Norway (2007, September). Actions and action effects. *NORSOK STANDARD N-003*.
- Sundland, M. (2013, June). Guidance and control of iceberg towing operation in open water, with experimental testing. Master's thesis, Norwegian University of Science and Technology (NTNU), Trondheim, Norway.

- Tran, D. N. (2014). Line-Of-Sight-based maneuvering control design, implementation, and experimental testing for the model ship C/S Enterprise I. MSc thesis, Norwegian University of Science and Technology, Trondheim, Norway. To be published in June, 2014.06.10.
- Voitkunsky, J. I. (1988). Resistance to ship motion. *Sudostroenie, Leningrad (In Russian)*, p. 287.
- WAMIT (2014, May). The state of the art in wave interaction analysis. <http://wamit.com/>. Accessed: 2014-05-29.

# Conference Paper





**22<sup>nd</sup> IAHR International Symposium on Ice**  
*Singapore, August 11 to 15, 2014*

---

**LOS guidance for towing an iceberg along a straight-line path**

**Andreas Orsten<sup>1</sup>, Petter Norgren<sup>1,2</sup>, and Roger Skjetne<sup>1,2</sup>**

<sup>1</sup> *Dept. Marine Technology, Norwegian Univ. of Science and Technology (NTNU).*

<sup>2</sup> *SFI Sustainable Arctic Marine and Coastal Technology (SAMCoT), NTNU.  
andreasorsten@gmail.com, Petter.Norgren@ntnu.no, Roger.Skjetne@ntnu.no*

Motivated by the need to develop a reliable and safe way of towing icebergs, this paper investigates the use of a feedback-based guidance algorithm for steering the iceberg along a pre-defined safe track.

A simplified, linear iceberg model is developed in 2 degrees of freedom (DOF) to capture the horizontal motion, including the effect of constant and irrotational ocean currents.

Previously, a Line-of-Sight (LOS) algorithm has been implemented for steering a ship along a pre-defined path. The algorithm has been modified to include the effect of an ocean current, using integral action. In this paper, the current-modified LOS algorithm is augmented in order to apply it to the 2-DOF horizontal iceberg model. The output of the iceberg LOS algorithm is the desired towline angle  $\alpha_{LOS}$ . Guidance of the model is achieved through a tow force  $T$  with direction  $\alpha$  that should conform to  $\alpha_{LOS}$ .

Simulation studies, showing the performance of the LOS algorithm, are performed in the presence of both a constant, and a slowly-varying ocean current. A towing vessel reference model is proposed in order to obtain a better resemblance between the change of the towline angle and the movements of the towing vessel.

The simulation studies all show that the iceberg trajectories converge to and move along the desired path, and that the vessel reference model provides feasible trajectories for the towing vessel.

## 1. Introduction

As oil and gas exploration moves further north, the problem of icebergs threatening stationary installations must be taken into account. This becomes relevant when considering installations, for example in the Barents Sea. Dealing with the risk of icebergs in offshore operations is called *Iceberg Management*.

Much experience on iceberg management is obtained in the Grand Banks area, out of Newfoundland, Canada, where there have been offshore installations in the area since 1997 (McClintock et al., 2007). Further research including model tests, numerical simulations and field experiments in the Barents sea has been performed (Eik, 2010; Marchenko and Eik, 2011). Iceberg management is roughly divided into:

1. Iceberg detection and tracking: Detecting and tracking icebergs that may instigate a threat.
2. Threat assessment: Forecasting iceberg drift pattern and deciding whether the iceberg is a threat to the installation.
3. Iceberg handling: If an iceberg is assessed as a threat, then alleviate the threat by performing some physical action on it.

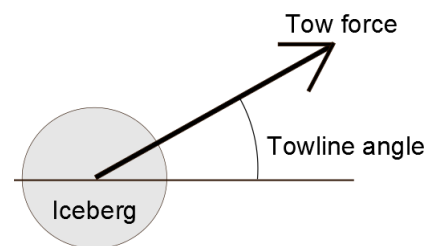
There is also *iceberg risk management* (McClintock et al., 2007), but this is not within the scope of this paper.

*Iceberg handling* in the Grand Banks area has been performed in many ways, but the most frequently used is *single vessel rope tow* (Rudkin et al., 2005). When towing an iceberg, the main target is changing its trajectory away from the installation, and ensuring it does not threaten the installation after the tow. In the Grand Banks, this has been performed manually, where according to McClintock et al. (2007, p.18), smaller icebergs are usually towed away. For larger icebergs, on the other hand, the objective of towing is mainly to deflect the iceberg heading a few degrees from its naturally preferred route.

As with other towing operations, one must avoid towline rupture. In addition, icebergs may be unstable, smooth-surfaced and slippery. Due to this, iceberg overturning and towline slippage are important limitations to iceberg towing (McClintock et al., 2002).

Instead of manually maneuvering the vessel performing the tow, automatic maneuvering could be used. Normally, when maneuvering a ship, the target is to make the ship follow a certain path. In this paper, however, we consider the problem of making the iceberg follow a certain path. With an iceberg steering algorithm in place, one could eventually implement ways to reduce the risk of towline rupture, towline slippage, and iceberg overturning by more intelligent control of the towing force. Better performance with respect to these challenges would make the towing operation safer and more reliable.

The objective of this paper is to steer an iceberg along a straight-line path, using a Line-of-Sight (LOS) algorithm. This is done in a simplified system, only considering the iceberg actuated by the towline (Figure 1). The towline has a force and a direction. By setting the tow force as constant and only controlling the towline angle, this paper investigates the feasibility of using the LOS method



**Figure 1.** A model of the simplified iceberg-towline system.

to steer the iceberg to and along a specified path.

The traditional LOS method for ships calculates the ship's desired yaw angle (Fossen et al., 2003), and uses this to converge to and move along a path. When towing icebergs, you must instead change the angle of the tow force by properly locating the towing vessel.

In addition, the iceberg may be affected by environmental loads, which for a traditional ship is implemented into the LOS method (Børhaug et al., 2008). In this paper we augment the implementation to include current in the iceberg towline model to robustly compensate the current forces.

## 2. Iceberg model

Consider the class of marine surface vessels described by the 3-DOF model (Fossen, 2011):

$$\dot{\eta} = R(\psi)\nu \quad [1]$$

$$M_{RB}\dot{\nu} + C_{RB}(\nu)\nu = -M_A\dot{\nu}_r - C_A(\nu_r)\nu_r - D\nu_r + \tau \quad [2]$$

**Assumption 1** *In order to develop an iceberg model of sufficient fidelity for a model-based guidance (or control) design, some simplifying assumptions are made as follows:*

1. *The iceberg is approximately cylinder-shaped.*
2. *The symmetric, cylinder-shaped iceberg has no correlated damping or added mass between yaw and surge/sway. This is a fair assumption for a cylindrical shape.*
3. *The symmetric, cylinder-shaped iceberg can be towed in every direction, regardless of the iceberg yaw angle. This is also a fair assumption for a cylindrical iceberg.*
4. *The tow force is assumed to act directly through the centres of gravity (CoG) and buoyancy (CoB) of the iceberg. This is fair for a stable iceberg with small roll/pitch motions. In reality roll and pitch motion would move CoG or CoB away from the tow force, causing yaw rotation. However, due to Assumption 1.3, this is ignored.*
5. *The Coriolis effect and nonlinear damping terms are disregarded, due to low velocities.*
6. *The ocean current  $\nu_c$  is assumed constant and irrotational, meaning that  $\dot{\nu}_c = 0$ .*

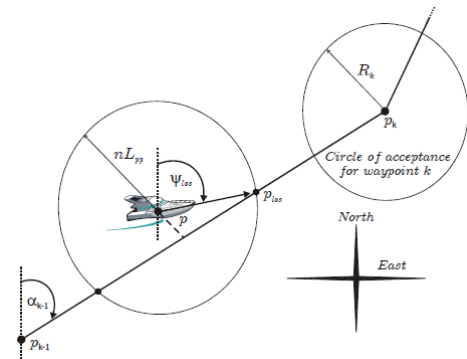
Thus, the simplified iceberg model is a linear, 2-DOF model, disregarding the rotational matrix:

$$\dot{\eta} = \nu \quad [3]$$

$$\nu_r = \nu - \nu_c \quad [4]$$

$$(M_{RB} + M_A)\dot{\nu} - M_A\dot{\nu}_c + D\nu_r = \tau, \quad [5]$$

where  $\eta = [x, y]^T$  and  $\nu = [u, v]^T$  describe the iceberg position and velocity in Cartesian coordinates,  $M_{RB}$ ,  $M_A$  and  $D$  are the rigid body mass-, added mass-, and linear damping matrices, respectively, and  $\nu_r$  is the relative velocity between iceberg velocity ( $\nu$ ) and current velocity  $\nu_c = [u_c, v_c]^T$ .



**Figure 2.** An interpretation of the desired path in a Cartesian coordinate system, courtesy of Fossen et al. (2003).

### 3. Line-of-Sight guidance

#### 3.1. Traditional LOS guidance

LOS guidance has been used to solve the geometric task of the maneuvering problem (Skjetne et al., 2011). Fossen et al. (2003) has described the LOS angle in Cartesian coordinates, as seen in Figure 2. Børhaug et al. (2008), on the other hand, described the LOS angle in a waypoint-path fixed coordinate system. As the iceberg model described in Equation (5) is in Cartesian coordinates, this paper will continue with Cartesian coordinates. The LOS angle for a ship is then described as:

$$\psi_{LOS} = \text{atan2}(y_{LOS} - y, x_{LOS} - x) \quad [6]$$

The use of  $\text{atan2}$ , as opposed to  $\text{arctan}$ , ensures that the LOS angle is placed in the correct quadrant and within the set  $(-\pi, \pi]$ .

The procedure for waypoint path-following, and the equations to obtain the LOS angle  $\psi_{LOS}$  are found in Fossen et al. (2003). Breivik (2003, pp.33-35) presented a way to solve these equations and obtain the projected point  $p_{LOS} = [x_{LOS}, y_{LOS}]^T$ .

#### 3.2. LOS algorithm with constant ocean current

The traditional LOS algorithm does not take into account environmental forces, such as ocean currents. Børhaug et al. (2008) suggested a guidance law, in the waypoint-path fixed coordinate system, using integral action, and obtained the current-modified LOS angle. To avoid confusion with yaw motion, this paper will replace  $\psi_{LOS}^m$  with an iceberg towline angle,  $\alpha_{LOS}$ :

$$\alpha_{LOS} \triangleq -\arctan\left(\frac{y' + \sigma y'_{int}}{\Delta}\right), \Delta > 0 \quad [7]$$

$$\dot{y}'_{int} = \frac{\Delta y'}{(y' + \sigma y'_{int})^2 + \Delta^2} \quad [8]$$

In order to apply it to the iceberg model, it must be transformed into Cartesian coordinates. Using the notation from Figure 3, the following relationships hold:

$$a = \sqrt{(x(t) - x_{k-1})^2 + (y(t) - y_{k-1})^2} \quad [9]$$

$$b = \sqrt{(x_{LOS} - x(t))^2 + (y_{LOS} - y(t))^2} \quad [10]$$

$$c = \sqrt{(x_{LOS} - x_{k-1})^2 + (y_{LOS} - y_{k-1})^2} \quad [11]$$

$$x' = \frac{a^2 + c^2 - b^2}{2c} \quad [12]$$

$$y' = \pm \sqrt{a^2 - (x')^2} \quad [13]$$

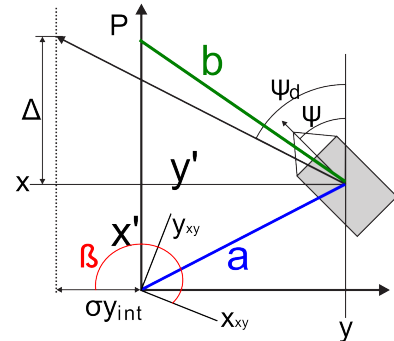
$$\Delta = c - x' \quad [14]$$

If the path lies on the iceberg's port side,  $y'$  is positive. Otherwise,  $y'$  is negative. When having obtained all these values,  $\dot{y}'_{int}$  is obtained and can be integrated. The integrated value  $y'_{int}$  must then be transformed into Cartesian coordinates:

$$\beta = \text{atan2}(y_k - y_{k-1}, x_k - x_{k-1}) + \frac{\pi}{2} \quad [15]$$

$$y_{int,x} = y_{int} \cos(\beta) \quad [16]$$

$$y_{int,y} = y_{int} \sin(\beta) \quad [17]$$



**Figure 3.** Notation for transforming between Path-fixed and Cartesian coordinates. Original illustration is found in Børhaug et al. (2008).



The index  $k$  denotes the selected waypoint.  $\beta$  is perpendicular to the angle between the Cartesian and the waypoint-path fixed coordinate system. Then, finally the Cartesian LOS angle can be calculated:

$$\Delta y_{LOS} = y_{LOS} - y \quad [18]$$

$$\Delta x_{LOS} = x_{LOS} - x \quad [19]$$

$$\alpha_{LOS}^{xy} = \text{atan2}(\Delta y_{LOS} + \sigma y_{int,y}, \Delta x_{LOS} + \sigma y_{int,x}) \quad [20]$$

#### 4. Iceberg guidance law

The main objective of this paper is to demonstrate the LOS method. For the purpose of testing the LOS method, a direct feed of the desired towline angle is used.

The model (Figure 1) consists of a tow force ( $T$ ) which is held constant, and a towline angle ( $\alpha$ ), which is set equal to the calculated towline angle from the LOS algorithm:

$$T = T_0 \quad [21]$$

$$\alpha = \alpha_{LOS}^{xy} \quad [22]$$

Simple trigonometry then suggests the following desired towing force:

$$\tau = \begin{bmatrix} \tau_x \\ \tau_y \end{bmatrix} = \begin{bmatrix} T_0 \cos(\alpha_{LOS}^{xy}) \\ T_0 \sin(\alpha_{LOS}^{xy}) \end{bmatrix} \quad [23]$$

It is imperative that the towing force amplitude  $T_0$  overcomes the environmental loads on the iceberg, such that a positive forward speed over ground is attained.

#### 5. Simulation studies

The proposed LOS algorithm was tested using *MatLab*<sup>TM</sup> and *Simulink*<sup>TM</sup>. The simulated iceberg was chosen as a *small berg* (McClintock et al., 2007) with the following dimensions:

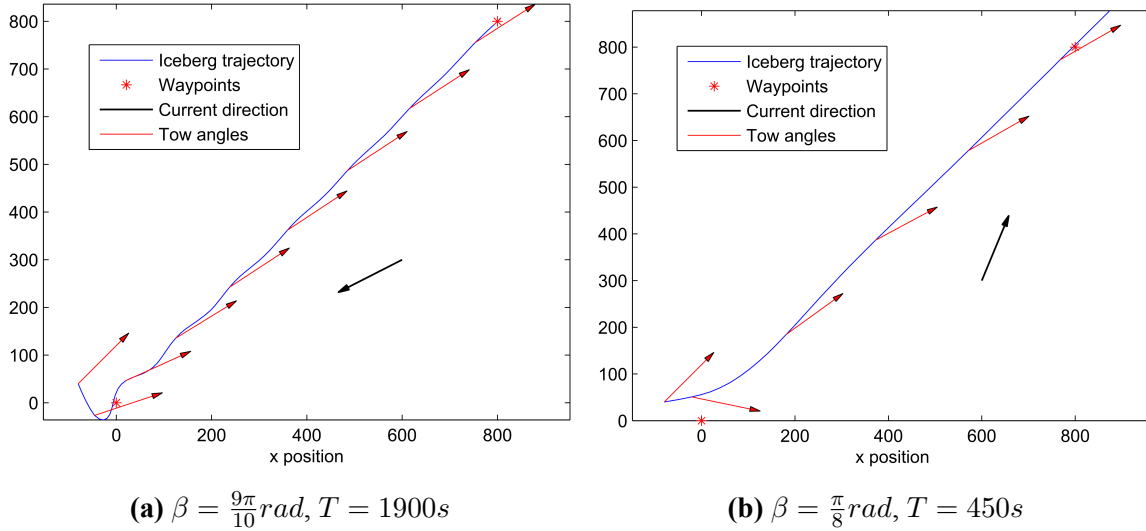
- Diameter/Length/Width: 25 m
- Height above waterline: 5 m
- Draught: 42.7465 m
- Water-iceberg form drag coefficient:  $C_{wi} = 0.75$  (Robe, 1980)
- Mass:  $2.1487 \times 10^7$  kg ( $\rho_i = 916.7$  kg/m<sup>3</sup>)

The maximum near-surface current in both Newfoundland and the Barents sea is  $1.3 \frac{m}{s}$ . (ISO 19906, 2010, pp.342-408) In order to overcome the current velocity, the constant tow force was chosen to be  $T_0 = 5 \times 10^6$ . The integral gain used was  $\sigma = 0.3$ .

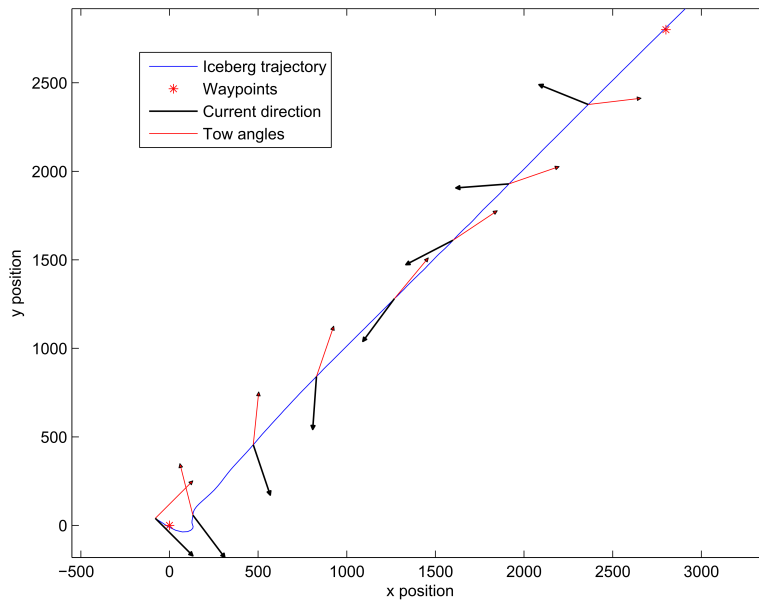
##### 5.1. Constant current

The algorithm was simulated with a constant ocean current of  $1.3 \frac{m}{s}$ , in 2 different directions. To create a straight-line path, the following waypoints were used:

$$WP = \begin{bmatrix} i & x & y \\ 1 & 0 & 0 \\ 2 & 800 & 800 \end{bmatrix} \quad [24]$$



**Figure 4.** Plotted Simulink results for a current with a  $\beta$  relative angle to the waypoint path. Simulation ran for  $T$  seconds.



**Figure 5.** Plotted Simulink results for a current rotating from  $-\pi$  to  $\pi$  relative angle to the waypoint path.

### 5.2. Slowly-varying current

The algorithm was tested in a scenario where the ocean current with an intensity of  $1.3 \frac{m}{s}$  changes direction from  $-\pi$  to  $\pi$  relative to the straight-line path during  $T = 5000s$ , as seen in Figure 5.

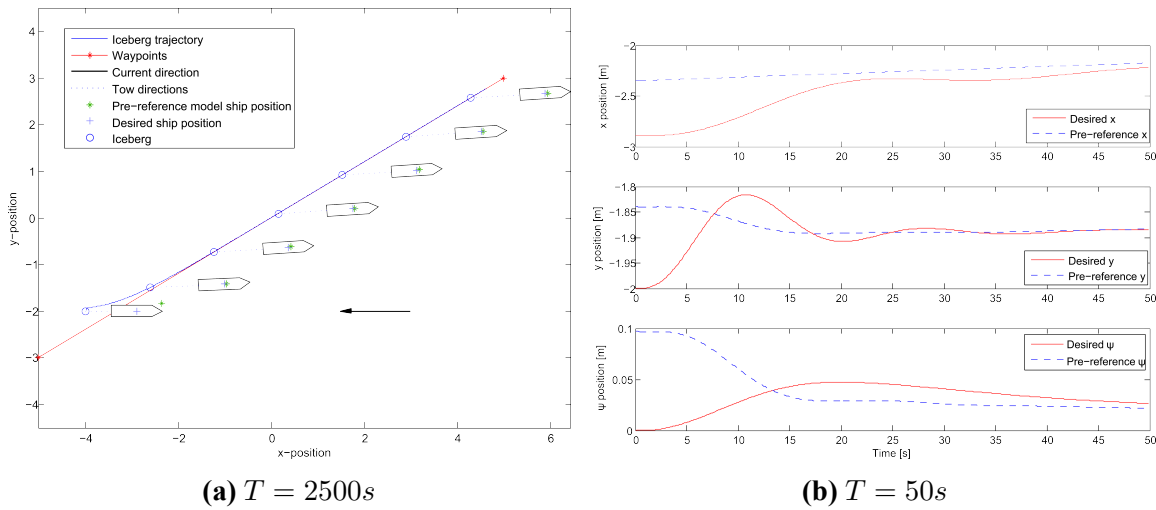
### 5.3. Towline with towing vessel dynamics

The main practical issue with the LOS algorithm is that the towline angle can not be changed without restriction. It must follow the dynamics of a towing vessel. The simulation setup has followed these few steps:

1. The current-modified LOS angle is calculated.

2. The desired towing vessel position is calculated. This position is placed in the direction of the LOS angle,  $\alpha_{LOS}^{xy}$ , and distance of the towline away from the iceberg.
3. The desired LOS-based position is then entered into a reference model for the towing vessel. The output of the reference model is a more realistic and feasible desired vessel position. The reference model is created to simulate the towing vessel's dynamics and provides smooth changes of the desired position.
4. The angle between the new, more realistic desired vessel position and the iceberg is then used as the desired towline angle, and fed into the controller as in the previous simulations.

In order to make a reference model work, data from the model vessel C/S Enterprise 1 at the Norwegian University of Science and Technology was used (Tran, 2014). The simulated iceberg is thus a model scaled, cylindrical iceberg with a diameter of 20cm and draught of 79.18cm.



**Figure 6.** (6a) Iceberg path following in a constant current, with towing vessel positions following vessel dynamics. (6b) Plots showing LOS ship position (pre-referenced) versus position obtained after the reference model (desired), during the initiation phase of the path following.

## 6. Conclusion

In this paper we have shown how we can tow an iceberg along a straight-line path by applying a Line-of-Sight-based algorithm to determine the towline direction, robustly in the presence of ocean currents.

The results seen in Figure 4 show that the algorithm makes the iceberg converge to the desired path when exposed to a constant ocean current, and the towline direction changed slowly enough to be feasible to determine the position of the towing vessel. Figure 5 shows that the iceberg also converges when exposed to a slowly varying ocean current. Similar scenarios in other waypoint directions were also tested, and worked satisfactorily.

As seen from Figure 6 it is possible to make the iceberg converge to the desired path, even when the tow angle is influenced by towing vessel dynamics. As seen in Figure 6b the initiation phase is important in order to obtain a stable tow angle. To avoid large oscillations during initiation, the LOS integral action  $\sigma$  value must be set sufficiently low.

In order to apply the LOS algorithm in real cases, it must be extended to include a towing vessel controller and towing vessel model, following the ideas of Section 5.3. Furthermore, with the algorithm working in a real case scenario, measures could be included in controlling the iceberg to avoid towline slippage, towline rupture and iceberg overturning. This would ensure safer and more reliable iceberg towing operations.

## References

- Breivik, M. (2003). Nonlinear maneuvering control of underactuated ships. Master's thesis, Department of Engineering Cybernetics, Norwegian University of Science and Technology.
- Børhaug, E., Pavlov, A., and Pettersen, K. Y. (2008). Integral los control for path following of underactuated marine surface vessels in the presence of constant ocean currents. *Proc. of the 47th IEEE Conference on Decision and Control, Cancun, Mexico*.
- Eik, K. (2010). *Ice Management in Arctic Offshore Operations and Field Developments*. PhD thesis, Norwegian University of Science and Technology, Trondheim.
- Fossen, T. I. (2011). *Handbook of Marine Craft Hydrodynamics and Motion Control*. John Wiley & Sons Ltd.
- Fossen, T. I., Breivik, M., and Skjetne, R. (2003). Line-of-sight path following of underactuated marine craft. *Proc. 6th IFAC Maneuvering and Control of Marine Craft, Girona, Spain*, pages pp. 244--249.
- ISO 19906 (2010). Petroleum and natural gas industries - arctic offshore structures. *International Organization for Standardization, Geneva*.
- Marchenko, A. and Eik, K. (2011). Iceberg towing in open water: Mathematical modeling and analysis of model tests. *Cold Regions Science and Technology 73 (2012)*, pages pp. 12--31.
- McClintock, J., Bullock, T., McKenna, R., Ralph, F., and Brown, R. (2002). Greenland iceberg management: Implications for grand banks management systems. *PERD/CHC Report 20-65. Report prepared for PERD/CHC, National Research Council Canada, Ottawa, ON. Report prepared by AMEC Earth & Environmental, St. John's, NF, R.F. McKenna & Associates, Wakefield, QC, and C-CORE, St. John's, NF*.
- McClintock, J., McKenna, R., and Woodworth-Lynas, C. (2007). Grand banks iceberg management. *PERD/CHC Report 20-84. Report prepared for PERD/CHC, National Research Council Canada, Ottawa, ON. Report prepared by AMEC Earth & Environmental, St. John's, NL, R.F. McKenna & Associates, Wakefield, QC, and PETRA International Ltd., Cupids, NL*.
- Robe, R. Q. (1980). Iceberg drift and deterioration. *Colbeck, S. (Ed.), Dynamics of Snow and Ice Masses, Academic Press, New York*, pages pp. 211--259.
- Rudkin, P., Boldrick, C., and Barron Jr., P. (2005). Comprehensive iceberg management database. *PERD/CHC Report 20-72, Report prepared by Provincial Aerospace Environmental Services*.
- Skjetne, R., Jørgensen, U., and Teel, A. R. (2011). Line-of-sight path-following along regularly parametrized curves solved as a generic maneuvering problem. *50th IEEE Conference on Decision and Control and European Control Conference (CDC-ECC)*.
- Tran, D. N. (2014). Line-Of-Sight-based maneuvering control design, implementation, and experimental testing for the model ship C/S Enterprise I. MSc thesis, Norwegian University of Science and Technology, Trondheim, Norway.

# Appendix



# Appendix A

## Tuning for LOS guidance and control

This appendix holds the tuning values for the LOS guidance and control simulations.

LOS Guidance:

$$\sigma = 0.005$$

Reference model:

$$\begin{aligned}A_{ref} &= \text{diag}([0.176, 0.5, 0.9642]) \\B_{ref} &= \text{diag}([0.0554, 0.22, 0.1741]) \\C_{ref} &= \text{diag}([0.0002, 0.047, 0.0109]) \\u_{max} &= 2 \frac{m}{s} \\v_{max} &= 1 \frac{m}{s} \\r_{max} &= \frac{\pi \text{ rad}}{30 \text{ s}}\end{aligned}$$

Controller:

$$\begin{aligned}K_p &= \text{diag}([10, 0.1, 0.1]) \\K_d &= \text{diag}([50, 10, 10])\end{aligned}$$

For the simulations in scenarios 5 and 6, the surge value used for  $K_p$  was 0.1. This was later changed for the latter scenarios. It should not mean anything for the results in scenarios 5 and 6, since it is not what is tested there.

Observer:

$$\begin{aligned}T_b &= \text{diag}([20, 200, 20]) \\K_2 &= \text{diag}([0.25, 1, 0.5]) \\K_3 &= \mathcal{I} \\K_4 &= \text{diag}([250, 300, 100])\end{aligned}$$

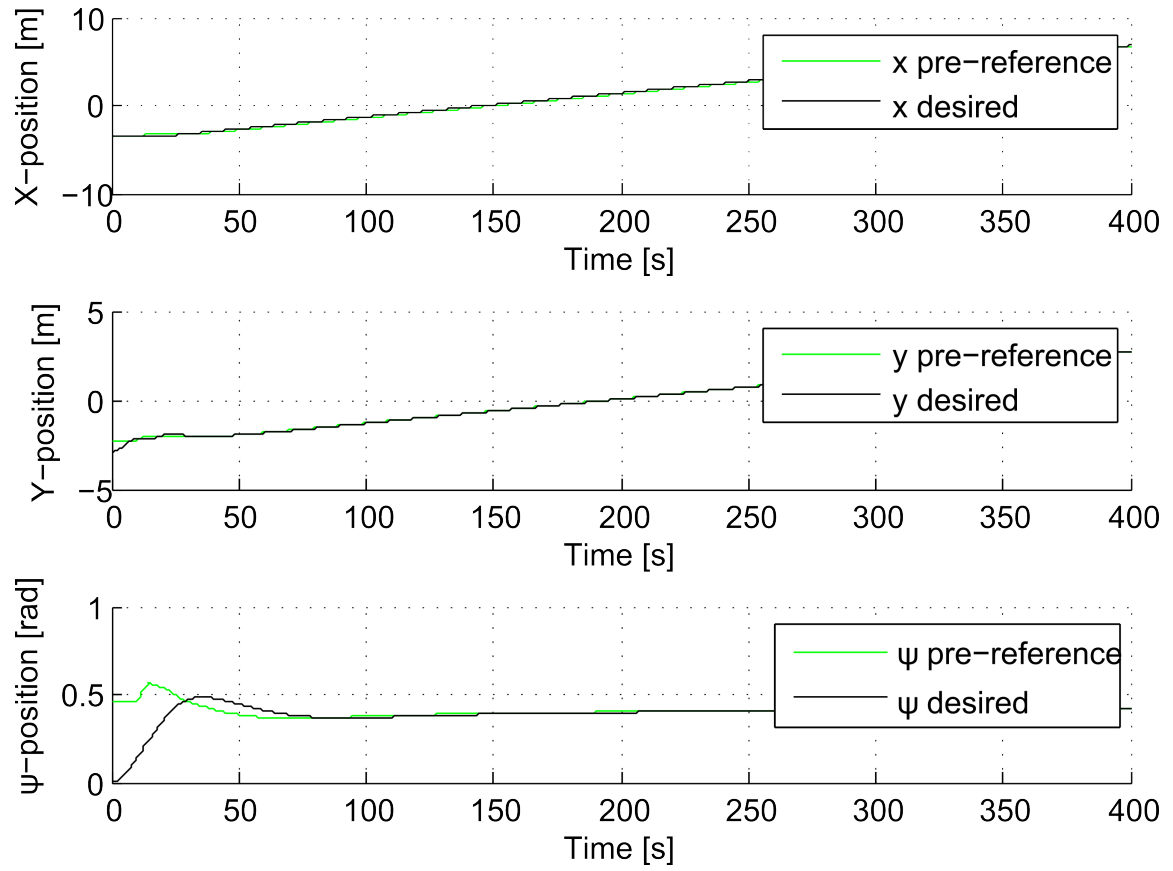


Figure A.1: Scenario 7,  $\beta_c = \pi$ : Pre-referenced position vs. desired towing vessel position.



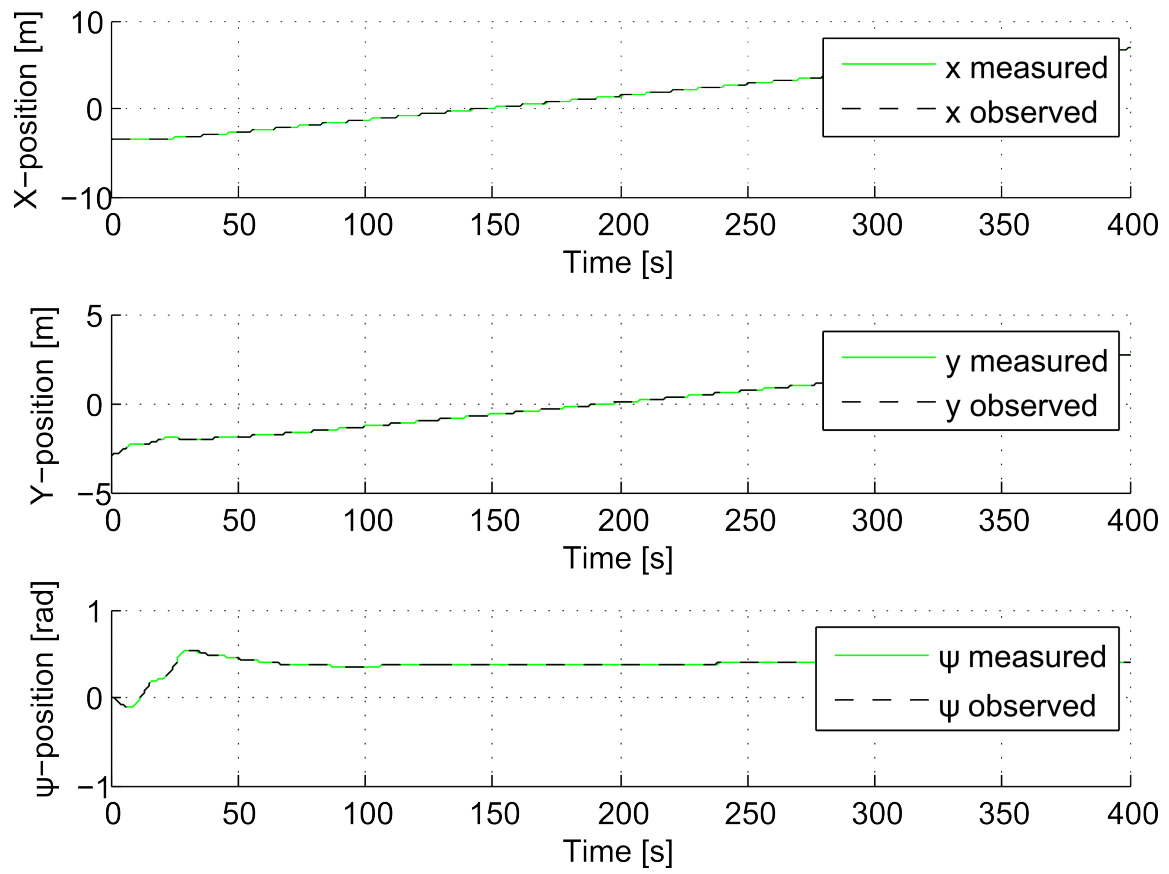


Figure A.2: Scenario 7,  $\beta_c = \pi$ : Measured vs. observed positions for the towing vessel.

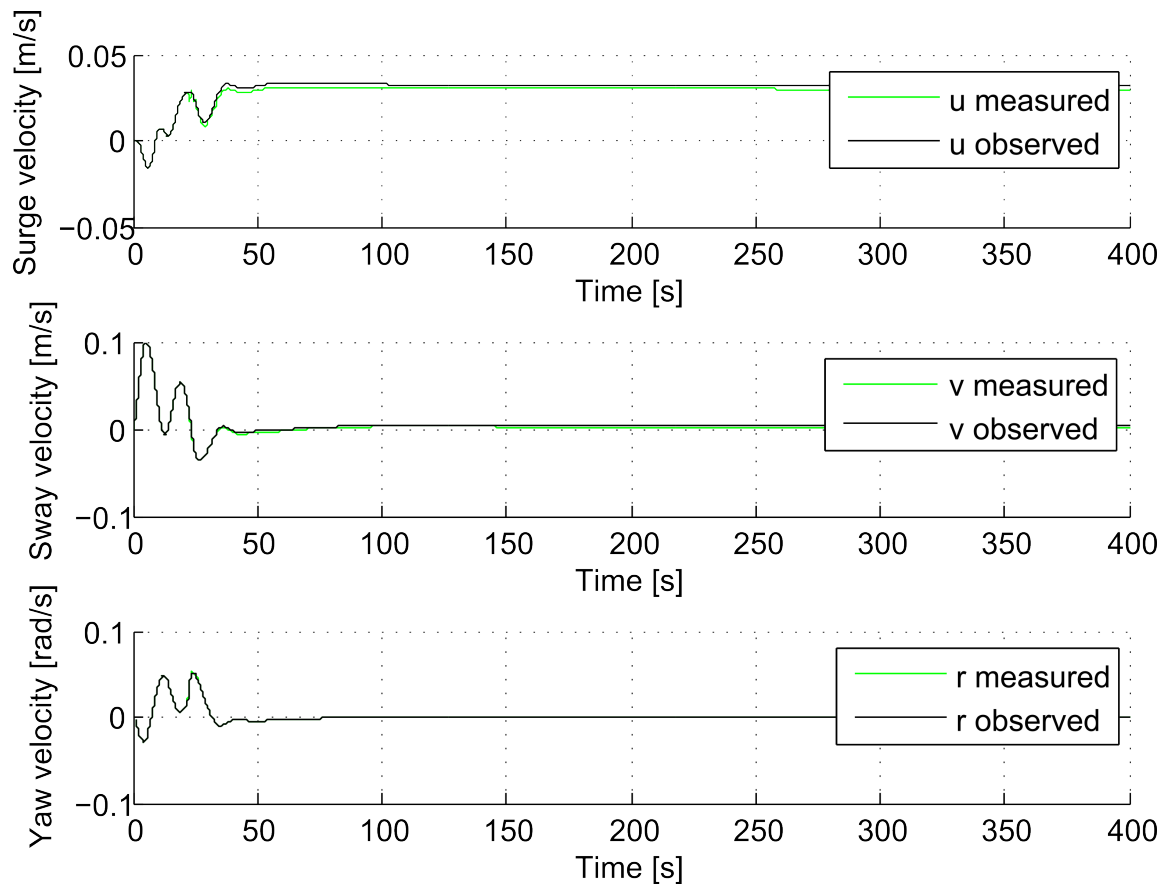


Figure A.3: Scenario 7,  $\beta_c = \pi$ : Measured vs. observed velocities for the towing vessel.

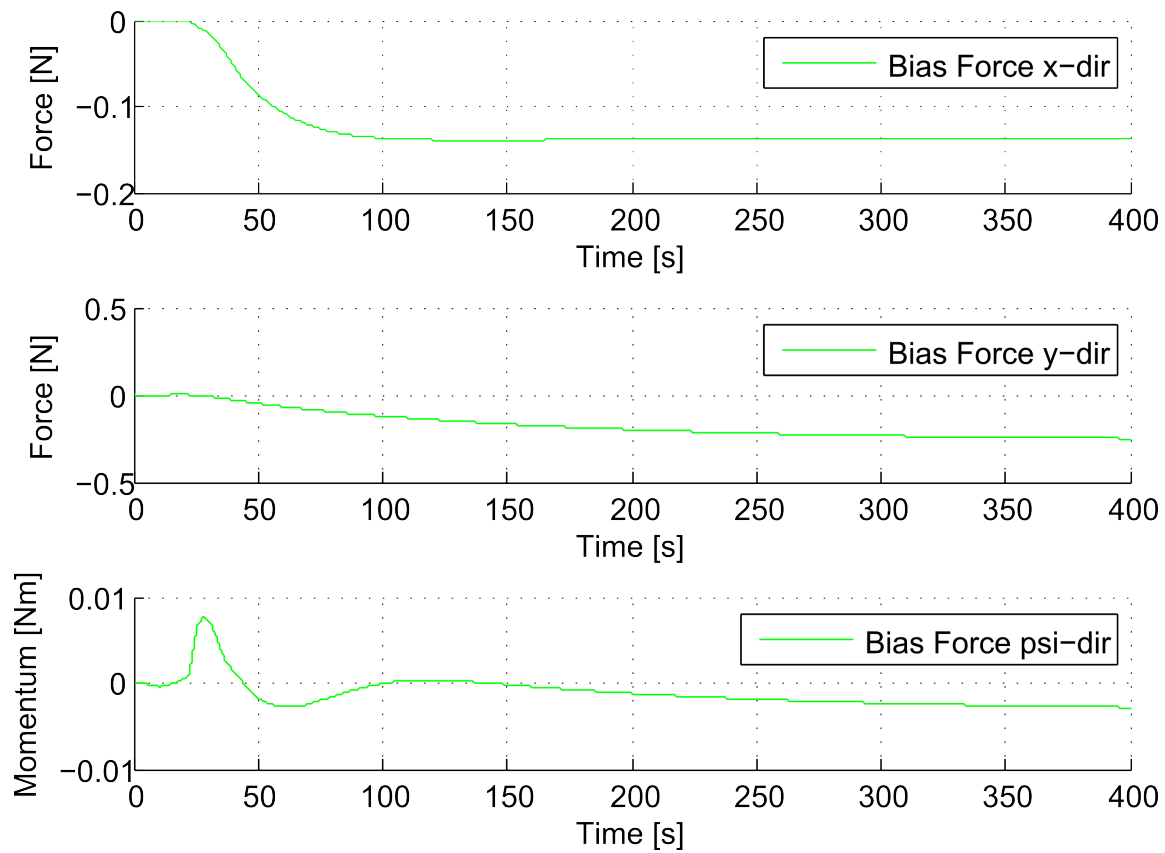


Figure A.4: Scenario 7,  $\beta_c = \pi$ : Measured vs. observed bias forces for the towing vessel.